INFORMATION TO USERS

This dissertation was produced from a microfilm copy of the original document. While the most advanced technological means to photograph and reproduce this document have been used, the quality is heavily dependent upon the quality of the original submitted.

The following explanation of techniques is provided to help you understand markings or patterns which may appear on this reproduction.

1. The sign or "target" for pages apparently lacking from the document photographed is "Missing Page(s)". If it was possible to obtain the missing page(s) or section, they are spliced into the film along with adjacent pages. This may have necessitated cutting thru an image and duplicating adjacent pages to insure you complete continuity.

2. When an image on the film is obliterated with a large round black mark, it is an indication that the photographer suspected that the copy may have moved during exposure and thus cause a blurred image. You will find a good image of the page in the adjacent frame.

3. When a map, drawing or chart, etc., was part of the material being photographed the photographer followed a definite method in "sectioning" the material. It is customary to begin photoing at the upper left hand corner of a large sheet and to continue photoing from left to right in equal sections with a small overlap. If necessary, sectioning is continued again — beginning below the first row and continuing on until complete.

4. The majority of users indicate that the textual content is of greatest value, however, a somewhat higher quality reproduction could be made from "photographs" if essential to the understanding of the dissertation. Silver prints of "photographs" may be ordered at additional charge by writing the Order Department, giving the catalog number, title, author and specific pages you wish reproduced.

University Microfilms

300 North Zeeb Road
Ann Arbor, Michigan 48106

A Xerox Education Company

72-19,716

YOON, Yo Kil, 1940-
GAS-LIQUID PHASE EQUILIBRIA IN THE HELIUM-CARBON TETRAFLUORIDE AND HELIUM-CHLOROTRIFLUOROMETHANE SYSTEMS AT LOW TEMPERATURES AND 20-120 ATMOSPHERES.

Georgia Institute of Technology, Ph.D., 1971
Engineering, chemical

University Microfilms, A XEROX Company, Ann Arbor, Michigan

GAS-LIQUID PHASE EQUILIBRIA IN THE HELIUM-CARBON TETRAFLUORIDE AND HELIUM-CHLOROTRIFLUOROMETHANE SYSTEMS AT LOW TEMPERATURES AND 20-120 ATMOSPHERES

A THESIS

Presented to

The Faculty of the Graduate Division

by

Yo Kil Yoon

In Partial Fulfillment

of the Requirements for the Degree

Doctor of Philosophy

In the School of Chemical Engineering

Georgia Institute of Technology

November, 1971

GAS-LIQUID PHASE EQUILIBRIA IN THE HELIUM-CARBON TETRAFLUORIDE AND HELIUM-CHLOROTRIFLUOROMETHANE SYSTEMS AT LOW TEMPERATURES AND 20-120 ATMOSPHERES

Approved:

W. T. Ziegler

Chairman

Date approved by Chairman: Nov. 17, 1971

PLEASE NOTE:

Some pages may have

indistinct print.

Filmed as received.

University Microfilms, A Xerox Education Company

In presenting the dissertation as a partial fulfillment of the requirements for an advanced degree from the Georgia Institute of Technology, I agree that the Library of the Institute shall make it available for inspection and circulation in accordance with its regulations governing materials of this type. I agree that permission to copy from, or to publish from, this dissertation may be granted by the professor under whose direction it was written, or, in his absence, by the Dean of the Graduate Division when such copying or publication is solely for scholarly purposes and does not involve potential financial gain. It is understood that any copying from, or publication of, this dissertation which involves potential financial gain will not be allowed without written permission.

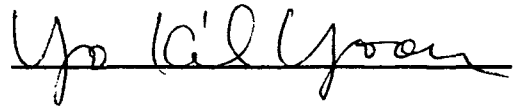

7/25/68

DEDICATION

To the memory of my mother and father

ACKNOWLEDGMENTS

It is my sincere wish to express a particular gratitute to Dr. W. T. Ziegler, my thesis advisor, for his encouragement, suggestions and fruitful discussions during this research. Especially, his broad and profound knowledge of thermodynamics was of great help in carrying out all theoretical treatments of this work. His continuous teaching and suggestions for the experimental techniques before and during the experimental work were also very helpful in developing attitutes necessary for an experimenter.

I wish to thank to Dr. B. S. Kirk, who built the phase equilibrium apparatus used in this work. I also extend my appreciation to Dr. J. D. Garber, who assisted me in learning the actual operation of the apparatus and whose several computer programs were of great help in making theoretical calculations.

Dr. R. A. Pierotti and Dr. J. D. Muzzy are acknowledged for serving on the Thesis Reading Committee.

I am also indebted to the School of Chemical Engineering for the financial support through teaching assistanships during 1969-1971. Thanks are due the Rich Electronic Computer Center for the use of their facilities.

My appreciation is also given to Korean Military Academy for allowing me a leave of absence to come the

United States and accomplish this research.

Finally, I am extremely grateful to my wife, Buhm Jin, for her endurance, encouragement and continuous love which have made the present work a reality. Particularly, her help with typing the final copy of this thesis is gratefully acknowledged.

TABLE OF CONTENTS

		Page
ACKNOWLEDGMENTS.		iii
LIST OF TABLES		viii
LIST OF FIGURES.		x
NOMENCLATURE		xiii
SUMMARY.		xx
Chapter		
I.	INTRODUCTION	1
II.	EXPERIMENTAL APPARATUS	8
	Description of Apparatus Experimental Procedure	
III.	EXPERIMENTAL RESULTS AND DISCUSSION	17
	Introduction Experimental Results Discussion of Results	
IV.	CALCULATION OF ENHANCEMENT FACTORS.	33
	Introduction Equations of State Considered Virial Equation of State Calculation of Virial Coefficients Benedict-Webb-Rubin Equation of State	
V.	COMPARISON OF PREDICTED AND EXPERIMENTAL GAS PHASE EQUILIBRIUM DATA.	63
	Interaction Second Virial Coefficient Enhancement Factor	
VI.	COMPARISON OF PREDICTED AND EXPERIMENTAL LIQUID PHASE EQUILIBRIUM DATA	96
	Experimental Henry's Law Constant and Partial Molar Volume at Infinite Dilution	

TABLE OF CONTENTS (Continued)

		Page
	Theoretical Prediction of Henry's Law Constant and Partial Molar Volume at Infinite Dilution	
VII.	CONCLUSIONS AND RECOMMENDATIONS.	129
	Conclusions Recommendations	
APPENDICES.		137
A.	TEMPERATURE SCALE USED AND CORRECTIONS FOR PRESSURE GAUGES.	138
B.	HELIUM-PROPYLENE SYSTEM MEASUREMENTS	140
C.	EXTRACTION OF KIHARA POTENTIAL PARAMETERS FROM EXPERIMENTAL SECOND VIRIAL COEFFICIENT DATA	143
D.	COMMENTS ON THE CALCULATION OF THE REDUCED VIRIAL COEFFICIENTS BASED ON THE LENNARD-JONES POTENTIAL.	149
E.	CALIBRATION OF GAS CHROMATOGRAPHS.	154
	General Analysis of Carbon Tetrafluoride in Helium Analysis of Chlorotrifluoromethane in Helium Analysis of Helium in Carbon Tetrafluoride and chlorotrifluoromethane	
F.	SUMMARY OF EXPERIMENTAL PHASE EQUILIBRIUM DATA FOR THE HELIUM-CARBON TETRAFLUORIDE AND HELIUM-CHLOROTRIFLUOROMETHANE SYSTEMS. . . .	163
G.	SMOOTHED EXPERIMENTAL AND THEORETICAL ENHANCEMENT FACTORS, AND SMOOTHED EXPERIMENTAL SOLUBILITY OF HELIUM	181
H.	SELECTION OF PHYSICAL PROPERTY DATA FOR PURE COMPONENTS.	186
	Helium Carbon Tetrafluoride Chlorotrifluoromethane	

TABLE OF CONTENTS (Concluded)

	page
I. PURITY OF GASES USED	206
BIBLIOGRAPHY.	207
VITA.	219

LIST OF TABLES

Table		Page
1.	B_{12} for the Helium-Carbon Tetrafluoride System	70
2.	B_{12} for the Helium-Chlorotrifluoromethane System	72
3.	Values of K_{12} for the Helium-Carbon Tetrafluoride and Helium-Chlorotrifluoromethane Systems.	79
4.	H_2^∞ and $\overline{V}_2^\infty$ for the Helium-Carbon Tetrafluoride System	104
5.	H_2^∞ and $\overline{V}_2^\infty$ for the Helium-Chlorotrifluoromethane System	106
6.	Boiling Point Data for Pure Components	117
7.	Parameters for the Method of Snider and Herrington	117
8.	Molar Volumes of the Pure Liquid Components at Saturation	125
9.	Comparison of Predicted and Experimental H_2^∞ and $\overline{V}_2^\infty$ for Some Binary Systems.	126
10.	Comparison of $B^*_{CL}(T^*)$'s and $C^*_{CL}(T^*)$'s Calculated Using Kirk's $b^{(j)}$'s and Kihara's $c^{(j)}$'s, Respectively	151
11.	Operating Conditions of Chromatographs	162
12.	Experimental Gas and Liquid Phase Equilibrium Compositions in the Helium-Carbon Tetrafluoride System.	165
13.	Experimental Gas and Liquid Phase Equilibrium Compositions in the Helium-Chlorotrifluoromethane System.	172

LIST OF TABLES (Continued)

Table		Page
14.	Smoothed Experimental and Theoretical Enhancement Factors of Carbon Tetrafluoride in Helium, and the Smoothed Experimental Solubility of Helium in Liquid Carbon Tetrafluoride	182
15.	Smoothed Experimental and Theoretical Enhancement Factors of Chlorotrifluoromethane in Helium, and the Smoothed Experimental Solubility of Helium in Liquid Chlorotrifluoromethane	184
16.	Input Parameters for the Calculation of Third Virial Coefficients Using the Method of Chueh and Prausnitz	189
17.	Intermolecular Potential Parameters and BWR Parameters.	190
18.	Compressibility Factors of Saturated Liquid Estimated Using the Generalized Correlation Given by Chueh and Prausnitz and the Critical Constants.	191
19.	Vapor Pressures of Carbon Tetrafluoride and Chlorotrifluoromethane.	200

LIST OF FIGURES

Figure		Page
1.	Schematic Diagram of Phase Equilibrium Apparatus	10
2.	Experimental Enhancement Factors of Carbon Tetrafluoride in Helium at 106.01, 117.33, 132.18, and 147.10 K. . . .	19
3.	Experimental Enhancement Factors of Carbon Tetrafluoride in Helium at 162.03 and 173.02 K	20
4.	Experimental Enhancement Factors of Carbon Tetrafluoride in Helium along Isobars	21
5.	Experimental Solubility of Helium in Liquid Carbon Tetrafluoride	22
6.	Experimental Enhancement Factors of Chlorotrifluoromethane in Helium at 145.21, 163.01, and 180.02 K.	23
7.	Experimental Enhancement Factors of Chlorotrifluoromethane in Helium at 196.01, 211.06, 221.27, and 231.08 K. . . .	24
8.	Experimental Enhancement Factors of Chlorotrifluoromethane in Helium along Isobars	25
9.	Experimental Solubility of Helium in Liquid Chlorotrifluoromethane	26
10.	Predicted and Experimental B_{12} for the Helium-Carbon Tetrafluoride System at Temperatures between 106 to 173 K	67
11.	Predicted and Experimental B_{12} for the Helium-Carbon Tetrafluoride System at Temperatures between 106 to 773 K	68
12.	Predicted and Experimental B_{12} for the Helium-Chlorotrifluoromethane System. . . .	71

LIST OF FIGURES (Continued)

Figure		Page
13.	Theoretical and Experimental Enhancement Factors in the Helium-Carbon Tetrafluoride System at 106.01 K	81
14.	Theoretical and Experimental Enhancement Factors in the Helium-Carbon Tetrafluoride System at 117.33 K	82
15.	Theoretical and Experimental Enhancement Factors in the Helium-Carbon Tetrafluoride System at 147.10 K	83
16.	Theoretical and Experimental Enhancement Factors in the Helium-Carbon Tetrafluoride System at 173.02 K	84
17.	Theoretical and Experimental Enhancement Factors in the Helium-Chlorotrifluoromethane System at 145.21 K.	85
18.	Theoretical and Experimental Enhancement Factors in the Helium-Chlorotrifluoromethane System at 180.02 K.	86
19.	Theoretical and Experimental Enhancement Factors in the Helium-Chlorotrifluoromethane System at 211.06 K.	87
20.	Theoretical and Experimental Enhancement Factors in the Helium-Chlorotrifluoromethane System at 231.08 K.	88
21.	Experimentally Determined Henry's Law Constants for the Helium-Carbon Tetrafluoride System	105
22.	Experimentally Determined Henry's Law Constants for the Helium-Chlorotrifluoromethane System.	107
23.	Comparison of Theoretical and Experimental H_2^{∞} for the Helium-Carbon Tetrafluoride System.	119
24.	Comparison of Theoretical and Experimental $\overline{V}_2^{\infty}$ for the Helium-Carbon Tetrafluoride System.	120

LIST OF FIGURES (Concluded)

Figure		Page
25.	Comparison of Theoretical and Experimental H_2^{∞} for the Helium-Chlorotrifluoromethane System	121
26.	Comparison of Theoretical and Experimental $\overline{V}_2^{\infty}$ for the Helium-Chlorotrifluoromethane System	122
27.	Experimental Enhancement Factors in the Helium-Propylene System at 200.01 K.	141
28.	Experimental Solubility of Helium in Liquid Propylene at 200.01 K.	142
29.	Comparison of Calculated Curves of the Reduced Third Virial Coefficient by Different Investigators.	152
30.	Calibration Curve of Carbon-Tetrafluoride in Helium.	157
31.	Calibration Curve of Chlorotrifluoromethane in Helium.	159
32.	Calibration Curve of Helium in Carbon Tetrafluoride and Chlorotrifluoromethane.	161
33.	Second Virial Coefficient of Helium.	194
34.	Third Virial Coefficient of Helium	195
35.	Second Virial Coefficient of Carbon Tetrafluoride	197
36.	Third Virial Coefficient of Carbon Tetrafluoride	198
37.	Second Virial Coefficient of Chlorotrifluoromethane	202
38.	Third Virial Coefficient of Chlorotrifluoromethane	203

NOMENCLATURE

$\mathring{A}$ = Angstrom unit, 1×10^{-8} cm.

A_o = empirical parameter in the BWR equation.

a = empirical parameter in the BWR equation and also used as Kihara core radius.

a_i = empirical parameter in the method of Snider and Herrington; see Equation (VI-22).

a_{12} = empirical parameter in the method of Snider and Herrington; see Equation (VI-23).

B = second virial coefficient.

$\overline{B}_i$ = experimental second virial coefficient.

B_{12} = interaction second virial coefficient.

B^*_{CL} = reduced classical second virial coefficient from classical Lennard-Jones (6-12) intermolecular potential function (also written as $B^*_{CL}(T^*)$).

B_K = second virial coefficient calculated from classical Kihara (6-12) intermolecular potential function.

B_o = empirical parameter in the BWR equation.

B^*_o = reduced translational quantum second virial coefficient for an ideal gas.

$\overline{BB}_i$ = see Equation (C-8).

BB_K = see Equation (C-5).

BWR = Benedict-Webb-Rubin equation of state.

B^*_I, B^*_{II} = first and second reduced translational quantum corrections for the second virial coefficient from the Lennard-Jones (6-12) potential function.

b = empirical parameter in the BWR equation.

b_o = volumetric parameter in the Lennard-Jones (6-12) intermolecular potential function, Equation (IV-24).

NOMENCLATURE (Continued)

$b^{(j)}$ = coefficients for series representation of $B^*_{CL}(T^*)$, Equation (IV-26).

$b_s^{(j)}$ = coefficients for series representation of F_s, Equation (IV-31).

C = third virial coefficient.

C^*_{CL} = reduced classical third virial coefficient from Lennard-Jones (6-12) intermolecular potential function (also written as $C^*_{CL}(T^*)$).

C_o = empirical parameter in BWR equation.

ΔC = non-additivity correction to the third virial coefficient, Equation (IV-52).

C^{add} = classical contribution to the third virial coefficient, Equation (IV-51).

c = empirical parameter in BWR equation.

$c^{(j)}$ = coefficient for series representation of $C^*_{CL}(T^*)$, Equation (IV-59).

d = parameter in correlation of Chueh and Prausnitz; see Equation (IV-62).

e = energy parameter in Lennard-Jones (6-12) intermolecular potential function.

exp = raise 2.71828 to the power of the number in parentheses.

e/k = energy parameter in Lennard-Jones (6-12) intermolecular potential function.

F_1, F_2, F_3 = reduced functions for second virial coefficient from Kihara core model (6-12); Equation (IV-30).

f = fugacity and also used in Equation (IV-53).

G^* = see Equation (C-15).

g^o = Gibbs' molar free energy of an ideal gas at 1 atmosphere pressure.

H = Henry's law constant.

NOMENCLATURE (Continued)

H_v = heat of vaporization.

h = Planck's constant = 6.6256×10^{-27} erg-sec; also used as peak height on chromatogram.

I = ionization potential.

i = summation index integer.

j = summation index integer.

KIH = Kihara core model (6-12).

KIHCK12 = Kihara core model (6-12) with correction applied to the geometric mixing rule using K_{12} calculated from Equation (V-5).

KIHEK12 = Kihara core model (6-12) with correction applied to the geometric mixing rule using experimental K_{12}.

$\overline{K}$ = Henry's law constant using consistency method.

K_{12} = constant representing the deviation from the Kihara potential geometric mean of the characteristic energy parameters of components i and j; see Equation (V-4).

k = Boltzmann constant = 1.38054×10^{-16} erg/k molecule.

LJCL = Lennard-Jones classical model.

ℓn = natural (base e) logarithm.

log = common (base 10) logarithm.

M = molecular weight.

M_o = core parameter in Kihara (6-12) core model.

m = mass of molecule, M/N_A.

N = a dummy quantity used to represent various equation of state parameters in writing mixture rules.

N_A = Avogadro's number 6.0238×10^{23} molecules/gm mole.

NOMENCLATURE (Continued)

n = number of gm moles and also used in the generalized correlation given by Chueh and Prausnitz; see Equation (IV-10).

n_i = number of moles of component i.

P = total absolute pressure.

P_{o1} = vapor pressure of condensible component.

R = gas law constant = 82.0560 atm-cc/gm mole K or 0.0820537 atm-liter/gm mole K.

R_i = residue.

r = intermolecular distance between centers of molecules and also used as hard sphere diameter.

S_o = core parameter in Kihara (6-12) core model.

s = summation index integer; also an attenuation factor on chromatograph (see Appendix D).

T = temperature, K (formerly $^{\circ}K$).

T^* = kT/e.

T_c^o = classical critical temperature at high temperature for quantum gases.

T_c = critical temperature.

T_{Ri} = reduced temperature, T/T_c, of component i.

t = temperature, $^{\circ}C$.

U = intermolecular potential energy.

U_o = minimum energy of the Kihara potential function.

U_o/k = energy parameter in Kihara (6-12) model.

V = total volume of gas.

V_c^o = classical critical volume at high temperature for the quantum gases.

V_c = critical molar volume.

NOMENCLATURE (Continued)

V_m = molar volume of gas mixture.

V_o = core parameter in Kihara core model.

V_{o1} = molar volume of component 1 gas at its vapor pressure.

V_1 = molar volume of component 1 gas.

V_2 = molar volume of component 2 gas.

$\overline{V}_i$ partial molar volume of component i.

v_l = molar volume of the compressed liquid phase.

v_{o1} = saturated liquid molar volume of the condensible component.

x = mole fraction in the condensed phase.

y_i = mole fraction of component i in the gas phase.

y_i^o = ideal mole fraction in the gas phase, P_{o1}/P.

W = see Equation (VI-25).

Z = compressibility factor, PV/nRT; also U_o/kT in Kihara core model.

GREEK LETTERS

α = parameter in BWR equation.

β = isothermal compressibility for the pure component

β^s = isothermal compressibility for the pure component at saturation.

Γ = gamma function.

γ = empirical parameter in BWR equation

γ_1' = activity coefficient of component 1 in liquid solutions referred to the pure liquid component at the system temperature and pressure.

Λ^* = translational quantum mechanical parameter.

μ = chemical potential.

NOMENCLATURE (Continued)

μ^o = chemical potential of ideal gas at 1 atmosphere.

μ^* = chemical potential of pure component.

π = pi = 3.14159265.

ρ = distance between molecular cores in the Kihara model.

$\overline{\rho}$ = number density of fluid molecules, N_A/v_l.

ρ_o = shortest distance between molecular cores at minimum potential energy.

ξ = see Equation (VI-20).

σ = length parameter in LJCL (6-12) intermolecular potential.

ω = Pitzer's acentric factor, Equation (IV-12).

$\emptyset$ = enhancement factor.

χ = see Equation (VI-19).

SUBSCRIPTS

1 = condensible component.

01 = gas at its normal vapor pressure (i.e. saturated vapor).

2 = helium.

c = condensible component.

m = gas mixture.

i,j,k = 1, 2, or m.

v = volatile component.

SUPERSCRIPTS

G = gas.

L = liquid

NOMENCLATURE (CONCLUDED)

$'$ = used to distinguish BWR parameters from virial equation parameters; Equation (IV-71).

∞ = refers to infinite dilution.

SUMMARY

The object of this work is to determine the experimental gas-liquid phase equilibria in pressurized, binary systems at low temperatures and compare these values with theoretically predicted data. The systems studied are the helium-carbon tetrafluoride and helium-chlorotrifluoromethane in which the condensed component is below its critical temperature and the gaseous component (helium) is well above its critical temperature.

For the determination of the gas and liquid phase compositions, a single-pass, continuous flow type, equilibrium apparatus previously described by Kirk[68] and Kirk and Ziegler[69] was used together with two gas chromatographs. Later, this same apparatus was also used by Mullins,[90,91] Liu,[77] and Garber[37] for their phase equilibrium studies in binary systems.

The gas and liquid phase equilibrium compositions in the helium-carbon tetrafluoride system were measured at six temperatures, 106.01, 117.33, 132.18, 147.10, 162.03 and 173.02 K and pressures from 20 to 120 atmospheres with an interval of 20 atmospheres. In the helium-chlorotrifluoromethane system, seven isotherms of 145.21, 163.01, 180.02, 196.01, 211.06, 221.27, and 231.08 K were studied in the gas-liquid region. The gas and liquid phase compositions

were determined at six pressure points, 20, 40, 60, 80, 100, and 120 atmospheres along each isotherm. The gas phase analysis in the helium-carbon tetrafluoride system is estimated to be accurate to ±2 mole percent of carbon tetrafluoride and in the helium-chlorotrifluoromethane system to ±3.5 mole percent of chlorotrifluoromethane. The uncertainty of liquid phase measurements in these two systems is estimated to be ±2 mole percent of helium. These uncertainties were determined by considering the uncertainties of the temperature measurement (±0.03 K), the pressure gauge (0.5 percent), and the chromatograph calibration curve.

Since no experimental phase equilibrium data for these systems were available in the literature, no comparison could be made for the experimental phase equilibrium data obtained in this work. The gas phase equilibria for these systems were described in terms of the enhancement factor, $\phi = Py_1/P_{o1}$. An exact thermodynamic expression for the enhancement factor was derived. For the evaluation of this expression, an assumption of ideal solution for liquid phase was made and the virial equation of state truncated after the third virial coefficient and Benedict-Webb-Rubin equation of state were used to describe the gas phase P-V-T properties for the helium-carbon tetrafluoride system. For the helium-chlorotrifluoromethane system, evaluation was restricted to the virial equation of state.

The pure and interaction second virial coefficients

of the virial equation of state were calculated utilizing the Lennard-Jones potential (classical), Kihara core potential, and Kihara core potential with the correction factor, K_{12},[51] for the geometric mixing rule. The Lennard-Jones potential (classical) and the method of Chueh and Prausnitz[18] were used for the prediction of the third virial coefficients. Both the Lorentz and linear averages were considered in this work for the evaluation of $(B_o)_{12}$ in the Benedict-Webb-Rubin equation of state.

The various theoretical models based on what has been described above were tested for the prediction of the enhancement factors. The predicted enhancement factors were compared with those experimentally determined for the helium binary systems of this work. The KIHEK12 model which utilizes the Kihara core potential with the experimentally determined K_{12} and the method of Chueh and Prausnitz[18] for the calculation of second and third virial coefficients, respectively, predicted the best enhancement factors. The Lennard-Jones classical model also predicted the enhancement factors which are in quite satisfactory agreement with the experimental values except at the highest temperatures. Contrary to expectation,[8,37,90] the Benedict-Webb-Rubin equation of state, with $(B_o)_{12}$ based on the Lorentz average, generally gave better results than that based on the linear average.

From the phase equilibrium data obtained here, also

extracted are the interaction second virial coefficients. The same theoretical models as used for the prediction of enhancement factors were also used for the prediction of B_{12} values. These predicted B_{12} values were compared with those experimentally determined. It was found that the discrepancy between the theoretically predicted and experimentally determined B_{12} values was principally responsible for the incorrect enhancement factors predicted from the various theoretical models. These theoretical models all failed to predict the satisfactory B_{12} values for the helium-carbon tetrafluoride system in the temperature range of 303 K to 773 K, where experimental B_{12} values were determined by Kalfoglou and Miller.[59]

Since the B_{12} values predicted from the Kihara core potential differs greatly from the experimental B_{12} values for the systems of this work, the Kihara core potential was used in conjunction with K_{12} to predict B_{12} values. This K_{12} factor is used to correct the geometric mixing rule for the energy parameter and has been employed by recent investigators.[18,19,33,50,51,77,90] The K_{12} value was determined simutaneously with the B_{12} values from the phase equilibrium data obtained in this work. The value of K_{12} thus determined (0.06 for the helium-carbon tetrafluoride system and 0.25 for the helium-chlorotrifluoromethane system) was compared with that calculated using the correlation given by Hiza and Duncan[51] (0.28 and 0.37 for the helium-carbon tetrafluoride

and helium-chlorotrifluoromethane system, respectively). Unlike other helium binary systems,[37,50,126] these two values differ considerably from each other, which resulted in large discrepancy between the B_{12} values predicted from the KIHEK12 model and KIHCK12 model which uses the calculated K_{12} value from the correlation of Hiza and Duncan[51] instead of experimental K_{12} value and also the predicted enhancement factors from these two models.

To determine the Henry's law constant, H_2^∞, and the partial molar volume at infinite dilution, $\overline{V}_2^\infty$, for helium from the experimental phase equilibrium data, the Krichevsky-Kasarnovsky[73] equation was used. This equation is based on the assumptions that the liquid solution is ideal and the change of $\overline{V}_2^\infty$ with pressure is negligible and enables one to evaluate the H_2^∞ and $\overline{V}_2^\infty$ values using the liquid composition and the fugacity of the gas phase. In this work, the fugacity of helium in the gas phase was evaluated using the virial equation of state.

For the theoretical prediction of H_2^∞ and $\overline{V}_2^\infty$ values, the method of Snider and Herrington[125] based on the hard sphere model of fluids has been used. The H_2^∞ and $\overline{V}_2^\infty$ values predicted using this method were compared with the experimental values and the agreement was found to be at most within 55 percent of the experimental values. Although in the application of this method Snider and Herrington[125], and Staveley[127] did not comment on the temperature dependency

of the parameter, a_{12}, which is a measure of background potential, a slight temperature dependency of this parameter has been found in this work.

CHAPTER I

INTRODUCTION

Knowledge of phase equilibria is fundamental to the understanding of separation processes and other chemical engineering operations. During the past ten years, extensive experimental measurements have been made of two phase equilibrium in binary systems. Comparison of these measurements with the results of theoretical calculations has been made possible with the availability of electronic degital computers which made practical the solution of the complicated thermodynamic relations involved in these theoretical calculations.

The purpose of this research has been to obtain the experimental phase equilibrium data and test various theoretical models for the prediction of gas-liquid phase equilibria of pressurized binary systems in which one component, 1, is below its critical temperature and the other component (helium), 2, is well above its critical temperature. Low concentrations of the gas in the condensed phase and activity coefficients near unity are the characteristics of such systems.

The single-pass flow type phase equilibrium apparatus which has been used in this laboratory by Kirk,[68] Mullins,[90]

Liu,[77] and Garber[37] was designed and built by Kirk. This apparatus is suitable for measurements of gas-liquid or gas-solid phase equilibria from liquid nitrogen temperature to room temperatures and at pressures up to 140 atmospheres. A schematic description of this apparatus is presented in the following chapter and detailed descriptions are given by Kirk[68] and Kirk and Ziegler.[69] Several other types of phase equilibrium apparatus such as the static type and the gas-recirculation type have been used by other investigators.

The binary systems which have been studied in this laboratory are the hydrogen-methane system by Kirk,[68] the hydrogen-argon and helium-argon systems by Mullins,[90] the helium-carbon dioxide system by Liu,[77] and the helium-ethylene and helium-propylene systems by Garber.[37] Many other binary systems have been also studied by other investigators and a recent paper by Hiza[50] gives a good summary of these systems.

The enhancement factor, $\phi = Py_1/P_{o1}$, where P is the total pressure of the system, y_1 is the mole fraction of component 1, the condensed component, and P_{o1} is the vapor pressure of component 1 at the system temperature has long been used by many investigators in describing the non-ideality of the gas phase in equilibrium with liquid or solid phase. (This enhancement factor can also be viewed as the ratio of the actual mole fraction y_1 to the ideal mole fraction $y_1^o = P_{o1}/P$ in the gas phase.) Since an exact thermodynamic expression for the enhancement factor is derivable, the

ability of the theoretical models for the prediction of gas phase equilibria can be readily tested simply by calculating the enhancement factors using those theoretical models with an assumption of ideal solution for the condensed phase and comparing these calculated enhancement factors with experimental values.

For a system at equilibrium between phases, thermodynamics requires that the chemical potential of each component in each phase must be equal. On the basis of this criterion, Dokoupil, et al.,[29] Kirk,[68] Kirk and Ziegler,[69] Kirk, et al.,[70] Mullins,[90] Liu,[77] Garber,[37] Smith, et al.,[123] Mackendrick, et al.,[80] Prausnitz, et al.,[99] Prausnitz and Chueh,[98] Chiu and Canfield,[17] Heck,[46] Hisa and Duncan[51] have derived an expression for the enhancement factor. The theoretical evaluation of the enhancement factor requires an equation of state for the pure components as well as for the mixture in the gas phase.

The equations of state to describe the gas phase have been the virial equation of state,[37,68,77,90] Benedict-Webb-Rubin equation of state,[46,68,69,80,90,124] Beattie-Bridgeman equation of state,[68,69,90] Redlich-Kwong equation of state,[97,98] and Martin-Hou equation of state.[16,82] Of these equations of state, all except the virial equation of state which has been most widely used are empirical equations of state. Early in the twentieth century, the virial equation was proposed as an empirical form for representing P-V-T data of a

gas. Later, it was shown that the virial equation for pure gases can be derived from the statistical mechanics,[25,49] which establishes exact relations between the virial coefficients and the intermolecular potential describing the forces between molecules. Thus, the second and third virial coefficients can be adequately described by the two and three body interactions of the intermolecular potential, respectively. The application of this virial equation to the gas mixture was also accomplished by Mayer[84] who presented the expressions for mixture virial coefficients in terms of mole fractions and pure and interaction virial coefficients. Even with this theoretical background, the virial equation of state has some limitations in its applications. The major disadvantage of this equation is that it is useful only for modest densities up to 3/4 of the critical density when virial coefficients after the third are neglected. Although the virial equation of state has a firm theretical basis in statistical mechanics, the interaction second virial coefficients predicted by the Kihara potential using the geometric mixing rule are in large disagreement with experimental values for the ehlium binary systems, necessiating a modification of the usual geometric mixing rule. The Beattie-Bridgeman equation of state is only able to represent the volumetric properties of fluids up to the critical.[113] Thus, Benedict-Webb-Rubin equation of state has been developed in an effort to overcome this limiation of the Beattie-Bridgeman equation. The Benedict-Webb-Rubin equa-

tion of state represents satisfactorily the volumetric properties of nonpolar gases and liquids to densities up to about 1.8 times the critical and was originally applied to pure hydrocarbons and their mixtures. The Martin-Hou equation of state is an empirical extention of van der Waals' equation and has 21 adjustable parameters in a recent version.[81] Containing so many adjustable parameters, this equation is generally superior to other empirical equations in describing the P-V-T data but is limited in its use for the prediction of mixture properties becuase of large number of empirical constants.[134]

In recent years, extensive attempts have been made to solve the problem of the solubility of gases in liquids in a high pressure system. As a result, some useful theoretical expressions and empirical correlations have been developed for the prediction of gas solubilities in liquids. Pierotti[94,95,96] has presented a method which can predict Henry's law constants and partial molar volumes at infinite dilution, using the scaled particle theory of Reiss.[106] Miller and Prausnitz,[88] Preston and Prausnitz,[101] and Snider and Herrington[125] have also presented correlations for Henry's law constants. The method given by Miller and Prausnitz[88] is based on the semi-empirical free volume theory,[102] while the generalized correlation given by Preston and Prausnitz[101] is based on the statistical mechanics of dilute liquid solutions in conjunction with Scott's[112] two-fluid theory and a

reduced empirical equation of state. The method of Snider and Herrington[125] based on hard-sphere model of fluid appears to require the least experimental data for the prediction of Henry's law constants and partial molar volumes at infinite dilution and its predicted values are in satisfactory agreement with experimental values.

In the selection of systems to study, several consideration were made for theoretical as well as practical aspects. The choice of binary system was largely influenced by the fact that there is some evidence that phase equilibrium data of multicomponent systems may be calculable from those of binary systems[20] and that one must necessarily be able to describe the simple binary systems before predicting the phase equilibria for more complicated ternary and multicomponent systems.

The binary systems with helium as a major gas phase component have been investigated not only Mullins,[90] Liu,[77] and Garber[37] in this laboratory, but also by numerous investigators such as Rodewald, et al.,[109] Herring and Barrick,[48] Sinor and Kurata,[119] Heck and Hiza,[47] Iomtev, et al.,[58] Hiza and Duncan,[51] and others.[4,14,27,28,34,38,54,62,63,80,85,91,122]

Therefore, the behavior of helium in its binary mixtures is well established. In addition to this, nonpolarity of helium molecules and their low solubility in the liquid enable one to make appropriate assumptions so that the theoretical or empirical models currently available in predicting

gas and liquid phase equilibria can be applied to the helium binary mixtures. One interesting phenomenon in helium binary systems is that, as pointed out by Hiza and Duncan[51] and Garber,[37] their isobars exhibit a minimum when the enhancement factor is plotted against temperature. This phenomenon seems to be unique to these helium binary systems.[37] Because of these several observations and the fact that the extention of study for phase equilibria to helium-halogen-substituted hydrocarbon systems might be interesting, the systems of helium-halogen substituted methane were decided to study in this work.

Carbon tetrafluoride and chlorotrifluoromethane were chosen as the second components. The main reason was that they can be treated as spherical nonpolar molecules together with helium. Other than this, the relative simplicity of the components from a molecular viewpoint, low toxicity, and the availability of their physical property data for the calculation of phase equilibria were also considered. Especially, the anomalous solvent properties of fluorocompounds which have aroused considerable interest in recent years afford a rather severe test for the theoretical models in predicting phase equilibria.

CHAPTER II

EXPERIMENTAL APPARATUS

Description of Apparatus

The entire phase equilibrium apparatus is shown schematically in Figure 1. This single-pass, flow-type device, used to determine the gas-liquid phase equilibria in this work, has been described in detail by Kirk[68,69] and was used by Kirk,[68] Mullins,[90] Liu[77] and Garber[37] in their phase equilibrium measurements. The apparatus was constructed primarily for the measurements of phase equilibria at temperatures between about 65 K and room temperature and pressures up to 140 atm. The description of the apparatus will be briefly discussed here in terms of its use for the helium-carbon tetrafluoride and helium-chlorotrifluoromethane systems.

Helium from a pressurized cylinder is admitted to the high-pressure panel which is used for the regulation and measurement of pressure in the system by means of a pressure regulating valve (V1) and two Bourdon pressure gauges G1 and G2. The gas flow is then directed into the phase equilibrium cell by controlling the needle valves V7, V8, V9, and V10. The pressure regulating valve (V1) is capable of regulating pressure from 0 to 4500 psi, and the high and low pressure gauges G1 and G2 read from 0 to 3000 psi and 0 to 600 psi, respectively. A gauge protector, set for 570 psi cut-off, is attached to G2 and protects the gauge from excess pressure. The

gauges G1 and G2 have recently been recalibrated by Garber [37] using the vapor pressures of argon and carbon dioxide (see Appendix A). The uncertainties of these gauges are within 0.5 percent of the indicated pressure.

A known amount of liquid component is introduced into the cell by means of a high pressure gas burette and the valves V2, V5, and V6 which are also located on the high pressure panel. A pressure gauge, not shown, is also mounted on the panel to measure the pressure in the high pressure burette.

The phase equilibrium cell whose internal volume and height are 46 cc and 9 inches, respectively, consists of an approximately cylindrical 9.5 pound copper body closed at both ends with threaded monel plugs sealed with soft solder. The cell is surrounded by a larger copper body which serves the function of a cryostat. A liquid nitrogen reservoir which provides the refrigeration for the cell is suspended beneath the copper cryostat. The entire assembly is suspended in an evacuated cylindrical container filled with an evacuated powder insulation containing metal flakes (Linde CS-5). The refrigeration of the cell is provided by transferring liquid nitrogen by means of a small tube from the reservoir to an annular space between the cell and the copper block cryostat surrounding the cell. The pressure inside the reservoir is maintained a little above atmospheric

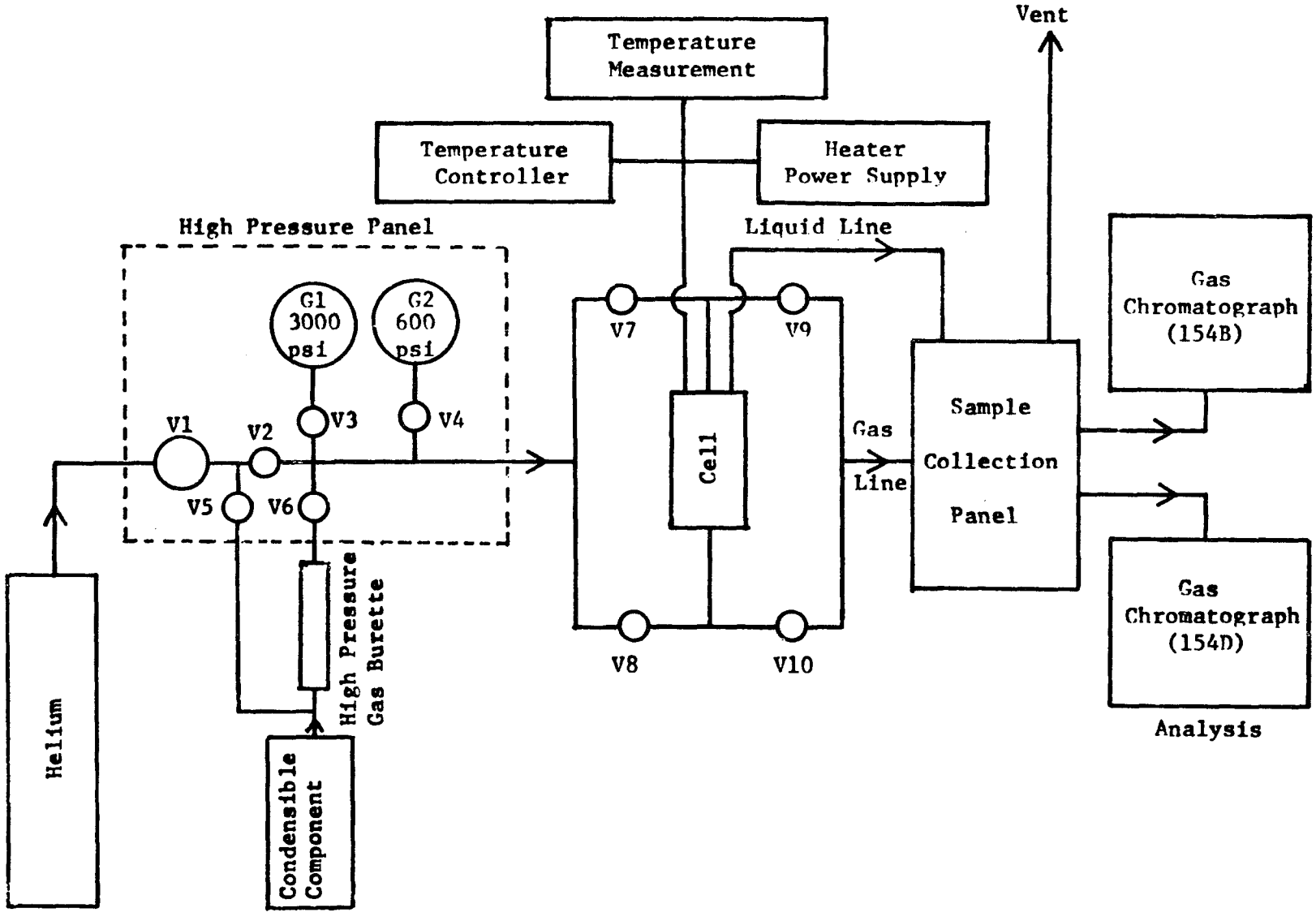

Figure 1. Schematic Diagram of Phase Equilibrium Apparatus

pressure by means of a differential pressure regulator. This facilitates controlling the rate of refrigeration by simply adjusting the throttling valve in the vent line, which increases or decreases the rate of transfer of liquid nitrogen.

Temperature control is established by a balancing a slight excess of refrigeration with heat from a direct current heater wrapped on the copper block. The energy input to this heater is controlled by an automatic temperature controller, which is a photoelectric, proportional device in which the output of a six-junction thermopile is balanced against a reference potentiometer.

The primary thermometer used for temperature measurements of the cell is a capsule-type platinum resistance thermometer manufactured by Leeds and Northrup Company and located in a well in the upper shoulder of the cell. This thermometer has been calibrated by the National Bureau of Standards on the International Practical Temperature Scale of 1948 (IPTS-48) above 90.18 K with an assigned ice point of 273.15 K. All temperatures reported in this work are on the (IPTS-68) as described in Appendix A. A number of difference thermocouples and thermopiles made of copper and constantan are mounted on the equilibrium cell and copper block to measure the temperature gradients along the cell and to monitor the temperature of the cell.

The liquid sample is collected on the sample collection panel which provides a mercury-filled glass burette to

hold the vaporized liquid sample until the sample is analyzed. A Perkin-Elmer vapor fractometer 154B is used for the analysis of the liquid sample. The gas flows continuously from the cell to the gas sample collecting copper burette and the flow rate of the exit gas can be measured with a wet-test meter. A gas sample from the equilibrium cell can be collected at any time and analyzed on a Perkin-Elmer vapor fractometer 154D. The calibration of these two gas chromatographs to determine the composition of the minor component of a sample is based on peak heights. The details of the choice of columns and the operating conditions for chromatographs and the calibration are described in Appendix E.

Experimental Procedure

A good vacuum between the copper block cryostat and the insulation powder-filled container is necessary for the stable temperature control of the cell. At first, this space is evacuated with a mechanical pump, while at the same time flushing out the equilibrium cell with helium gas to remove all impurities in it. An acceptable vacuum of about 0.1 torr at the top and about 50 microns at the bottom of the insulation container could be always established at the room temperature. The cryostat is then cooled down with refrigerant. The reservoir is filled with approximately two liters of liquid nitrogen with the differential pressure

regulator open. After filling the reservoir, the differential pressure regulator and the filling line at the top of the insulation container are closed. With the throttle valve wide open about six hours are required to cool down the cryostat from the room temperature to around 100 K and uses up about three liters of liquid nitrogen. A slight overpressure in the liquid nitrogen reservoir caused by the differential pressure regulator injects the liquid nitrogen via the capillary tube into the space between the cell and the copper block. This cools down the block and the cell. With the cryostat cooled a vacuum of 0.05 torr at the top and 30 microns at the bottom of the insulation container is usually obtained. To maintain the temperature of the cell constant after the desired temperature has been reached, the rate of refrigeration and the rate of heating are adjusted so as to provide a slight cooling. The cooling down below the desired temperature causes the heat input to be increased through the automatic temperature controller. In this way, the temperature of the cell could be always controlled within ±0.02 K at any point throughout this work. Two liters of liquid nitrogen provide sufficient refrigeration for about 20 hours of operation.

After establishing the temperature of the cell, the pressure of the system is set using the pressure regulating valve (V1). The resulting gas flow rate is measured with the valves V8 and V9 open and V7 and V10 closed using the

wet-test meter and set at approximately 100 cc/hr (at cell T and P) by adjusting the flow rate regulating needle valve V11 on the high pressure panel. The next step is to introduce the liquid component into the cell. A known amount of the liquid component is first isolated in the high pressure gas burette with the valves V5 and V6 closed and then slowly flushed into the cell and condensed there with the valve V2 closed and V5 and V6 open. About 10-12 cc of the liquid volume is initially introduced into the cell. This quantity brings the liquid level in the cell slightly above the constriction in the middle of the cell and allows about 4-6 cc of liquid above the end of the liquid sample line which extends downwards through the upper monel plug to a point slightly below the middle of the cell. Too much liquid in this cell may cause undesirable entrainment. These 4-6 cc of liquid are sufficient for the analyses of the gas and liquid phases after allowing for some evaporation of the liquid in the cell. (A liquid level indicator is located on the liquid capillary line and was out of order at the time of this work.) After charging the cell with liquid and establishing the desired temperature and pressure in the system, gas samples are continuously collected and analyzed with the 154D chromatograph until the peak heights of three consecutive samples differ no more than two percent. The liquid sample is then withdrawn through the liquid sample line and collected on the sample collecting panel. Two or three

aliquot analyses are made using the 154B chromatograph. During this period of analysis, the temperature of the platinum resistance thermometer, the pressure inside the cell, and the temperature gradients along the cell are continuously measured.

After the measurement of each point on an isotherm, it was necessary to locate the liquid level since addition of too much liquid may cause entrainment. This is done by continuously withdrawing liquid samples and analyzing them; a sudden change of helium concentration indicates that the liquid level is just below the end of the liquid sample line. For the next measurement, approximately 4 to 6 cc of the liquid component is again added into the cell using the high pressure gas burette and the pressure is adjusted to the next desired point. Analysis of gas and liquid samples for each point on an isotherm takes about one and one-half to two and one-half hours.

Throughout this work, the temperature gradients along the cell during phase equilibrium measurements were always less than 0.03 K. Considering these temperature gradients and the cell temperature fluctuation, the uncertainty of temperature measurements was estimated to be ±0.03 K.

In the analysis of helium in the liquid, an additional column of silica gel installed outside the 154B chromatograph in series with the molecular sieve column was used to retain the second component long enough so that after

analysis of helium it can be vented directly from the silica gel column to the atomosphere. This modification of the equipment is described in detail in Appendix E.

CHAPTER III

EXPERIMENTAL RESULTS AND DISCUSSION

Introduction

In this investigation the equilibrium gas and liquid phase compositions of two binary systems, helium-carbon tetrafluoride and helium-chlorotrifluoromethane were measured. Since no experimental phase equilibrium data were available for these systems in the literature, no comparison could be made. However, the results are discussed in relation to those of similar binary systems.

Six isotherms for the helium-carbon tetrafluoride system and seven isotherms for the helium-chlorotrifluoromethane system were studied from 20 to 120 atm with an interval of 20 atm. The results are presented in Figures 2 through 9. Since the gas phase compositions at 20 atmospheres at the highest temperatures in these measurements were beyond the composition range of the chromatograph calibration curve (see Appendix E), those compositions were not measured.

The gas phase compositions are expressed in terms of enhancement factor which is the ratio of the actual composition to the ideal composition of the gas phase. The detailed experimental data and their smoothed values are given numerically in Appendices F and G, respectively.

Experimental Results

Six isotherms of 106.01, 117.33, 132.18, 147.10, 162.03, and 173.02 K in the gas-liquid region were studied for the helium-carbon tetrafluoride system and those for the gas phase are shown in Figures 2 and 3 with enhancement factor on the ordinate and total pressure on the abscissa. The points in the figures represent the average values of two or more samples for given pressures. The curves are smoothly drawn by eye through the experimental points so that the curves intersect the abscissa at the values of pressure equal to the vapor pressures of carbon tetrafluoride at given temperatures. From these smoothed curves also drawn are ±2 percent error bars inherent of the enhancement factors. In Figure 4, the smoothed enhancement factors obtained from Figures 2 and 3 are plotted against 1000/T for a given pressure and the resulting isobars show an interesting phenomenon which is discussed in later part of this chapter. These isobars correspond to the pressures 20, 40, 60, 80, 100 and 120 atm. The 20 atm isobar is smoothly extended by a dotted line so as to join the abscissa at the temperature at which the vapor pressure of carbon tetrafluoride is 20 atm. The experimental solubilities of helium in liquid carbon tetrafluoride are presented in Figure 5 together with ±2 percent error bar. The smoothed experimental data given in Appendix G were read from the smoothed

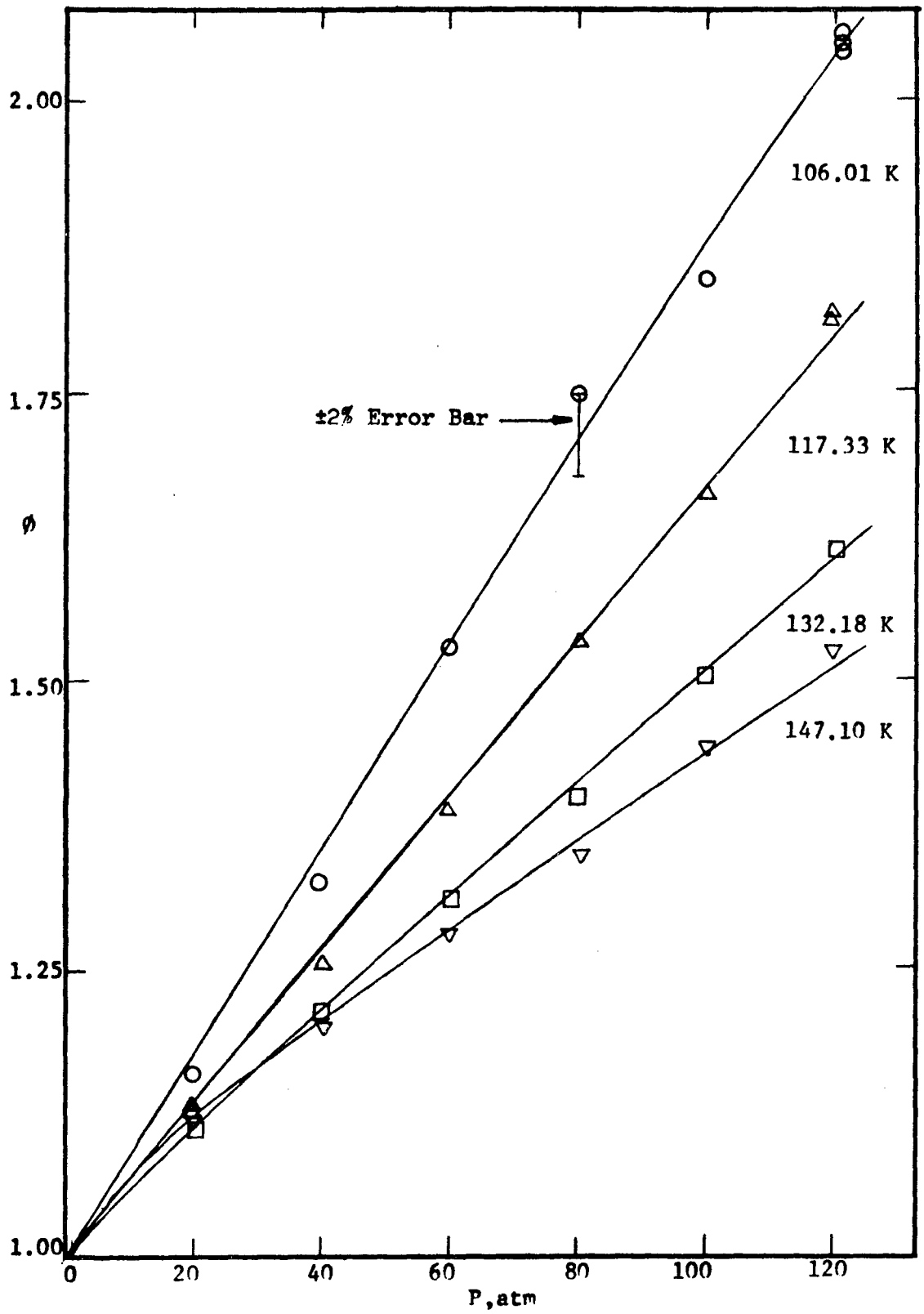

Figure 2. Experimental Enhancement Factors of Carbon Tetrafluoride in Helium at 106.01, 117.33, 132.18, and 147.10 K.

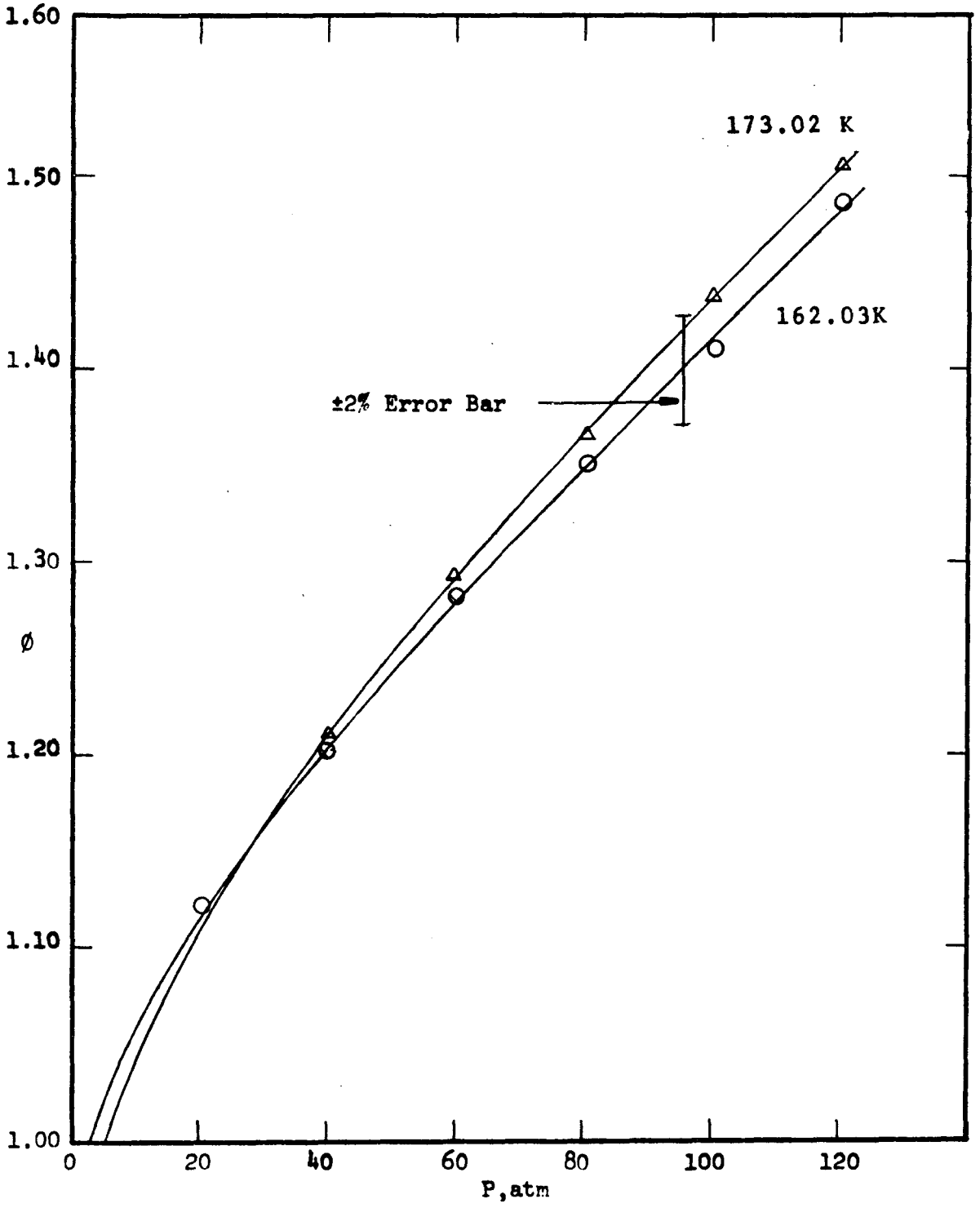

Figure 3. Experimental Enhancement Factors of Carbon Tetrafluoride in Helium at 162.03 and 173.02 K.

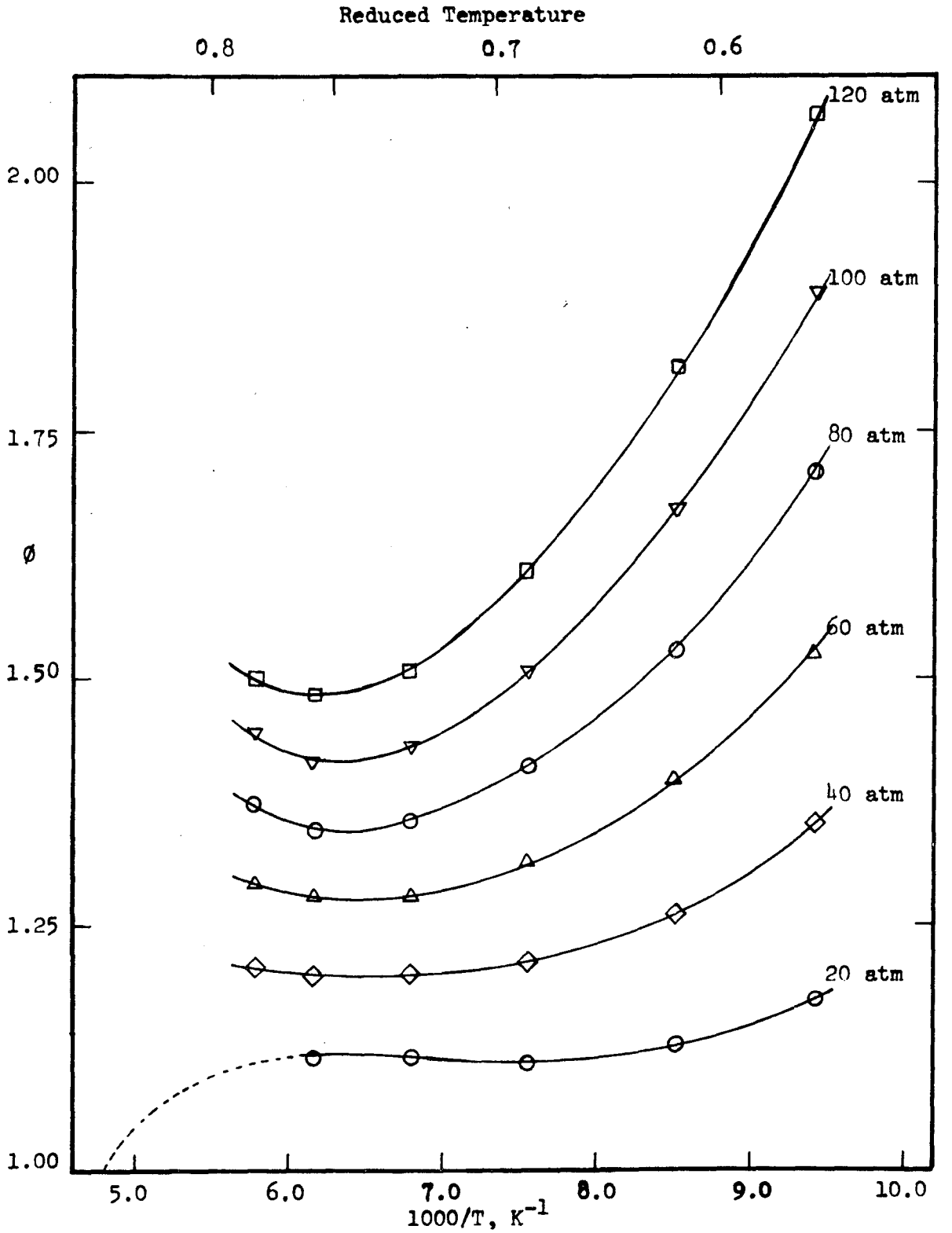

Figure 4. Experimental Enhancement Factors of Carbon Tetrafluoride in Helium along Isobars.

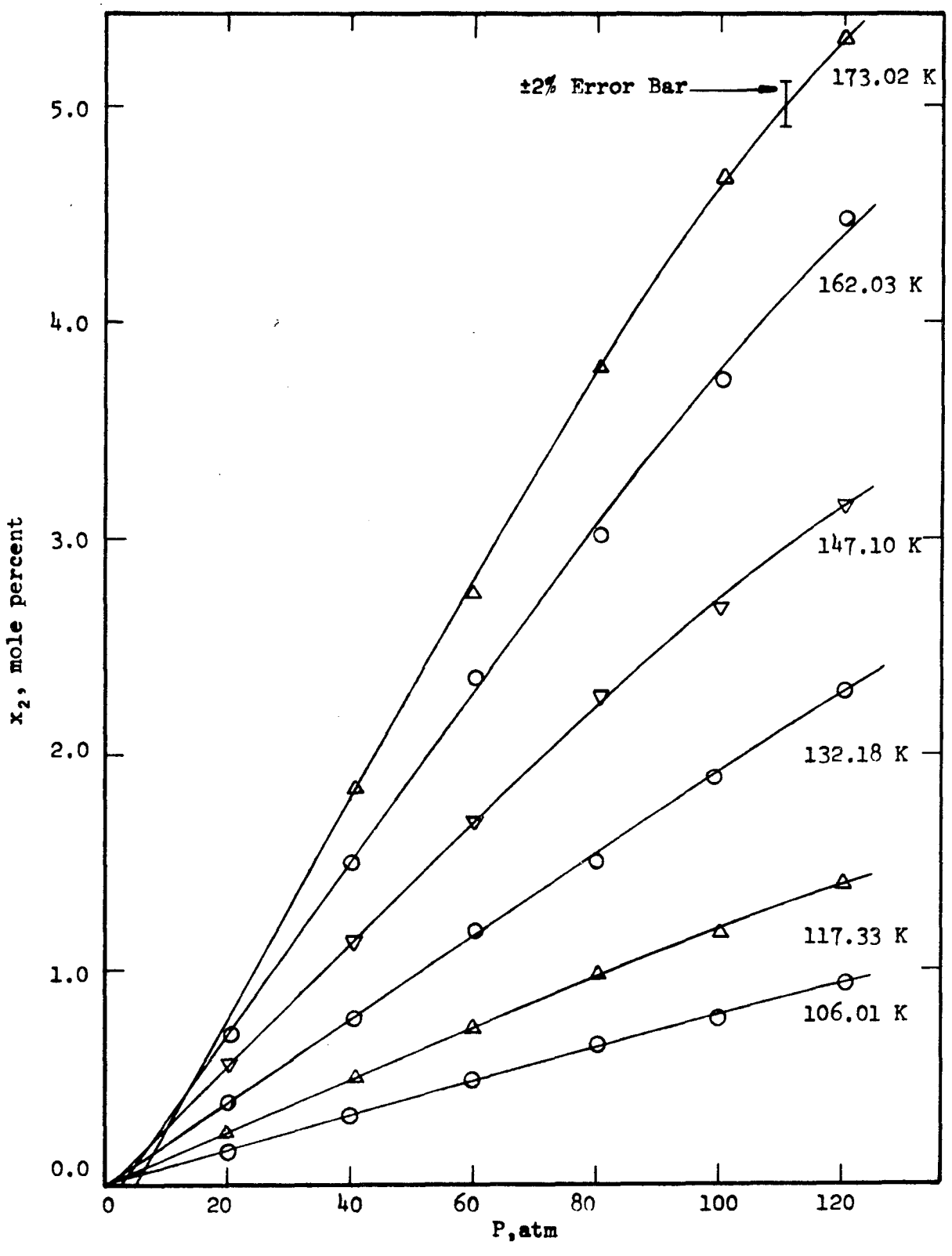

Figure 5. Experimental Solubility of Helium in Liquid Carbon Tetrafluoride.

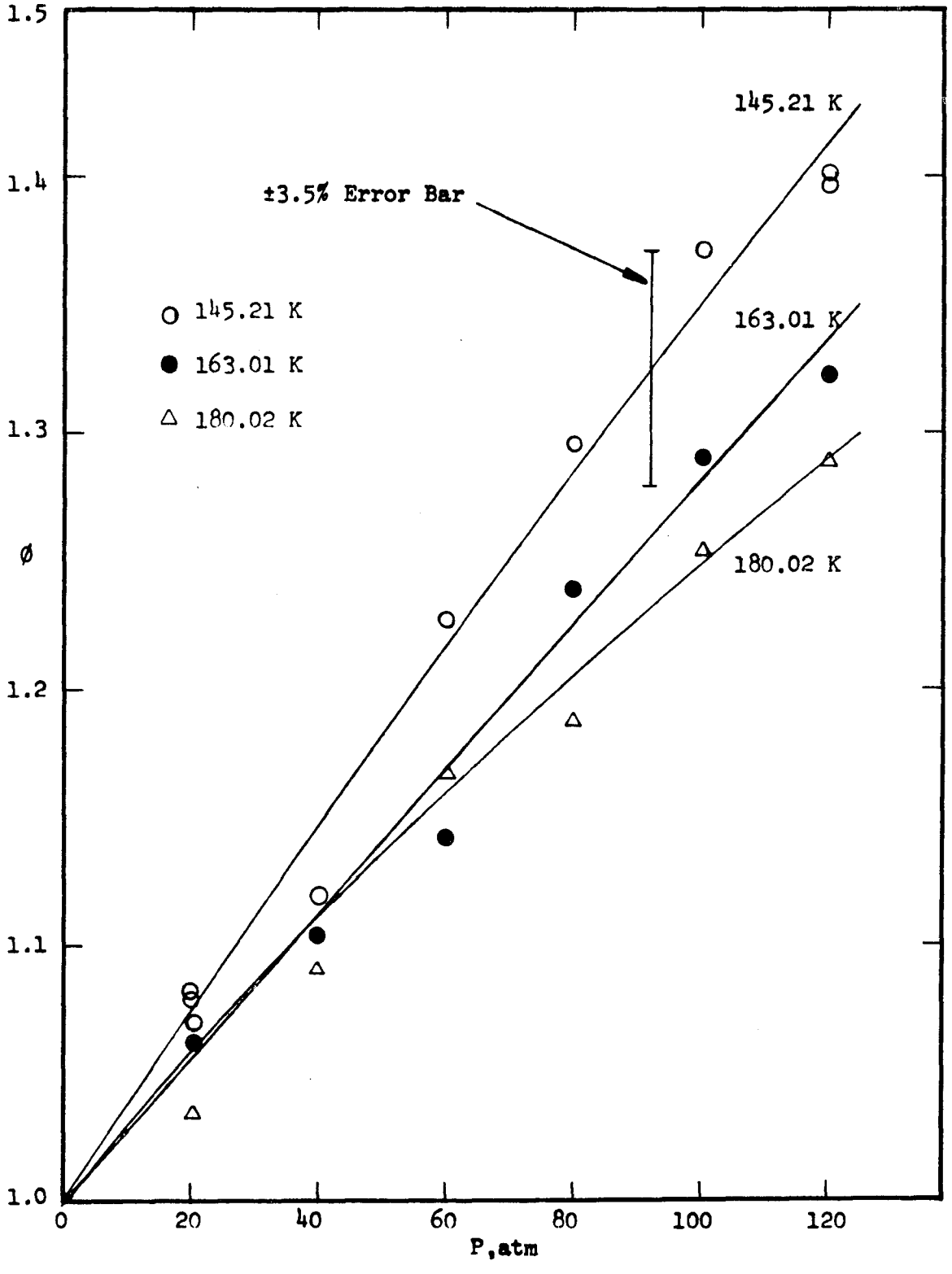

Figure 6. Experimental Enhancement Factors of Chlorotrifluoromethane in Helium at 145.21, 163.01, and 180.02 K.

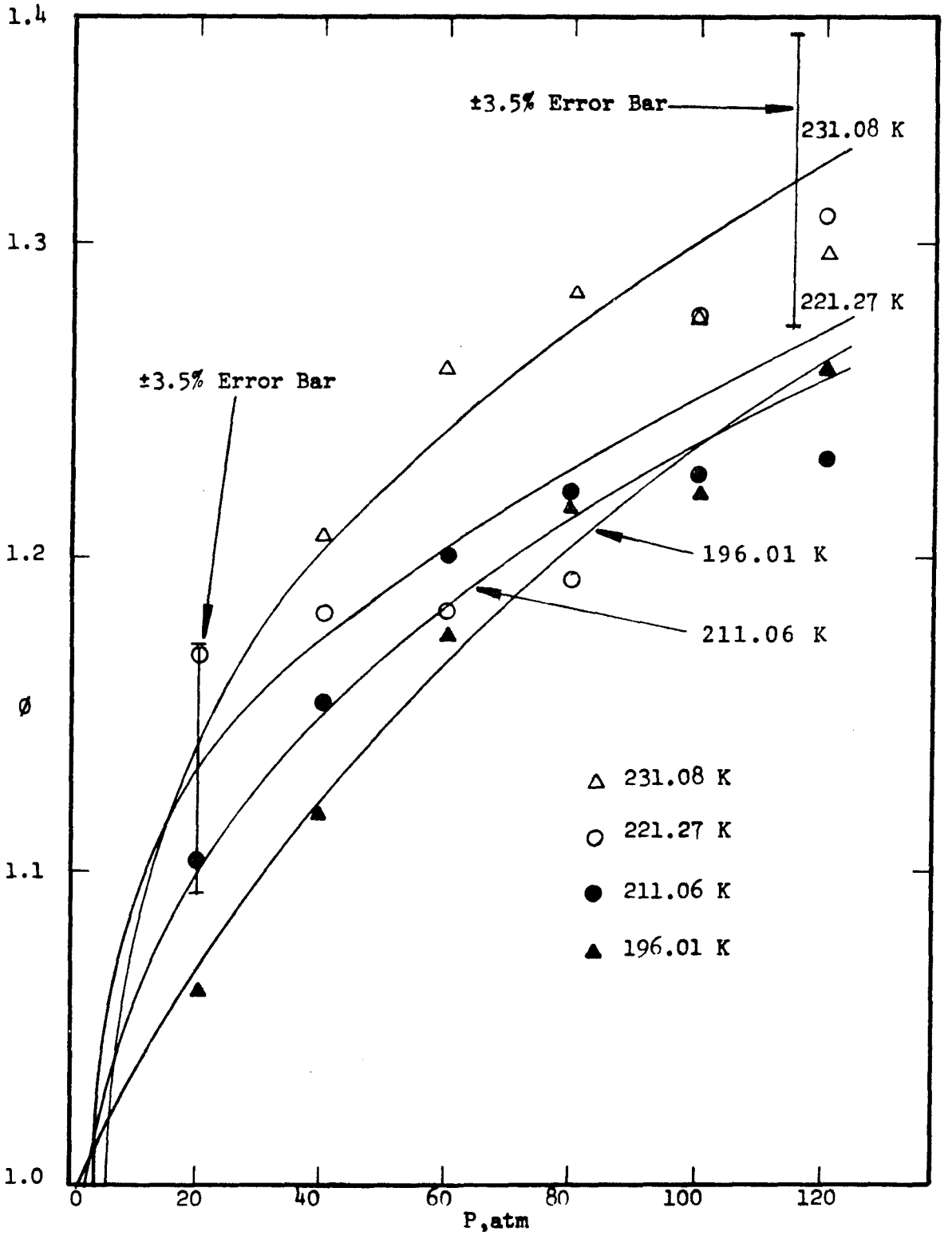

Figure 7. Experimental Enhancement Factors of Chlorotrifluoromethane in Helium at 196.01, 211.06, 221.27 and 231.08 K.

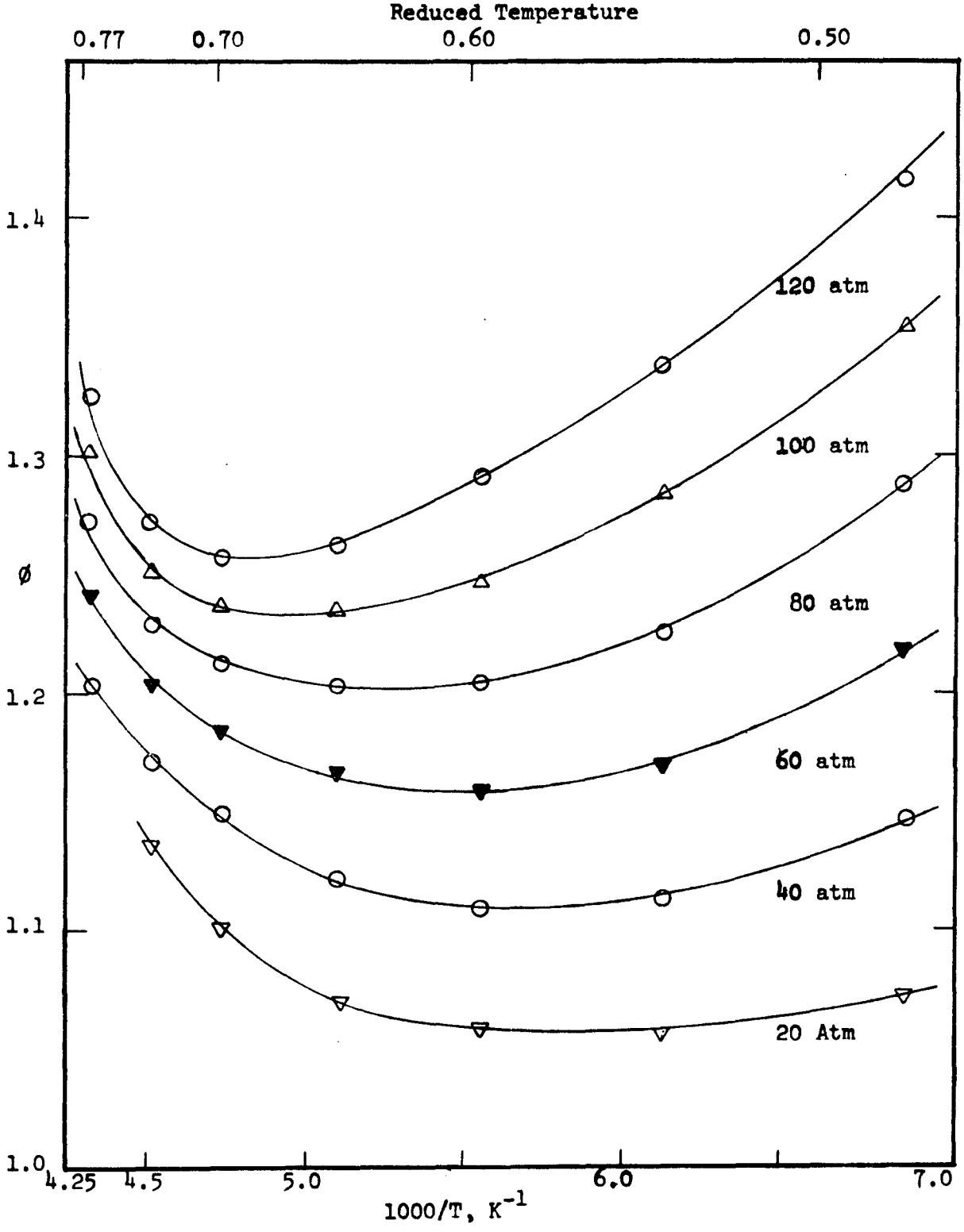

Figure 8. Experimental Enhancement Factors of Chlorotrifluoromethane in Helium along Isobars.

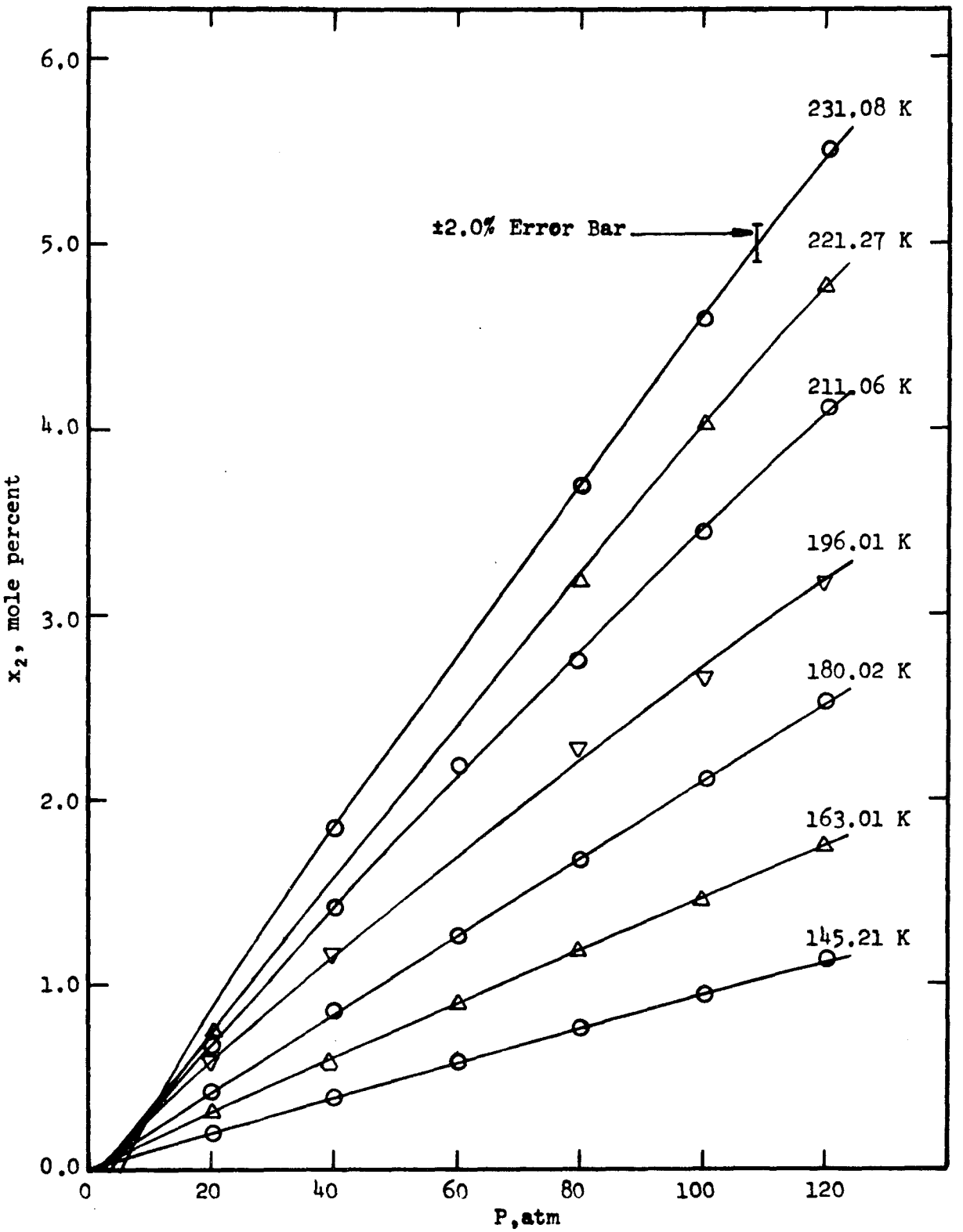

Figure 9. Experimental Solubility of Helium in Liquid Chlorotrifluoromethane.

curves in Figures 2, 3, and 5.

The seven isotherms in the gas-liquid region for the helium-chlorotrifluoromethane system are shown as a plot of enhancement factor vs temperature with ±3.5 percent error bar: three isotherms at 145.21, 163.01, and 180.02 K in Figure 6 and four isotherms at 196.01, 211.06, 221.27, and 231.08 K in Figure 7. The enhancement factors for this system are also plotted against 1000/T along six isobars - 20, 40, 60, 80, 100 and 120 atm - and presented in Figure 8. The liquid compositions along seven isotherms are shown as a function of pressure in Figure 9. The smoothed experimental equilibrium data for the helium-chlorotrifluoromethane system given in Appendix G were read from the smoothed curves in Figures 6, 7, and 9.

Discussion of Results

In most helium binary systems with light hydrocarbons,[37,38,46,47,51,54,63,111,122] the enhancement factors have been shown to be usually between one and two in the gas-liquid region at pressures up to 120 atm, and those in the helium-saturated hydrocarbon systems are greater than those in the corresponding unsaturated hydrocarbon systems,[37,51] at the same pressures and reduced temperatures. Liu[77] has also shown that the enhancement factors in the helium-carbon dioxide system are smaller than those in other binary systems such as helium-argon,[90] -oxygen,[48] -nitrogen,[27,109] and

-methane[47,54,122] systems; the maximum enhancement factors at pressures up to 120 atm in the gas-liquid region in the latter systems are not much greater than two. In other words, the helium binary systems involving nonpolar spherical molecules generally give greater enhancement factors than those with less spherical molecules. These interesting facts are also true in the systems studied in this work. As shown in Figures 2, 3, 5, and 6, the enhancement factors are between one and two, and those in helium-carbon tetrafluoride system are greater than those in helium-chlorotrifluoromethane system at the same pressures and reduced temperatures, with carbon tetrafluoride being more spherical than chlorotrifluoromethane. Thus, the behavior of these helium-halogen-substituted methane systems is not much different from other helium binary systems. In this work the approximate ranges of the gase phase equilibrium compositions were found to be between 0.03 to 15.1 mole percent carbon tetrafluoride in helium-carbon tetrafluoride system and between 0.04 to 16.6 mole percent chlorotrifluoromethane in helium-chlorotrifluoromethane system (see Appendix F).

Figures 2 and 3 show the general trend of the enhancement factor isotherms in the helium-carbon tetrafluoride system. As the temperature increases, the enhancement factors at the constant pressure decrease and then after passing the minimum point at around the normal boiling point of

carbon tetrafluoride, 145.12 K,[16] the enhancement factors begin to increase with increasing temperature. This phenomenon was first noted by Hiza and Duncan[51] in their study of the helium-ethane system. Figure 4 clearly shows these minimum points on the isobar curves and their shift to the higher temperatures as the pressure increases. These interesting phenomena have been found in several other helium binary systems such as helium-methane,[47] -ethylene,[37] and -propane.[111] The lowest isobar curve in Figure 4, is extended with dotted line such that after passing a maximum point it crosses the abscissa at the temperature at which the vapor pressure of carbon tetrafluoride is 20 atm. Since the enhancement factor should be one when the total pressure is equal to the vapor pressure of the liquid and the critical pressure of carbon tetrafluoride is 36.96 atm,[17] the 20 atm isobar curve in Figure 4 is natually expected to have a maximum point before it joins the abscissa.

The enhancement factor isotherms for the helium-chlorotrifluoromethane system are presented in Figures 6 and 7, and the trends of these isotherms are somewhat similar to those of the helium-carbon tetrafluoride system. The enhancement factors in Figure 6 decrease with increasing temperature and those in Figure 7 show the reverse trend. A plot of enhancementfactor versus 1000/T at even pressures for the helium-chlorotrifluoromethane system is shown in Figure 8. The minimum points on the isobars are located

near the normal boiling point of chlorotrifluoromethane, 191.75 K,[1] and these minimum points move to the higher temperature as the pressure increases. Although it is not shown in Figure 8, a maximum point on the 20 atm isobar is also expected to lie somewhere between the minimum point on the curve and its intersection with the abscissa on the same grounds that have been described for the helium-carbon tetrafluoride system.

The solubilities of helium in carbon tetrafluoride and in chlorotrifluoromethane are similar to each other and greater than other helium binary systems[37,122] for the same pressure and reduced temperature. The liquid compositions in the helium-carbon tetrafluoride and the helium-chlorotrifluoromethane systems range from 0.165 to 5.37 and from 0.197 to 5.46 mole percent of the condensible component, respectively, as shown in Figures 5 and 9. These systems also show the reverse solubility effect exhibited by other helium binary systems,[37,122] that is, the solubility of helium increases with increasing temperature for a given pressure. The solubility curves in both systems bend downward with increasing pressure as can be seen in Figures 5 and 9 which indicates that the behavior of these systems deviates negatively from Henry's law. In Figure 9, several high temperature isotherms have less than six experimental points as the liquid samples were lost during the gas phase analysis due to the high evaporation rate of liquid at those

temperatures. The liquid samples lost were all rerun in the helium-carbon tetrafluoride system. The highest isotherm in Figure 5 has five experimental points and all others have six.

The experimental error in the gas phase analysis for the helium-carbon tetrafluoride system was estimated to be ±2 percent of the stated analysis and for the helium-chlorotrifluoromethane system ±3.5 percent, and in the liquid phase analysis for both systems ±2 percent. The corresponding error ranges are shown as a bar on the smoothed curves in Figures 2, 3, 5, 6, 7, and 9. These uncertainties were determined from the scatter in the chromatograph calibration curves (see Appendix E), the pressure gauge uncertainty of ±0.5 percent, and the temperature uncertainty of ±0.03 K. The scatter of points along an experimental isotherm is within the corresponding uncertainty as expected.

Kirk,[68] Mullins,[90] Liu,[77] and Garber[37] have all proved that a flow rate of 100 cc/hr at the cell temperature and pressure was adequate for establishing the gas-liquid phase equilibrium in the single-pass flow type apparatus used in this work. In this kind of phase equilibrium apparatus, non-equilibrium steady state can occur if the flow rate through the equilibrium cell is too fast. To see if this same flow rate is proper for the systems studied here, the flow rate was varied at several points. In the helium-

carbon tetrafluoride system, five points at 20 and 120 atm on the two lowest isotherms were reproduced as shown in Figure 2: three of them with a flow rate of 150-200 cc/hr and the others with that of 50 cc/hr at the cell temperature and pressure. In addition to these, one more point at 20 atm on the 117.33 K isotherm was rerun after reducing the temperature from 132.18 K to see if there is any difference in the liquid phase compositions, since the usual procedure followed in this work was to start from the lowest temperature and work to the higher temperature. This additional point is shown in Figure 5. These results are in good agreement with the earlier measurements within the experimental error and thus verified that a flow rate near 100 cc/hr was satisfactory for the helium-carbon tetrafluoride system. (Very recently Shiau[117] has reproduced the 147.10 K isotherm in the helium-carbon tetrafluoride system and his experimental results are in excellent agreement with those of this work.)

In the helium-chlorotrifluoromethane system, four points at 20 and 120 atm on the two lowest isotherms were rerun: two of them at twice the normal flow rate and the others at half of it. Their agreement with the earlier measurements was again satisfactory. The flow rate of 100 cc/hr at the cell temperature and pressure is thus verified to be adequate for the helium-chlorotrifluoromethane system also and was used in all the runs in this work.

CHAPTER IV

CALCULATION OF ENHANCEMENT FACTORS

Introduction

A more sensitive parameter than the mole fraction in describing the non-ideality of gas phase in equilibrium with a condensed phase is the enhancement factor, which is defined as

$$\phi = \frac{Py_1}{P_{01}} \qquad \text{(IV-1)}$$

To predict the enhancement factor, that is, to calculate ϕ without the experimental value of y_1 in Equation (IV-1), an exact thermodynamic expression for the enhancement factor is necessary.

For the equilibrium between phases in a multicomponent system, the chemical potential of each component in every phase must be equal, that is,

$$\mu_i^L = \mu_i^G = \mu_i^S \qquad i = 1, 2 \cdots\cdots \qquad \text{(IV-2)}$$

For the condensible component 1 in the gas-liquid equilibrium at the temperature T and pressure P in a binary system, the following relation holds:

$$\mu_1^L(P,T,x_1) = \mu_1^G(P,T,y_1) \qquad \text{(IV-3)}$$

The chemical potential of the liquid mixture can be expressed in terms of that for the pure liquid under the same temperature and pressure as follows:

$$\mu_1^L(P,T,x_1) = \mu_1^{*L}(P,T) + RT \ln (\gamma_1' x_1) \qquad \text{(IV-4)}$$

$$\gamma_1' \to 1, \text{ as } x_1 \to 1$$

where

$$\mu_1^{*L}(P,T) = \mu_1^{*L}(P_{o1},T) + \int_{P_{o1}}^{P} v_1 dP \qquad \text{(IV-5)}$$

The chemical potential of the pure liquid under its saturation pressure P_{o1} must be the same as that of the pure gas at P_{o1}.

$$\mu_1^{*L}(P_{o1},T) = \mu_1^{*G}(P_{o1},T) = \int_{V_{o1}}^{\infty} \left[\left(\frac{\partial P_1}{\partial n_1}\right)_{V_1,T} - \frac{RT}{V_1}\right] dV_1 \qquad \text{(IV-6)}$$

$$- RT \ln \frac{V_{o1}}{RT} + g_1^o$$

where g_1^o is the Gibbs free energy of one mole of component 1 in the ideal gas state at the temperature T and one atmosphere pressure.

For the chemical potential of component 1 in a binary

gas phase, the following equation holds:

$$\mu_1^G(P,T,y_1) = \int_{V_m}^{\infty} \left[\left(\frac{\partial P}{\partial n_1}\right)_{V_m,T,n_2} - \frac{RT}{V_m}\right] dV_m - RT \ln \frac{V_m}{RT} \quad \text{(IV-7)}$$

$$+ RT \ln y_1 + g_1^o$$

By combining Equations (IV-3), (IV-4), (IV-5), (IV-6), and (IV-7) and adding RT ln (P/P_{o1}) to both sides of Equation (IV-3), the final expression for the enhancement factor is obtained.

$$\ln \phi = \ln \frac{Py_1}{P_{o1}} = \ln \frac{PV_m}{P_{o1}V_{o1}} + \frac{1}{RT}\int_{P_{o1}}^{P} v_1 dP \quad \text{(IV-8)}$$

$$+ \frac{1}{RT}\int_{V_{o1}}^{\infty} \left[\left(\frac{\partial P_1}{\partial n_1}\right)_{V_1,T} - \frac{RT}{V_1}\right] dV_1 - \frac{1}{RT}\int_{V_m}^{\infty} \left[\left(\frac{\partial P}{\partial n_1}\right)_{V_m,T,n_2}$$

$$- \frac{RT}{V_m}\right] dV_m + \ln (\gamma_1' x_1)$$

An expression for the enhancement factor similar to Equation (IV-8) has been reported by a number of authors;[6, 29,37,46,68,90] in some cases the condensed phase is assumed to be pure, the term ln $(\gamma_1' x_1)$ being dropped out. To evaluate the enhancement factor using Equation (IV-8), the following information is required:

1. Composition of liquid phase.
2. Experimental data or an assumption about γ_1'.
3. Molar volume of pure liquid component as a function of temperature and pressure.
4. Equation of state for the gas phase of pure component 1 and for the gas mixture.

The composition of liquid phase has been experimentally determined for the helium-carbon tetrafluoride and helium-chlorotrifluoromethane systems in this work and found to be always less than 5.5 mole percent. Due to this low concentration of helium in the liquid phase, the solutions investigated here are assumed to be ideal, that is, the activity coefficient γ_1' is one. This assumption is based on the work of Mullins[90] in which the activity coefficient of argon in the helium-argon system is computed along three-phase line, where the composition of helium in condensed phase is negligible, and shown to be one.

Since no data are available for the molar volumes of liquid carbon tetrafluoride and chlorotrifluoromethane as a function of pressure except the saturated molar volumes at given temperatures, a generalized correlation for the compressibilities of normal liquids given by Chueh and Prausnitz[21] has been used for these liquids to estimate the liquid molar volumes as a function of pressure. This correlation uses the compressibility of liquids at saturation. The compressibility β is defined by

$$\beta = -\frac{1}{v_1}\left(\frac{\partial v_1}{\partial P}\right)_T \qquad \text{(IV-9)}$$

For a given liquid, β is a function of both temperature and pressure. Chueh and Prausnitz[21] have shown that, after rearranging their original equation, the molar volume of liquid can be expressed as:

$$v_1 = v_{o1}[1 + n\beta^s(P - P_{o1})]^{-\frac{1}{n}} \qquad \text{(IV-10)}$$

This equation holds for the interval $0.4 \leq T_{R1} \leq 0.98$, which fully covers the temperature range of this work. The compressibility of saturated liquid, β^s, is given by them as follows:

$$\beta^s = \frac{V_{c1}}{RT_{c1}}(1.0 - 0.89\omega^{\frac{1}{2}})\,[\exp(6.9547 - 76.2853T_{R_1} \qquad \text{(IV-11)}$$

$$+ 191.3060T_{R1}^2 - 203.5472T_{R1}^3 + 82.7361T_{R1}^4)]$$

ω in Equation (IV-11) is Pitzer's acentric factor and given by

$$\omega = -\log P_{R1} - 1.0 \qquad \text{(IV-12)}$$

where P_{R_1} is the reduced vapor pressure of the component 1 evaluated at a reduced temperature of 0.7. The value of n

in Equation (IV-10) has been suggested as 9 for normal liquids by Chueh and Prausnitz[21] and this value of n has been used in this work. The calculated values of β^s for carbon tetrafluoride and chlorotrifluoromethane are presented in Table 18 of Appendix H. Using Equation (IV-10), the first integral in Equation (IV-8) is evaluated as:

$$\frac{1}{RT}\int_{P_{o1}}^{P} v_1 dP = \frac{V_{o1}}{8\beta^s RT}\left[\{1 + 9\beta^s(P - P_{o1})\}^{\frac{8}{9}} - 1\right] \quad \text{(IV-13)}$$

The evaluation of the second and third integrals in Equation (IV-8) can be accomplished using a equation of state for the gas phase for both the pure component 1 and the gas mixture. The correct evaluation of these integrals is one of the primary objectives of this work.

Equations of State Considered

From the time of Boyle, some 300 years ago, one has attempted to describe the volumetric behavior of gases using an equation of state. But no one equation of state has been found yet which satisfactorily describes the volumetric properties of all fluids. A number of equations of state have been therefore developed; some are theoretical, some are empirical, and some are combined forms of the first two types. A good summary of equations of state has been recently given by Tsonopoulos and Prausnitz.[134]

The most commonly used equations of state for engineering applications are the virial equation, the Benedict-Webb-Rubin

equation,[7,8,9] the Beattie-Bridgeman equation,[5] the Stockbridge equation,[128] the Martin-Hou equation[82] and the Redlich-Kwong equation.[103] Of these, the virial equation of state and the Benedict-Webb-Rubin equation of state have been chosen and used in this work. The details of these two equations of state and their applications to the systems of this work are given in the following sections following closely the description of Garber.[37]

Virial Equation of State

The virial equation of state was first proposed as an empirical form for representing P-V-T data of gas by Kamerlingh Onnes early in twentieth century. Later, it was shown that this virial equation of state can be derived from the statistical mechanics.[25,49] This virial equation of state is used here in a form truncated after the third virial coefficient.

$$\frac{PV}{nRT} = 1 + \frac{nB}{V} + \frac{n^2C}{V^2} \qquad \text{(IV-14)}$$

The second and third virial coefficients, B and C in Equation (IV-14) are a function of temperature. When these virial coefficients are applied to a binary gas mixture, they can be given as Equations (IV-15) and (IV-16).

$$B_m = y_1^2 B_{11} + 2y_1 y_2 B_{12} + y_2^2 B_{22} \qquad \text{(IV-15)}$$

$$C_m = y_1^3 C_{111} + 3y_1^2 y_2 C_{112} + 3y_1 y_2^2 C_{122} + y_2^3 C_{222} \qquad \text{(IV-16)}$$

Applying Equation (IV-14) to the second integral of Equation (IV-8), following expressions are obtained.

$$\left(\frac{\partial P}{\partial n}\right)_{V,T} = RT\left(\frac{1}{V} + \frac{2nB_{11}}{V^2} + \frac{3n^2C_{111}}{V^3}\right) \qquad \text{(IV-17)}$$

$$\frac{1}{RT}\int_{V_{o1}}^{\infty}\left[\left(\frac{\partial P_1}{\partial n_1}\right)_{V,T} - \frac{RT}{V_1}\right] dV_1 = \frac{2B_{11}}{V_{o1}} + \frac{3C_{111}}{2V_{o1}^2} \qquad \text{(IV-18)}$$

Similarily, using Equations (IV-14), (IV-15), and (IV-16), the third integral of Equation (IV-8) can be evaluated. With these integrals evaluated and Equation (IV-3), Equation (IV-19) is obtained from Equation (IV-8) for the enhancement factor.

$$\ln \phi = \frac{V_{o1}}{8\beta^s RT}\left[\{1 + 9\beta^s(P - P_{o1})\}^{\frac{8}{9}} - 1\right] + \frac{2B_{11}}{V_{o1}} \qquad \text{(IV-19)}$$

$$+ \frac{3C_{111}}{2V_{o1}^2} - \ln Z_{o1} - \frac{2(y_1B_{11} + y_2B_{12})}{V_m}$$

$$- \frac{3(y_1^2C_{111} + 2y_1y_2C_{112} + y_2^2C_{122})}{2V_m^2} + \ln Z_m + \ln x_1$$

This equation is the working equation used for the prediction of the enhancement factor in the gas-liquid region of this work. In Equation (IV-19), there are still two unknown y_1 and V_m which have to be obtained by solving Equations (IV-14) and

(IV-19) simultaneously.

Equation (IV-19) can also be applied to the binary gas-solid system. In this case two more assumptions are added to simplify the calculation. The first assumption is that the solid phase is pure solid component 1, that is, in Equation (IV-19) the $\ell n\ x_1$ term can be eliminated. This assumption is experimentally supported by Mullins,[90] who studied the freezing point curve in the helium-argon system up to 120 atmospheres and concluded that the solid phase in this system was essentially pure argon. The other assumption is that the solid phase is incompressible. Considering the pressure of 120 atmospheres on the solid phase, this assumption appears to be reasonable and simplifies the first integral of Equation (IV-8) to

$$\frac{1}{RT}\int_{P_{o1}}^{P} v_1\,dP = \frac{v_1}{RT}\,(P - P_{o1}) \qquad \text{(IV-20)}$$

Calculation of Virial Coefficients

Second Virial Coefficient

If the interaction potential between molecules of the same chemical species or different chemical species is known, the corresponding virial coefficient can be calculated from the statistical mechanics. A variety of intermolecular potential functions have been developed to describe the different types of intermolecular forces which exist. In this investi-

gation two potential functions have been studied: the Lennard-Jones potential[49] and the Kihara core potential.[66,67]

The Lennard-Jones intermolcular potential function has been widely used to describe the potential energy between spherically symmetrical non-polar molecules and especially the noble gases. This potential function treats the molecule as a point mass and does not take into account the size and shape of the interacting molecules. The Lennard-Jones potential[49] function is given as

$$U(r) = 4e\ [(\frac{\sigma}{r})^{12} - (\frac{\sigma}{r})^{6}] \qquad \text{(IV-21)}$$

where r is the distance between two point masses, σ is the value of r at $U(r) = 0$, and e is the minimum energy which occurs at $r = 2^{\frac{1}{6}}\sigma$. As can be seen in Equation (IV-21), this function is a two-parameter function with an attractive energy inversely proportional to the sixth power of the distance between the molecules and a repulsive force inversely proportional to the twelfth power of the distance between the molecules.

The Kihara core potential[66,67] takes into account the size and shape of the molecules by assuming the molecules to have an impenetrable core and is given by Equation (IV-22).

$$U(\rho) = U_o\ [(\frac{\rho_o}{\rho})^{12} - 2\ (\frac{\rho_o}{\rho})^{6}] \qquad \text{(IV-22)}$$

The parameter ρ represents the shortest distance between the molecular cores of two interacting molecules and ρ_o is the value of ρ when $U(\rho)$ is minimum, U_o.

Lennard-Jones (6-12) Classical Model (LJCL). Hirschfelder, et al.[49] have calculated the second virial coefficient based on Equation (IV-12). Using their method, the second virial coefficient between molecules i and j is written as follows.

$$B_{ij} = (b_o)_{ij} \, B^*_{CL} \, (T^*_{ij}) \qquad \text{(IV-23)}$$

where

$$(b_o)_{ij} = \frac{2\pi \, N_A \, \sigma^3_{ij}}{3} \qquad \text{(IV-24)}$$

$$T^*_{ij} = \frac{T}{(e/k)_{ij}} \qquad \text{(IV-25)}$$

and

$$B^*_{CL}(T^*_{ij}) = \sum_{j=0}^{\infty} b^{(j)} \, (T^*_{ij})^{-(1+2j)/4} \qquad \text{(IV-26)}$$

The expression for $b^{(j)}$ in Equation (IV-26) is given by Equation (IV-27).

$$b^{(j)} = \left(\frac{2^{j+\frac{1}{2}}}{4j!}\right) \Gamma\left(\frac{2j-1}{4}\right) \qquad \text{(IV-27)}$$

The value of $B^*_{CL}(T^*)$ in Equation (IV-26) can be well represented by the summation of the first forty-one terms in the series (see Appendix D). The first forty-one values of $b^{(j)}$ are presented by Hirschfelder, et al.[49] and later Kirk[68] has recomputed these values. These two sets of the values of $b^{(j)}$ agree very well except at $b^{(16)}$, where Kirk's value was $-0.3386316 \times 10^{-5}$ as compared to $-0.33872440 \times 10^{-5}$ computed by Hirschfelder, et al. The values of Kirk have been selected for use in this work.

The mixture rules for $(b_o)_{ij}$ and $(e/k)_{ij}$ in Equations (IV-23) and (IV-25) are

$$(b_o)_{ij} = \frac{1}{8}\left(b_{oi}^{\frac{1}{3}} + b_{oj}^{\frac{1}{3}}\right)^3 \qquad \text{(Lorentz average)} \qquad \text{(IV-28)}$$

and

$$\left(\frac{e}{k}\right)_{ij} = \left(\frac{e}{k}\right)_i^{\frac{1}{2}} \left(\frac{e}{k}\right)_j^{\frac{1}{2}} \qquad \text{(geometric average)} \qquad \text{(IV-29)}$$

The Lennard-Jones (6-12) parameters used for the estimation of the second virial coefficients in this work are given in Table 17 of Appendix H.

Kihara Core Model (KIH). Using Equation (IV-22), Kihara[66,67] has derived the following expression for the pure and mixed second virial coefficients from the statistical mechanics.

$$\frac{(B_k)_{ij}}{N_A} = \frac{2\pi}{3}(\rho_o)_{ij}^3 F_3 + \frac{M_{oi} + M_{oj}}{2}(\rho_o)_{ij}^2 F_2 \qquad \text{(IV-30)}$$

$$+\left[\frac{S_{oi} + S_{oj}}{2} + \frac{M_{oi}M_{oj}}{4\pi}\right](\rho_o)_{ij} F_1$$

$$+ \frac{M_{oi}S_{oj} + M_{oj}S_{oi}}{8\pi} + \frac{V_{oi} + V_{oj}}{2}$$

The three functions F_1, F_2, and F_3 are functions of Z ($Z = (U_o)_{ij}/kT$) and can be calculated from Equation (IV-31).

$$F_s = \sum_{j=0}^{\infty} b_s^{(j)} Z^{(6j+s)}/12 \qquad \text{(IV-31)}$$

where

$$b_s^{(j)} = \left(\frac{s}{12}\right)\left(\frac{2^j}{j!}\right)\Gamma\left(\frac{6j - s}{12}\right) \qquad \text{(IV-32)}$$

The first forty values of $b_s^{(j)}$ for s = 1, 2 and 3 have been computed by Mullins[90] and given by Kirk.[68] These values have been used in this work. The mixture rules for $(\rho_o)_{ij}$ and $(U_o)_{ij}$ in Equation (IV-30) are given as

$$(\rho_o)_{ij} = \frac{(\rho_o)_i + (\rho_o)_j}{2} \qquad \text{(IV-33)}$$

and

$$(U_o)_{ij} = U_{oi}^{\frac{1}{2}} \; U_{oj}^{\frac{1}{2}} \qquad \text{(IV-34)}$$

The parameters M_o, S_o, and V_o in Equation (IV-30) are related to the size and shape of the molecular core and have the dimensions of length, area, and volume. For the spherical core [66, 100] as in the case of helium, carbon tetrafluoride, and chlorotrifluoromethane whose molecules have been assumed to have a spherical core in this work, these parameters are defined as

$$M_o = 4\pi a \qquad \text{(IV-35)}$$

$$S_o = 4\pi a^2 \qquad \text{(IV-36)}$$

and

$$V_o = \frac{4}{3}\pi a^3 \qquad \text{(IV-37)}$$

where a is the radius of the core.

For the light gases like helium, hydrogen, and neon, it is necessary to include quantum corrections in the calculation of the second virial coefficient as pointed out by Prausnitz and Myers.[100] They have also indicated that these corrections may still be required for the mixture of a quantum and non-quantum gases and presented the following equation for the second virial coefficient considering the first two translational quantum corrections when the quantum deviations are not too large.

$$B_{ij} = (B_k)_{ij} + (b_o)_{ij} [\Lambda^{*2}_{ij} B^*_I + \Lambda^{*4}_{ij} B_{II} - \Lambda^{*3}_{ij} B^*_o] \quad \text{(IV-38)}$$

The second term in Equation (IV-38) applies only as a quantum correction for the Lennard-Jones potential, which is the same as the Kihara core potential in the special case of a vanishing core. As an approximation, this term can also be applied as the quantum correction to the Kihara potential. The reduced quantum mechanical parameter Λ^* is given as

$$\Lambda^{*2}_{ij} = \frac{h^2}{2k\sigma^2_{ij} m_{ij} (U_o/k)_{ij}} \quad \text{(IV-39)}$$

The parameter σ_{ij} is related to the Kihara parameter by

$$\sigma_{ij} = 2^{-\frac{1}{6}} (\rho_o)_{ij} + \frac{M_{oi} + M_{oj}}{4\pi} \quad \text{(IV-40)}$$

Equation (IV-40) is exact for a spherical core and approximation for other cores. The parameter m_{ij} in Equation (IV-39) is defined as

$$m_{ij} = \frac{M_{ij}}{N_A} \quad \text{(IV-41)}$$

where

$$\frac{1}{M_{ij}} = \frac{1}{M_i} + \frac{1}{M_j} \qquad \text{(IV-42)}$$

The first two translational quantum correction terms B_I^* and B_{II}^* in Equation (IV-38) have been derived by Kihara [49,67] and are given as follows:

$$B_I^* = \sum_{j=o}^{\infty} b_I^{(j)} (T^*)^{-(6j+13)/12} \qquad \text{(IV-43)}$$

$$B_{II}^* = \sum_{j=o}^{\infty} b_{II}^{(j)} (T^*)^{-(6j+23)/12} \qquad \text{(IV-44)}$$

where

$$b_I^{(j)} = -\left(\frac{11-36j}{768\pi^2}\right)\left(\frac{2^{(6j+13)/6}}{j!}\right)\Gamma\left(\frac{6j-1}{12}\right) \qquad \text{(IV-45)}$$

$$b_{II}^{(j)} = -\left(\frac{3024j^2+4728j+767}{491520\pi^4}\right)\left(\frac{2^{(6j+23)/6}}{j!}\right) \qquad \text{(IV-46)}$$

$$\times\,\Gamma\left(\frac{6j+1}{12}\right)$$

The first forty-two values for $b_I^{(j)}$ and $b_{II}^{(j)}$ computed by Kirk[68] have been used in this work. The ideal gas quantum correction B_o^* is given by

$$B_o^* = \frac{3}{32\pi^{\frac{5}{2}}\,(T^*)^{\frac{3}{2}}} \qquad \text{(IV-47)}$$

The second virial coefficient based on the Kihara potential as shown in Equation (IV-38) has been used here for helium and gas mixtures. The parameters needed for calculating the second virial coefficients for the Kihara core model in this work are given in Table 17 of Appendix H.

Kihara Core Model with K_{12}(KIHCK12 and KIHEK12). This model is esstially the same as KIH except that the geometric mixing rule for the energy parameter is changed, that is, instead of Equation (IV-34), the following mixing rule is adopted for a binary system.

$$(U_o)_{12} = (1 - K_{12})\ (U_o)_{12G} \qquad \text{(IV-48)}$$

where

$$(U_o)_{12G} = U_{o1}^{\frac{1}{2}}\ \ U_{o2}^{\frac{1}{2}} \qquad \text{(IV-49)}$$

In this modification of the Kihara core model, the mixing rule for $(\rho_o)_{12}$, Equation (IV-33), is not changed. K_{12} in Equation (IV-48) is an empirical factor to correct for deviations from the geometric mean.

Recently Hiza and Duncan[51] have reported an empirical correlation for K_{12} of simple binary gas mixtures (see Chapter V). Using their equation, K_{12} can be evaluated from the ionization potentials of the two components. The Kihara core model with this predicted K_{12} for the geometric mixing rule for the energy parameter is called KIHCK12, and when K_{12} which is

evaluated so as to fit the experimental interaction second virial coefficients data is used, it is designated as KIHEK12.

Third Virial Coefficient

The theoretical calculation of the third virial coefficient in Equation (IV-14) is much more complicated than that of the second virial coefficient since it is concerned with three-body interactions. As Sherwood and Prausnitz[116] have pointed out, the third virial coefficient is more sensitive to the shape of the potential function than the second virial coefficient and its calculation allows a more severe test of the potential model.

As presented by Sherwood and Prausnitz,[115] the classical third virial coefficient of a gas for an angle-independent potential function $U_{ij}(r_{ij})$ is formally written as

$$C = C^{add} + \Delta C \qquad \text{(IV-50)}$$

where

$$C^{add} = -\frac{8\pi^2 N_A^2}{3} \iiint f_{12}f_{13}f_{23}\, r_{12}r_{13}r_{23}\, dr_{12}dr_{13}dr_{23} \qquad \text{(IV-51)}$$

$$\Delta C = -\frac{8\pi^2 N_A^2}{3} \iiint \exp\left[-\frac{\Sigma U_{ij}}{kT}\left\{\exp\left(-\frac{\Delta U}{kT}\right) - 1\right\}\right] \qquad \text{(IV-52)}$$

$$\times\, r_{12}r_{13}r_{23}\, dr_{12}dr_{13}dr_{23}$$

$$f_{ij} = \exp\left(-\frac{U_{ij}}{kT}\right) - 1 \qquad \text{(IV-53)}$$

and

$$\Sigma U_{ij} = U_{12} + U_{13} + U_{23} \qquad \text{(IV-54)}$$

the nonadditivity correction ΔC is the sum of the two portions, the dispersion and the overlap, and therefore Equation (IV-50) can be written as follows.

$$C = C^{add} + \Delta C \text{ (dispersion)} + \Delta C \text{ (overlap)} \qquad \text{(IV-55)}$$

Equation (IV-50) is based on the fact that the total potential energy of the three-molecule interaction is equal to the sum of the three pairwise interactions and the three-body interaction energy $\Delta U\ (r_{12}, r_{13}, r_{23})$, that is,

$$U_{123} = U_{12} + U_{13} + U_{23} + \Delta U \qquad \text{(IV-56)}$$

If one assume the pairwise additivity for the total potential energy of the three-molecule interaction (i.e., $U_{123} = \Sigma U_{ij}$), Equation (IV-50) becomes

$$C = C^{add} \qquad \text{(IV-57)}$$

which is the customary expression for the third virial coefficient.

Equation (IV-51) has been numerically calculated for the Lennard-Jones potential by Bird, et al.,[11] Bergeon,[9] Kihara,[64],

[65] Rowlinson, et al.,[110] and Sherwood and Prausnitz,[115] and for the Kihara core potential by Sherwood and Prausnitz [115] assuming a spherical core.

ΔC (dispersion) in Equation (IV-55) represents the contribution of the attractive force to the third virial coefficient and has been estimated for the Lennard-Jones (6-12) potential by Fowler and Graben,[36] Graben and Present, [39] and Sherwood and Prausnitz,[115] and for the Kihara potential by Sherwood and Prausnitz.[115] These investigations confirmed that ΔC (dispersion) is always positive and becomes more significant with decreasing temperature. The repulsive portion of the nonadditivity contribution is ΔC (overlap), the evaluation of which has been performed only for the Lennard-Jones (6-12) potential by Graben, et al.[40] and Sherwood, et al.[114] From their calculations, it is found that ΔC (overlap) is negative and its magnitude is nearly same as that of ΔC (dispersion). Thus, the net contribution of the nonadditivity ΔC to the third virial coefficient can be set negligible even though their estimated values contain large uncertainty.

Due to the lack of experimental third virial coefficient data in the temperature range of this work for the substances considered here, except helium, and the large uncertainty in the theoretical calculation of the third virial coefficient, two models have been selected for the estimation of the third virial coefficient in this work;

one is the Lennard-Jones (6-12) classical model and the other is the corresponding-states correlation of Chuech and Prausnitz.[18] These models are discussed in detail in the succeeding sections.

Lennard-Jones (6-12) Classical Model. Hirschfelder, et al.[49] have presented the following expression for the LJCL third virial coefficient, which is based on the potential additivity neglecting the three-body (nonadditive) interaction energy among molecules i, j and k.

$$C_{ijk} = C^{add}_{ijk} = (b_o)^2_{ijk} \, C^*_{CL}(T^*_{ijk}) \qquad \text{(IV-58)}$$

The reduced third virial coefficient is given as

$$C^*_{CL}(T^*_{ijk}) = \sum_{j=o}^{\infty} c^{(j)} (T^*_{ijk})^{-(j+1)/2} \qquad \text{(IV-59)}$$

The expression for $c^{(j)}$ is also presented by Hirschfelder, et al.[49] and several investigators[10,65,110] have computed the values of $c^{(j)}$. A comparison of C^*_{CL} values calculated using these different sets of $c^{(j)}$ is given in Appendix D. The first eighteen values of $c^{(j)}$ calculated by Kihara[65] have been presented by Hirschfelder, et al.[49] and these values were used in this work. The mixing rules used for the two parameters are

$$\left(\frac{e}{k}\right)_{ijk} = \left(\frac{e}{k}\right)_i^{\frac{1}{3}} \left(\frac{e}{k}\right)_j^{\frac{1}{3}} \left(\frac{e}{k}\right)_k^{\frac{1}{3}} \qquad \text{(IV-60)}$$

and

$$(b_o)_{ijk} = \frac{1}{27}\left[(b_o)_i^{\frac{1}{3}} + (b_o)_j^{\frac{1}{3}} + (b_o)_k^{\frac{1}{3}}\right]^3 \qquad \text{(IV-61)}$$

The Lennard-Jones (6-12) third virial coefficient used here does not include quantum and nonadditivity corrections. The parameters needed for the evaluation of the third virial coefficients for the Lennard-Jones (6-12) model are presented in Table 17 of Appendix H.

Method of Chueh and Prausnitz. The third virial coefficient estimated by the method of Chueh and Prausnitz[18] has been used for the Kihara program to predict the enhancement factor and also used for the fugacity and B_{12} calculations.

Chueh and Prausnitz[18] have shown a correlation for the third virial coefficient within the framework of the corresponding states principle. This correlation is intended for estimating the third virial coefficients of pure and mixed nonpolar gases including quantum gases. The general expression for the reduced third virial coefficient is given by

$$\frac{C}{V_c^2} = \left(0.232\, T_R^{-0.25} + 0.468\, T_R^{-5} \right) \qquad \text{(IV-62)}$$

$$\times \left(1 - e^{(1-1.89\, T_R^2)}\right) + d\, e^{-(2.49-2.30 T_R+2.70 T_R^2)}$$

This equation requires reliable experimental data to estimate the value of d and is recommended to be used at reduced temperatures above 0.8. To take into account of the deviations among the reduced third virial coefficients of different gases, Chueh and Prausnitz[18] have set these deviations proportional to the parameter d. This parameter is some measure of the size, shape, and polarizability of the molecule and becomes significant at reduced temperatures below 1.75. They have also presented some values of d for pure gases, based on a zero value of d for argon and nitrogen. The d values for carbon tetrafluoride and chlorotrifluoromethane have been estimated in this work by plotting the third virial coefficient data in a reduced form on the figure of generalized correlation for third virial coefficients presented by Chueh and Prausnitz.[18] These third virial coefficient data are given in Appendix H. For helium they set the parameter d equal to zero. All input data for the calculation of the third virial coefficient using the method of Chueh and Prausnitz are given in Table 16 of Appendix H.

The configurational properties of light gases such as

helium, hydrogen, and neon must be described by quantum rather than classical, statistical mechanics. For these quantum gases, Chueh and Prausnitz[18] use the effective critical constants as the reducing parameters instead of the true critical constants. These effective critical constants are given by Equations (IV-63) and (IV-64)

$$T_c = \frac{T_c^\circ}{1 + \frac{c_1}{MT}} \qquad \text{(IV-63)}$$

$$V_c = \frac{V_c^\circ}{1 + \frac{c_2}{MT}} \qquad \text{(IV-64)}$$

In these equations, c_1 and c_2 are set equal to 21.8 and - 9.91 K, respectively. For helium the classical critical temperature T_c° which is the effective critial temperature in the limit of high temperature is given as 10.47 K and the classical, high temperature critical volume V_c° as 37.5 cc/gm mole by Chueh and Prausnitz.[18] With the effective critical constants, given as Equation (IV-63) and (IV-64) the third virial coefficients of quantum gases can be calculated from Equation (IV-62). For the mixtures of gases, the mixing rules suggested by Chueh and Prausnitz[18] are used for the evaluation of the mixture virial coefficients. They are

$$C_{ijk} = (C_{ij}\ C_{ik}\ C_{jk})^{\frac{1}{3}} \tag{IV-65}$$

where

$$C_{ij} = (V_c)^2_{ij}\ f_c\ \left(\frac{T}{(T_c)_{ij}},\ d_{ij}\right) \tag{IV-66}$$

The function f_c is that given by Equation (IV-62). For a binary gas mixture containing a classical gas 1 and a quantum gas 2, the following critical constants are used.

$$(T_c)_{12} = \frac{(1 - K_{12})\ T_{c_1}^{o\frac{1}{2}}\ T_{c_2}^{o\frac{1}{2}}}{\left(1 + \frac{c_1}{M_{12}T}\right)} \tag{IV-67}$$

$$(V_c)_{12} = \frac{(V_{c_1}^{o\frac{1}{3}} + V_{c_2}^{o\frac{1}{3}})^3}{8\left(1 + \frac{c_2}{M_{12}T}\right)} \tag{IV-68}$$

In this case,

$$d_{12} = \frac{d_1 + d_2}{2} \tag{IV-69}$$

and

$$M_{12} = \frac{2M_1\ M_2}{M_1 + M_2} \tag{IV-70}$$

Since the correction factor K_{12} for the geometric mixing rule in Equation (IV-67) is obtained from the interaction second virial coefficient data[18] and is the same as that for the Kihara potential given in Equation (IV-48), the method of Chueh and Prausnitz has been used for the calculation of the third virial coefficients for all of the Kihara programs in this work. Because of the large uncertainty of the third virial coefficient at temperatures below $T_R = 0.8$, the third virial coefficient in Equation (IV-62) has been set equal to zero at $T_R < 0.8$ in this work, that is, C_{111} and C_{112} are zero at $T_{R1} < 0.8$ from Equation (IV-65) and C_{122} is also zero at $T_{R12} < 0.8$.

Benedict-Webb-Rubin Equation of State (BWR)

The empirical Benedict-Webb-Rubin (BWR)[7,8,9] equation of state is a modification of the Beattie-Bridgeman equation[5,6] of state to represent the properties of fluids at high densities and was originally developed for light hydrocarbons. Recently, however, this equation has been applied to non-hydrocarbons and also to several helium binary systems.[37,46,80] The BWR equation contains eight adjustable parameters and can be written by Equation (IV-71) for the mixtures of fluids.

$$P = \frac{RT}{V_m} + \frac{RTB'_m}{V_m^2} + \frac{RTC'_m}{V_m^3} + \frac{a_m\alpha_m}{V_m^6} + \frac{c_m(1+\frac{\gamma_m}{V_m^2})\exp(-\frac{\gamma_m}{V_m^2})}{V_m^3 T^2} \qquad \text{(IV-71)}$$

The parameters B'_m and C'_m are defined as

$$B'_m = (B_o)_m - \frac{(A_o)_m}{RT} - \frac{(C_o)_m}{RT^3} \qquad \text{(IV-72)}$$

and

$$C'_m = b_m - \frac{a_m}{RT} \qquad \text{(IV-73)}$$

The mixture rules as originally proposed for binary systems and used in this work are

$$N_m = y_1^2 N_{11} + 2y_1 y_2 N_{12} + y_2^2 N_{22} \qquad \text{(IV-74)}$$

for $N = A_o$, B_o, C_o, and γ with N_{12} defined as

$$N_{12} = (N_1 N_2)^{\frac{1}{2}} \qquad \text{(IV-75)}$$

for A_o, C_o, γ. Two different averages, linear and Lorentz have been commonly used for the value of $(B_o)_{12}$. These are

$$(B_o)_{12} = \frac{B_{o1} + B_{o2}}{2} \qquad \text{(linear)} \qquad \text{(IV-76)}$$

and

$$(B_o)_{12} = \frac{1}{8}\left(B_{o1}^{\frac{1}{3}} + B_{o2}^{\frac{1}{3}}\right)^3 \quad \text{(Lorentz)} \qquad \text{(IV-77)}$$

The BWR equation based on the linear average of $(B_o)_{12}$ is, hereafter, called BWR (LINEAR) and on the Lorentz average BWR (LORENTZ).

The mixture rules for the remaining four parameters, a, b, c, and α are

$$N_m = y_1^3 N_{111} + 3y_1^2 y_2 N_{112} + 3y_1 y_2^2 N_{122} + y_2^3 N_{222} \qquad \text{(IV-78)}$$

with the definition of $N_{ijk} = (N_i N_j N_k)^{\frac{1}{3}}$.

Benedict, et al.[8] have shown that the Lorentz average is better than the linear average in fitting the P-V-T data of their hydrocarbon systems but in the prediction of phase equilibria, the linear average gives a better fit than the Lorentz average. Mullins [90] and Garber[37] have also proved that in their study of the phase equilibria for hydrogen and helium binary systems the linear average gives the better results than the Lorentz average. In this work, both methods have been tested.

Using Equation (IV-8), (IV-13), and (IV-71) for mixtures and pure components, the following equation for the enhancement factor can be written.

$$\ln \phi = \ln \frac{PV_m}{P_{o1}V_{o1}} + \frac{V_{o1}}{8\beta^s RT}\left[\left\{1 + 9\beta^s (P-P_{o1})\right\}^{\frac{8}{9}} - 1\right] \qquad \text{(IV-79)}$$

$$+ \frac{2B'_{11}}{V_{o1}} + \frac{3C'_{111}}{2V_{o1}^2} + \frac{6a_1\alpha_1}{5RTV_{o1}^5} + \frac{c_1}{RT^3\gamma_1} + \frac{c_1}{RT^3}$$

$$\times \exp\left(-\frac{\gamma_1}{V_{o1}^2}\right)\left[\frac{\gamma_1}{V_{o1}^4} + \frac{1}{2V_{o1}^2} - \frac{1}{\gamma_1}\right] - \frac{2[y_1(B'_{11}-B'_{12})+B'_{12}]}{V_m}$$

$$- \frac{3\left[y_1^2(C'_{111}-2C'_{112}+C'_{122}) + 2y_1(C'_{112}-C'_{122}) + C'_{122}\right]}{2V_m^2}$$

$$- \frac{3(a_m\alpha_{1mm}+\alpha_m a_{1mm})}{5RTV_m^5} - \frac{3c_{1mm}}{RT^3\gamma_m} + \frac{2c_m\gamma_{1m}}{RT^3\gamma_m^2} + \frac{\exp\left(-\frac{\gamma_m}{V_m^2}\right)}{RT^3}$$

$$\times \left(\frac{3c_{1mm}}{\gamma_m} - \frac{2c_m\gamma_{1m}}{\gamma_m^2} + \frac{3c_{1mm}}{2V_m^2} - \frac{2c_m\gamma_{1m}}{\gamma_m V_m^2} - \frac{c_m\gamma_{1m}}{V_m^4}\right)$$

$$+ \ln(\gamma'_1 x_1)$$

The mixing rules for α, a, and c in Equation (IV-79) are

$$N_{1mm} = (N_1 N_m^2)^{\frac{1}{3}} \qquad \text{(IV-80)}$$

with N_m given by Equation (IV-78), and for γ,

$$N_{1m} = (N_1 N_m)^{\frac{1}{2}} \qquad \text{(IV-81)}$$

with N_m given by Equation (IV-74).

The second and third virial coefficients in Equation (IV-14) can be expressed in terms of the parameters in (IV-71) by putting Equation (IV-71) in a form similar to Equation (IV-14). They can be written as follows.

$$B_{ij} = (B_o)_{ij} - \frac{(A_o)_{ij}}{RT} - \frac{(C_o)_{ij}}{RT^3} \qquad \text{(IV-82)}$$

$$C_{ijk} = b_{ijk} - \frac{a_{ijk}}{RT} + \frac{c_{ijk}}{RT^3} \qquad \text{(IV-83)}$$

These relations have been obtained by expanding the exponential term in Equation (IV-71) and equating the same order volume terms to the ocrresponding same order volume terms in equation (IV-14) as shown by Kirk.[68] The second and third virial coefficients based on Equations (IV-82) and (IV-83) are given in Chapter V and Appendix H. The parameters needed for the evaluation of the BWR equation are presented in Table 17 of Appendix H.

CHAPTER V

COMPARISON OF PREDICTED AND EXPERIMENTAL GAS PHASE EQUILIBRIUM DATA

Interaction Second Virial Coefficient

The correct prediction of the thermodynamic properties of a gas mixture depends mainly on the interaction potential between dissimilar molecules if the molecular potentials of the pure components are well known. Unfortunately, the prediction of this interaction potential is formidable and therefore, the interaction second virial coefficient B_{12} which is the most important measure of the interaction between two dissimilar molecules is usually derived from experimental data. There are various ways[13,23,24,90,135,138] to obtain the interaction second virial coefficient as presented by Garber.[37] Of these, the indirect method for the extraction of B_{12} from experimental phase equilibrium data has been widely used by many investigators[17,28,37,68,77,90,108] since other direct methods either require precise P-V-T measurements which are very difficult or present experimental difficulties at low temperatures. This indirect method is adopted in this work and is described here in detail.

Extraction of Interaction Second Virial Coefficient from Phase Equilibrium Data

By rearranging the enhancement factor Equation (IV-19) for binary phase equilibrium, the expression for B_{12} can be obtained as

$$B_{12} = \frac{V_m}{2y_2}\left[\frac{2B_{11}}{V_{o1}} + \frac{3C_{111}}{2V_{o1}^2} - \ln Z_{o1} - \frac{3}{2V_m^2}\left(y_1^2 C_{111}\right.\right. \qquad \text{(V-1)}$$

$$\left.\left. + 2y_1 y_2 C_{112} + y_2^2 C_{122}\right) + \frac{V_{o1}}{8\beta^s RT}\left\{\left(1 + 9\beta^s (P-P_{o1})\right)^{\frac{8}{9}} - 1\right\}\right.$$

$$\left. - \frac{2y_1 B_{11}}{V_m} + \ln Z_m + \ln x_1 - \ln \frac{Py_1}{P_{o1}}\right]$$

The evaluation of V_m requires the values of the additional virial coefficients B_{22}, B_{12} and C_{222} other than those shown in Equation (V-1). As shown in Figures 36 and 38 of Appendix H, the third virial coefficients (C_{111}) of the condensed components considered here are best described by the method of Chueh and Prausnitz.[18] This method has been used for the calculation of the third virial coefficients C_{111}, C_{112}, and C_{122} in estimating the experimental B_{12} values. The selected curve in Figure 34 of Appendix H represents the experimental third virial coefficients (C_{222}) of helium very well and the input values of C_{222} are taken directly from this curve.

The Lennard-Jones model is used for representing the second virial coefficient (B_{22}) of helium, and the second virial coefficients (B_{11}) of the condensed components are evaluated using both the Lennard-Jones and Kihara core models.

To solve Equation (V-1), the trial input values of B_{12} for the calculation of V_m and K_{12} for the calculation of the third virial coefficients are necessary. Initially, these values of B_{12} and K_{12} are calculated using the Lennard-Jones model and the empirical equation of Hiza and Duncan,[51] respectively.

This B_{12} program was originally written by Mullins[90] and later modified by Garber,[37] and this modified program has been used in this work with one more modification, that is, instead of using the average isothermal compressibility[46] for the evaluation of the compressed liquid molar volume, as was used by Garber,[37] the generalized correlation for the compressibilities given by Chueh and Prausnitz[21] was used as has been described in Chapter IV. It is now possible to solve Equation (V-1) to obtain the experimental B_{12} at each pressure point along an isotherm. The values of B_{12} obtained are plotted against $(P - P_{o1})$ and extrapolated down to $(P - P_{o1}) = 0$. The true value of B_{12} is the intercept of this extrapolated line.

Solving Equation (V-1) with those input values described above, the new and improved values of B_{12} can be obtained. For a new K_{12} value, the B_{12} curves based on Kihara model at the

values of K_{12} from 0 to 1 with an interval of 0.1 are prepared as a function of temperature in a graphical form and the new and improved values of B_{12} are plotted in this graph. In this way, a new input value of K_{12} can be obtained. The third virial coefficients C_{112} and C_{122} do not appear too sensitive to this parameter K_{12}. Two iterations of the B_{12} program were enough to obtain the final estimates of B_{12} and K_{12}. This method has been described and used by Mullins,[90] Liu,[77] and Garber.[37]

Since B_{11} in Equation (V-1) is calculated using two models, the Lennard-Jones potential and Kihara core potential, two experimental values of B_{12} were obtained. These two values are shown in Figures 10 and 12 together with the theoretically calculated values of B_{12}. The theoretical models used for comparison are LJCL, KIH, KIHCK12, KIHEK12, BWR (LINEAR), and BWR (LORENTZ) for the helium-carbon tetrafluoride system. Since no BWR parameters are available for chlorotrifluoromethane, only the LJCL, KIH, KIHCK12 and KIHEK12 models were used for the helium-chlorotrifluoromethane system. All of these theoretical models have been described in detail in Chapter IV.

B_{12} for the Helium-Carbon Tetrafluoride System. Phase equilibrium data have been extensively used by Hiza and Duncan,[51] Liu,[77] and Garber[37] for the extraction of B_{12} for the helium binary systems. But no phase equilibrium data were available for the extraction of B_{12} for the helium-

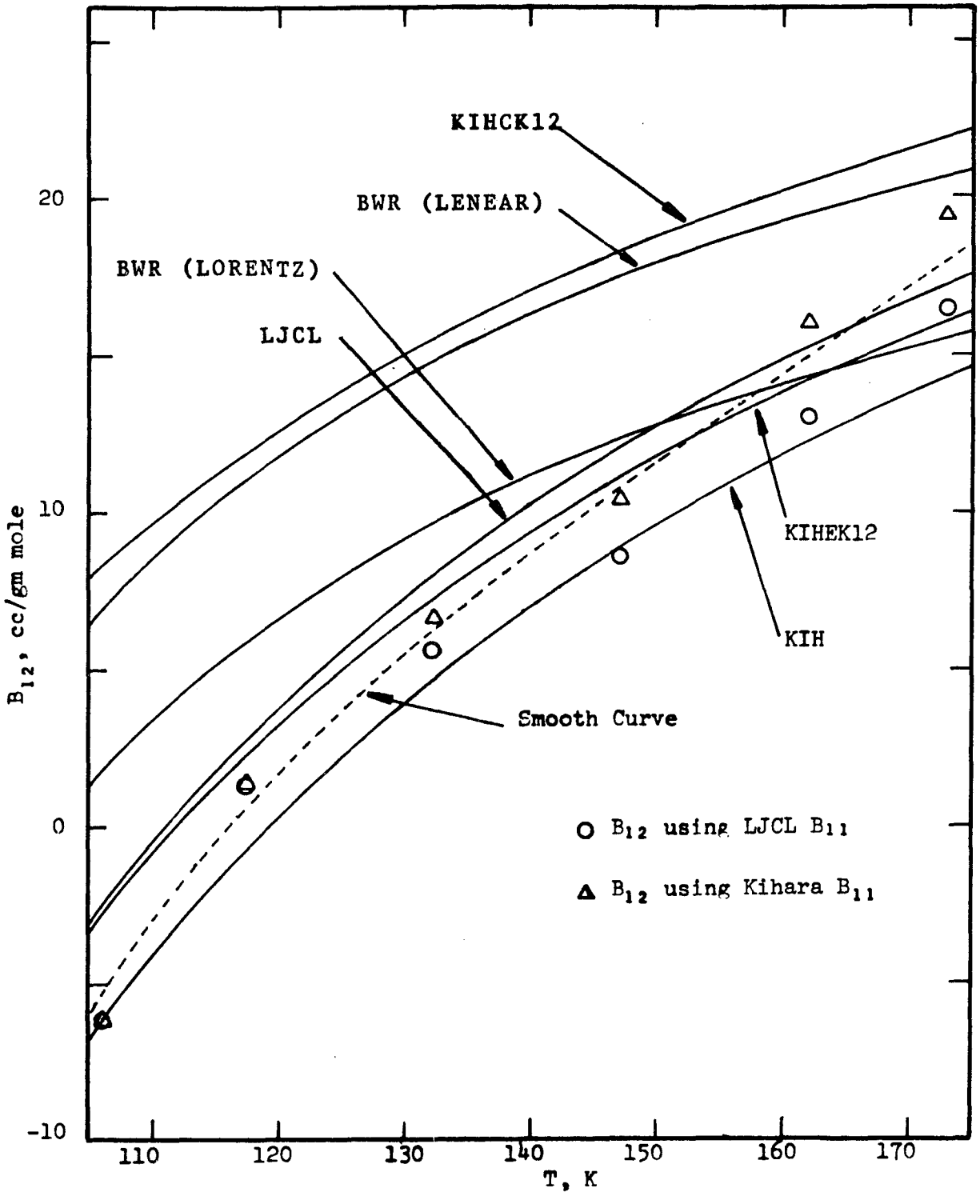

Figure 10. Predicted and Experimental B_{12} for the Helium-Carbon Tetrafluoride System at Temepratures between 106 and 173 K.

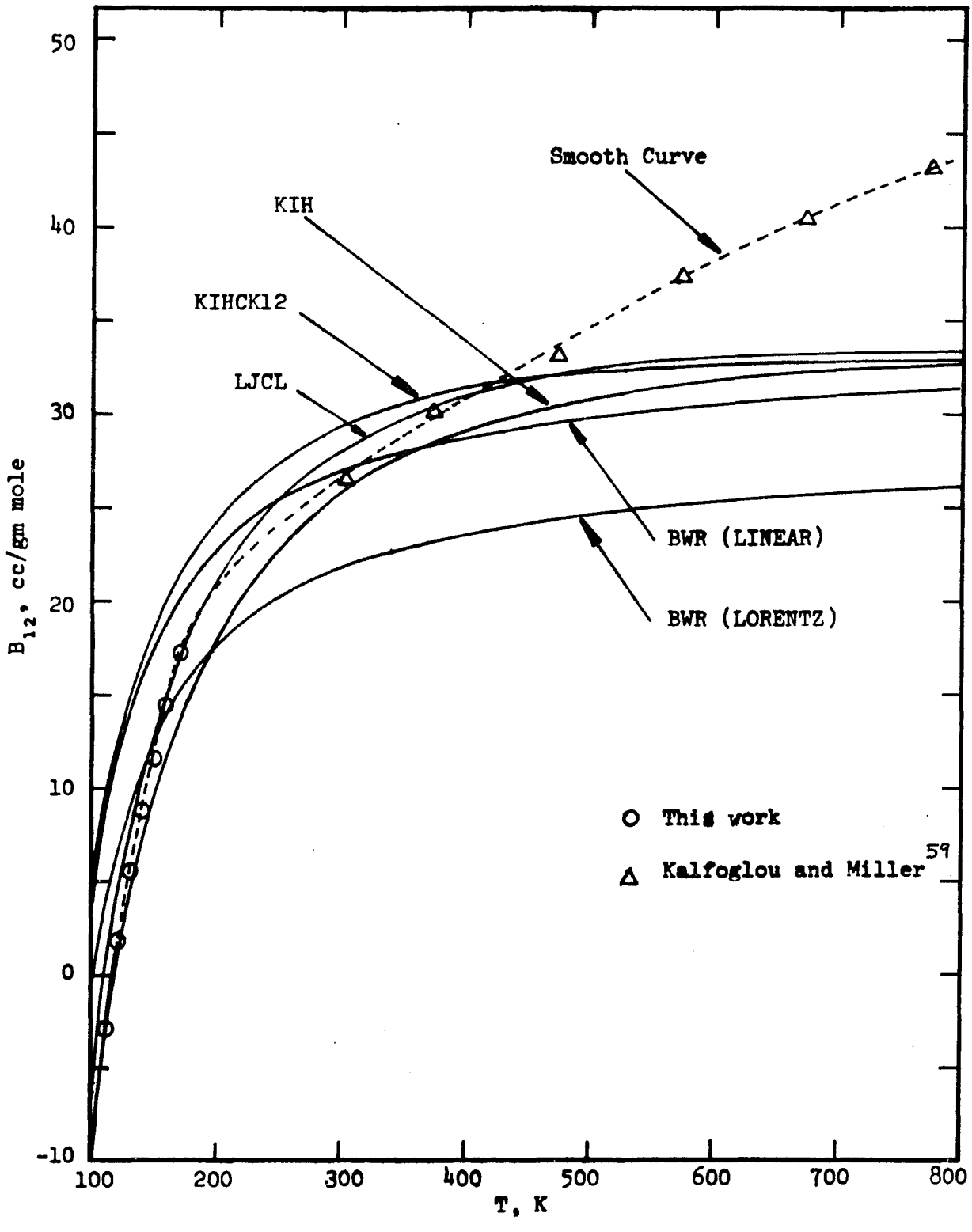

Figure 11. Predicted and Experimental B_{12} for the Helium-Carbon Tetrafluoride System at Temperatures between 106 and 773 K.

carbon tetrafluoride system prior to the present work. The data used here are the smoothed experimental values for ϕ and x_2 presented in Table 14 of Appendix G.

The B_{12} values obtained in this work are shown in Figure 10 together with those predicted using the various theoretical models. The B_{12} values for this system at the higher temperatures 303-773 K have been experimentally determined by Kalfoglou and Miller[59] using Burnett method.[13] These values are plotted in Figure 11, and a smooth curve is drawn through these experimental values and extrapolated to the lower temperatures so as to fit the B_{12} values of this work. All theoretical models used appear to fail to predict the B_{12} values satisfactorily in the temperature region of 303-773 K. Table 1 presents the B_{12} values from the smooth curve at the temperatures of 300 to 700 K in Figure 11 and those from the smooth curve in Figure 10 in the temperature range of 110 to 170 K.

The error range for the B_{12} values of this work is determined by varying the input enhancement factor and x_2 values by the assigned experimental error, ±2.0 percent in ϕ and x_2, and is also shown in Table 1. The masimum error for the B_{12} values at 300-700 K is given as less than 1.0 cc/mole by Kalfoglou and Miller.[59]

B_{12} for the Helium-Chlorotrifluoromethane System. The B_{12} data for the helium-chlorotrifluoromethane system determined in this work are shown in Figure 12. No values of

Table 1. B_{12} for the Helium-Carbon Tetrafluoride System

T, K	B_{12}, cc/gm mole
110	-3.0 ± 3.0
120	1.8 ± 3.0
130	5.5 ± 3.0
140	8.7 ± 3.0
150	11.6 ± 3.0
160	14.4 ± 3.0
170	17.2 ± 3.0
300	26.7 ± 1.0*
400	30.9 ± 1.0*
500	34.7 ± 1.0*
600	38.3 ± 1.0*
700	41.3 ± 1.0*

* Smoothed values from Kalfoglou's[59] experimental B_{12} data

B_{12} could be found in the literature. The smoothed gas and liquid phase equilibrium data used for the extraction of B_{12} data are presented in Table 15 in Appendix G. The smoothed B_{12} values read from the smooth curve in Figure 12 are given in Table 2 at even temperature intervals with the corresponding error range. This error range was produced by varying the enhancement factor by ±3.5 percent and the liquid composition x_2 by ±2.0 percent.

Theoretical models considered for the calculation of the interaction second virial coefficients for this system are the KIH, KIHCK12, KIHEK12, and LJCL models and shown in Figure 12.

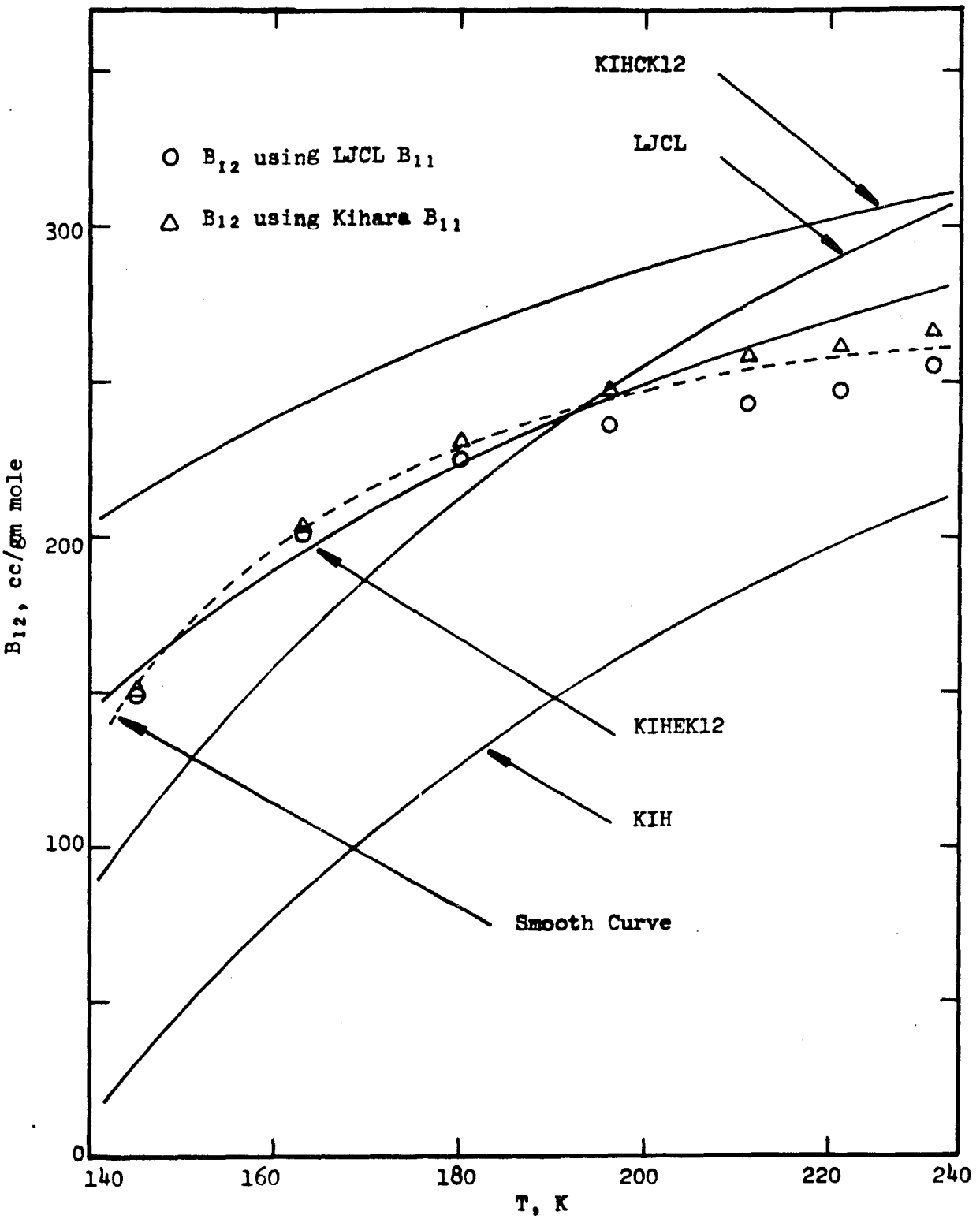

Figure 12. Predicted and Experimental B_{12} for the Helium-Chlorotrifluoromethane System.

Table 2. B_{12} for the Helium-Chlorotrifluoromethane system

T, K	B_{12}, cc/gm mole
150	17.1 ± 6.0
160	19.6 ± 6.0
170	21.5 ± 6.0
180	22.9 ± 6.0
190	24.0 ± 6.0
200	24.8 ± 6.0
210	25.4 ± 6.0
220	25.8 ± 6.0
230	26.0 ± 6.0

Discussion of Results

A good summary of B_{12} data for the helium binary systems has been presented by Garber.[37] In his paper, he has discussed in detail the general trend of B_{12} curves of these systems as a function of temperature and his discussion appears to shed some light on the unusual behavior of the B_{12} curves which is specific for the helium binary systems. In the following, the results of the B_{12} data of this work are discussed and the main emphasis is given on the comparison of these results with the general trend of the interaction second virial coefficients for the helium binary systems as stated by Garber.[37]

Of the theoretical models shown in Figure 10, the KIHEK12, LJCL, and BWR (LORENTZ) models fit the experimental B_{12} data for the helium-carbon tetrafluoride system quite

well, the KIHCK12 and BWR (LINEAR) models predict the values that are too high, and the predicted B_{12} values from the KIH model are somewhat too low. All of these B_{12} values are positive except at the lowest temperature and increase with increasing temperature, which accounts for the fact that that the enhancement factors for this system are close to one. This is the general trend of the helium binary systems as pointed out by Garber.

The B_{12} data of Kalfoglou and Miller[59] at the higher temperatures (303-773 K) are plotted together with the smoothed B_{12} values of this work in Figure 11. A smooth curve passes through all of the experimental points very nicely, proving the consistency of the two experimental results. Unfortunately, all of the theoretical models considered here fail to predict the B_{12} values satisfactorily at the elevated temperatures. As can be seen in Figure 11, no maximum is shown in the experimental B_{12} values at this temperature range though the theoretical curves tend to bend downward at the higher temperatures, giving a mixiumum at the temperatures above 750 K. The maximum have been shown in the experimental B_{12} curves for the helium-hydrogen, helium-nitrogen, helium-neon, and helium-argon systems, and Garber[37] stated that these maxima in the B_{12} curves are not unusual at all in the helium binary systems. The large discrepancy between the experimental and theoretical B_{12} values in the temperature region of 303-773 K in Figure 11 is pro-

bably due to the inadequacy of the theoretical models used in that temperature region. No further attempt is made here to account for this discrepancy.

Of the theoretical models shown in Figure 12, the KIHEK12 model predicts the best B_{12} values of the helium-chlorotrifluoromethane system. The values of B_{12} obtained from the KIHCK12 and KIH models are either too high or too low. The LJCL model predicts values that are too high at higher temperatures, too low at lower temperatures, and quite satisfactory in the middle. Garber[37] has observed that within a given series such as the helium-hydrocarbon series or helium-inert gases it appears that, for a given reduced temperature T_{R1}, the values of B_{12} increase as the molecules become larger. As can be seen in Figure 12, the B_{12} values of this system are somewhat higher than those of the helium-carbon tetrafluoride system, where the chrlotrifluoromethane molecules are larger than the carbon tetrafluoride molecules. Although the uncertainty of the B_{12} values for the helium-chlorotrifluoromethane system is large (±6.0 cc/mole), it can be seen in Figure 12 that the B_{12} values increase with increasing temperature and the rate of this increase decreases at the higher temperatures. No maximum is shown on the B_{12} curve in the temperature region studied here.

Deviations from the Geometric Mixing Rule

For pure gases, the evaluation of virial coefficients

requires the knowledge of interactions among like molecules. These interactions are approximated by some functional form such as the Lennard-Jones or Kihara potential. Assuming that the interactions among unlike molecules can be characterized by the same functional form, the hybrid interaction parameters are estimated from the pure component data using combining rules.

Numerous investigators[18,37,50,51,56,57,79,90,118] have shown that the interaction energy parameters can not be obtained simply using the geometric mixing rule (Equation (IV-29) or (IV-34)) for all molecular species. Hudson and McCoubrey[56] have derived the following mixing rule for the energy parameter of the Lennard-Jones (6-12) potential from the London theory of dispersion forces.

$$e_{12} = \left[\frac{2(I_1 I_2)}{I_1 + I_2}\right]^{\frac{1}{2}} \left[\frac{2^6 \sigma_1^3 \sigma_2^3}{(\sigma_1+\sigma_2)^6}\right] (e_1 e_2)^{\frac{1}{2}} \qquad \text{(V-2)}$$

If the ionization potentials and the collision diameters of two interacting molecules are the same, that is, $I_1 = I_2$ and $\sigma_1 = \sigma_2$, Equation (V-2) reduces to the geometric mixing rule. In the derivation of Equation (V-2) the repulsive part of the potential function was entirely reglected. Recently, Sikora[118] has presented a more complicated mixing rule for the Lennard-Jones (6-12) potential energy parameter, considering both the repulsive and attractive parts of the inter-

action potential. This mixing rule is an improved form of Equation (V-2). In an attempt to correct the deviations from the geometric mixing rule, Liu[77] has also used the following type of the combining rule for the Lennard-Jones (6-12) potential.

$$\left(\frac{e}{k}\right)_{12} = (1 - K_{LJ}) \left[\left(\frac{e}{k}\right)_1 \left(\frac{e}{k}\right)_2\right]^{\frac{1}{2}} \qquad \text{(V-3)}$$

Although much attention has given on the estimation of the interaction energy parameters for the Lennard-Jones (6-12) potential, it is of less interest to correlate the Lennard-Jones (6-12) potential parameters, e and σ, to obtain the interaction energy parameter since these potential parameters have the strong temperature dependency so that the extraction of these parameters from second virial coefficient data is quite difficult as has been pointed by Lin and Robinson[76] and Hanley and Klein.[43] The Kihara core potential function has three adjustable parameters and these parameters are not so sensitive to the temperature as those of the Lennard-Jones (6-12) potential function. Therefore, it has proven to be more meaningful to examine the combining rule for the interaction energy parameter for this potential.

Mullins,[90] Garber,[37] Chueh and Prausnitz,[18,19] Eckert, et al.,[33] Hiza and Duncan,[51] and Hiza[50] have used the following combining rule for the interaction energy parameter

for the Kihara core potential.

$$(U_o)_{12} = (1 - K_{12}) (U_{o1} U_{o2})^{\frac{1}{2}} \qquad (V\text{-}4)$$

K_{12} in Equation (V-4) is a correction factor for the geometric mixing rule. Hereafter, all values of K_{12} discussed are in reference to Equation (V-4).

Hiza and Duncan[51] have presented an empirical correlation for K_{12} which is based on the experimental B_{12} data for helium, hydrogen, neon, and some other binary systems. This is

$$K_{12} = 0.17 (I_v - I_c)^{\frac{1}{2}} \ln(\frac{I_v}{I_c}) \qquad (V\text{-}5)$$

where v and c represent the volatile and condensible components, respectively. Hiza and Duncan,[51] Hiza,[50] and Garber[37] have shown that the values of K_{12} calculated using Equation (V-5) are in good agreement with those of K_{12} experimentally determined, in spite of the temperature dependency of K_{12} as pointed out by Hiza and Duncan[51] and Garber.[37] In this work, the experimental values of K_{12} were simultaneously determinted with those of B_{12} from the phase equilibrium data using the Kihara second virial coefficients with quantum corrections, Equation (VI-38). The values of B_{12} obtained are presented in Table 3. The method of extrac-

tion of K_{12} value has been given in the early part of this chapter. Since the K_{12} values for the helium binary systems of this work have also shown the apparent temperature dependency, these values are determined as an average value over a specified temperature range.

The values of K_{12} determined experimentally and those computed using Equation (V-5) are compared in Table 3. No other experimental K_{12} values for the helium-carbon tetrafluoride and helium-chlorotrifluoromethane systems were available for comparison. Very recently, a good summary of K_{12} values for the helium binary systems has been given by Garber.[37] It can be seen from his results that within the helium-hydrocarbon series, the helium interactions with large molecules tend to give large values of K_{12}. The K_{12} value of the helium-chlorotrifluoromethane system is larger than that of the helium-carbon tetrafluoride as is shown in Table 3.

The difference between the experimental and calculated K_{12} values for these systems are seen to be very large. The value of K_{12} for the helium-carbon tetrafluoride system is surprisingly small compared with that of the helium-methane system, or any helium-hydrocarbon system. So far, no satisfactory explanation could be found for this unusual behavior of K_{12} values for these helium-hologen-substituted methane systems, but it is certainly true that Equation (V-5) is inadequate for the prediction of the K_{12} values for the systems

Table 3. Values of K_{12} for the Helium-Carbon Tetrafluoride and Helium-Chlorotrifluoromethane Systems

Gas	I (eV)	Calculated K_{12} From Eqation (V-5)	Experimental K_{12}**
Helium	24.46[104]		
Carbon Tetrafluoride	15.0[71]	0.28	0.06 (106-173 K)
Chlorotrifluoromethane	12.91[136]	0.37	0.25 (145-231 K)

** These values represent an average value over the specified temeprature range

considered here. No further consideration has been made for the theoretical basis of Equation (V-5) in this work.

Enhancement Factor

For the prediction of enhancement factors for the helium-carbon tetrafluoride system, the LJCL, KIH, KIHCK12, KIHEK12, BWR (LINEAR), and BWR (LORENTZ) models have been used. For the helium-chlorotrifluoromethane system only four models, the LJCL, KIH, KIHCK12, and KIHEK12, have been studied for the theoretical prediction of enhancement factors since no BWR parameters were available for chlorotrifluoromethane. All of these theoretical models are described in detail in Chapter IV. The predicted values of enhancement

factors are presented in Tables 14 and 15 in Appendix G. Four representative isotherms for each system have been selected and presented for comparison in Figures 13 through 20. All pure virial coefficients used for the calculation of enhancement factors using various theoretical models are shown in Figures 33 through 38 of Appendix H.

Of the two equations of state used here, the virial equation is designated as the LJCL, KIH, KIHCK12 or KIHEK12 model depending on which model is used for the calculation of virial coefficients. The Lennard-Jones (6-12) potential is used in evaluating all virial coefficients in the LJCL model. The three models, KIH, KIHCK12, and KIHEK12, differ only in their combining rule for the calculation of the interaction virial coefficients, B_{12}, C_{122}. For these three models the Kihara potential is used for the calculation of all the second virial coefficients while for the third virial coefficients the method of Chueh and Prausnitz[18] is used. The calculation of the enhancement factor based on the BWR equation make use of two different mixing rules for the calculation of the parameter $(B_o)_{12}$ (see Equations (IV-76) and (IV-77)) for the gas mixture. The two models, BWR (LINEAR) and BWR (LORENTZ) are based on the use of these mixture rules.

Four enhancement factor isotherms for the helium-carbon tetrafluoride system are shown in Figures 13 through 16 in the order of low temperature to high temperature. At

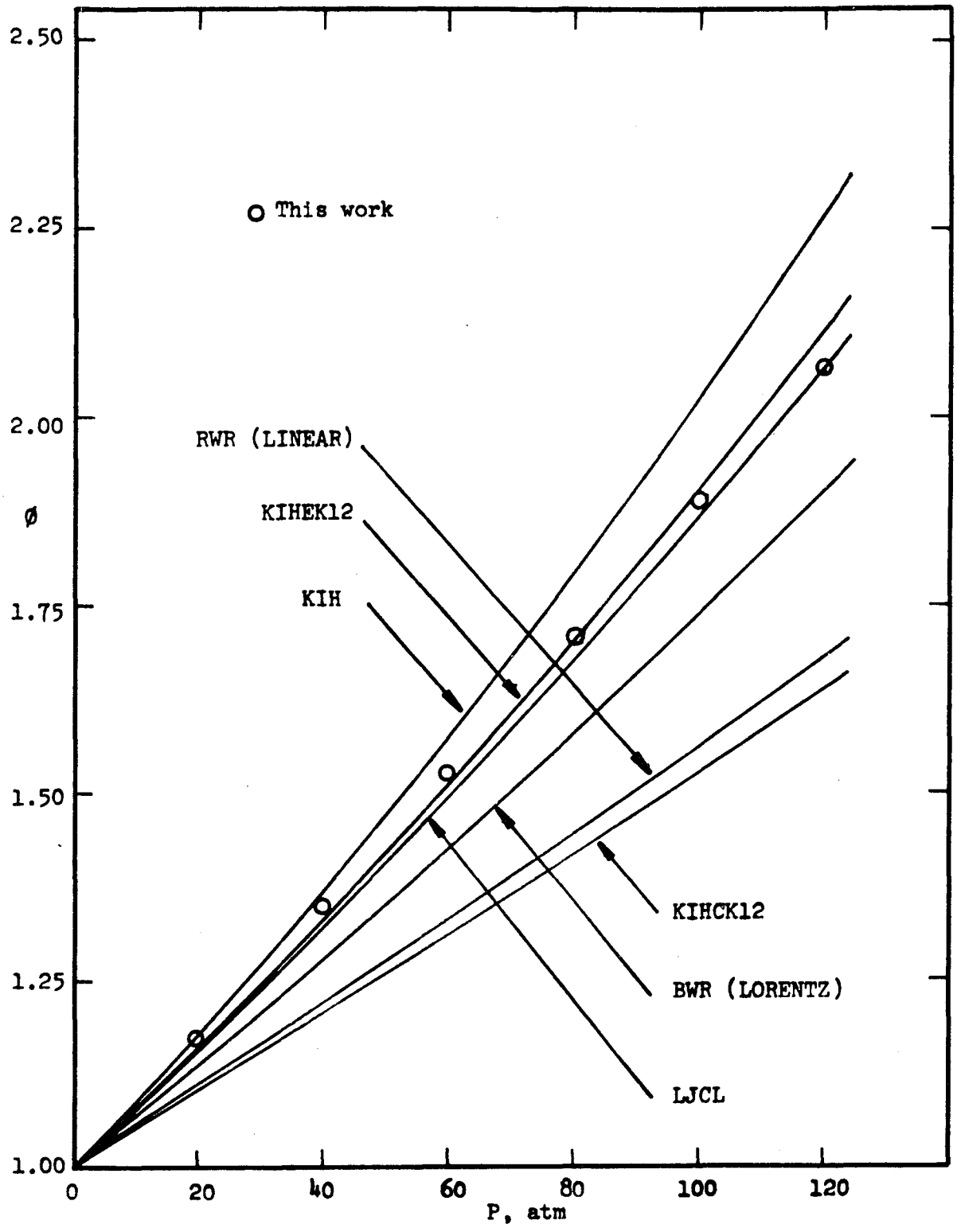

Figure 13. Theoretical and Experimental Enhancement Factors in the Helium-Carbon Tetrafluoride Sysem at 106.01 K.

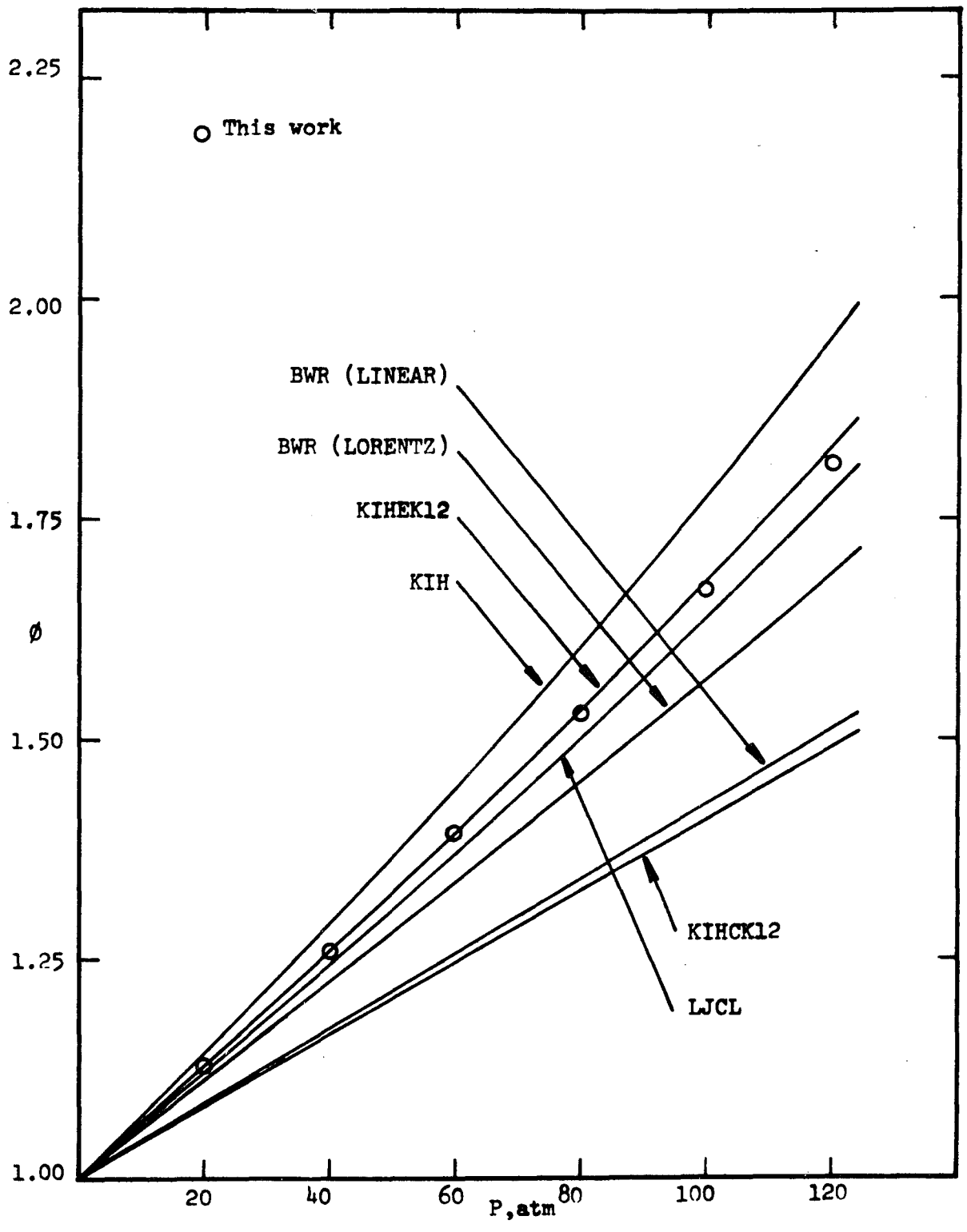

Figure 14. Theoretical and Experimental Enhancement Factors in the Helium-Carbon Tetrafluoride System at 117.33 K.

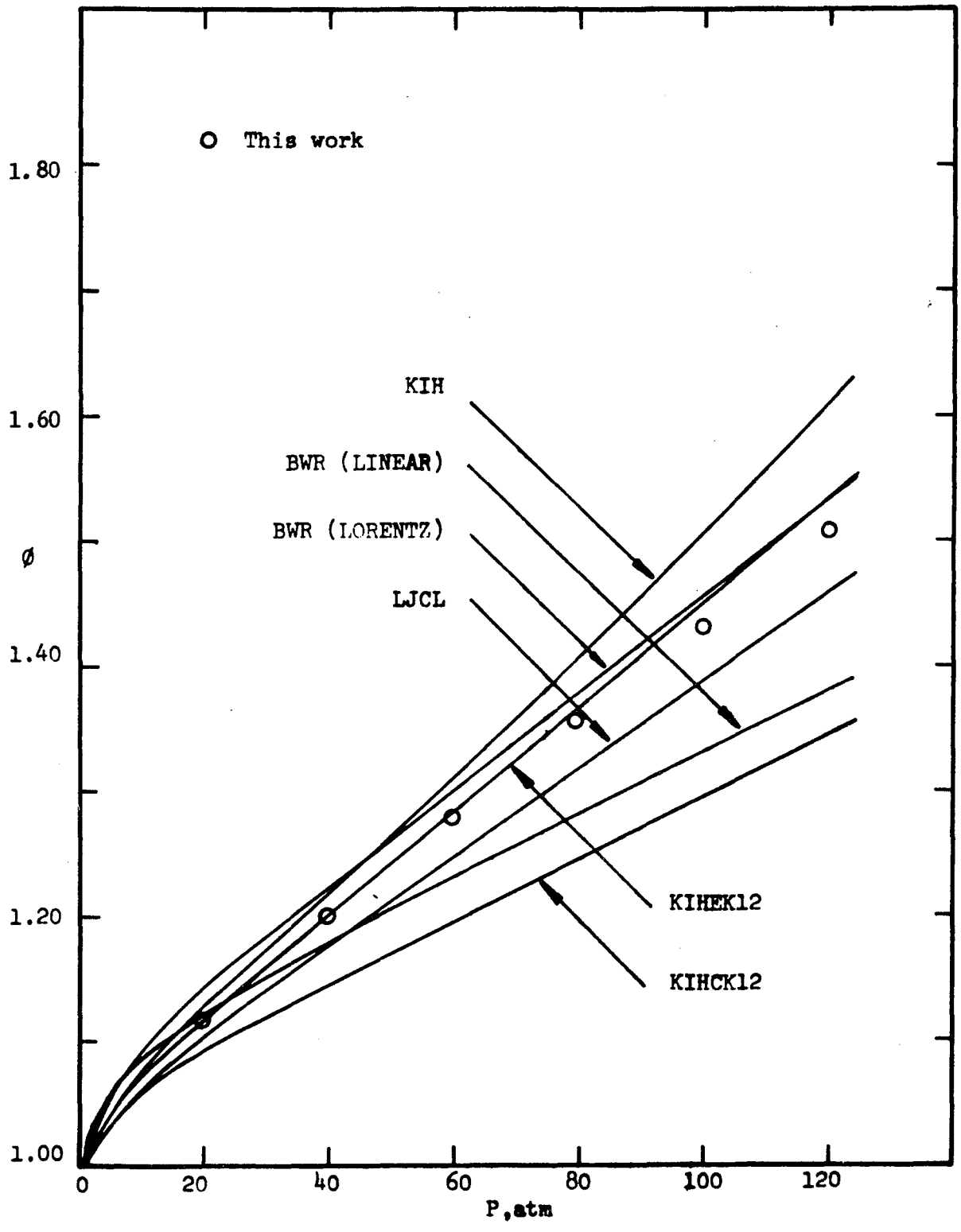

Figure 15. Theoretical and Experimental Enhancement Factors in the Helium-Carbon Tetrafluoride System at 147.10 K.

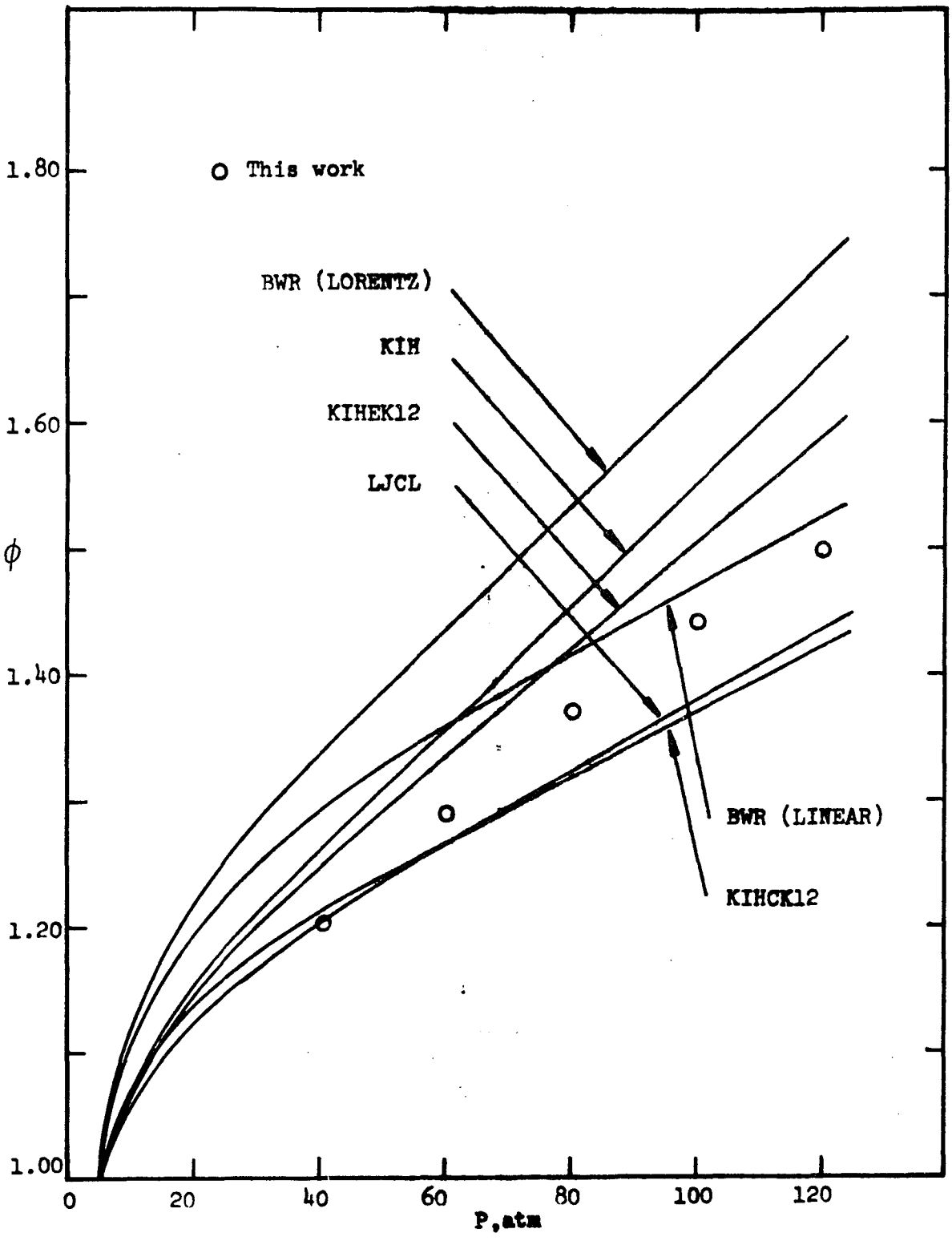

Figure 16. Theoretical and Experimental Enhancement Factors in the Helium-Carbon Tetrafluoride System at 173.02 K.

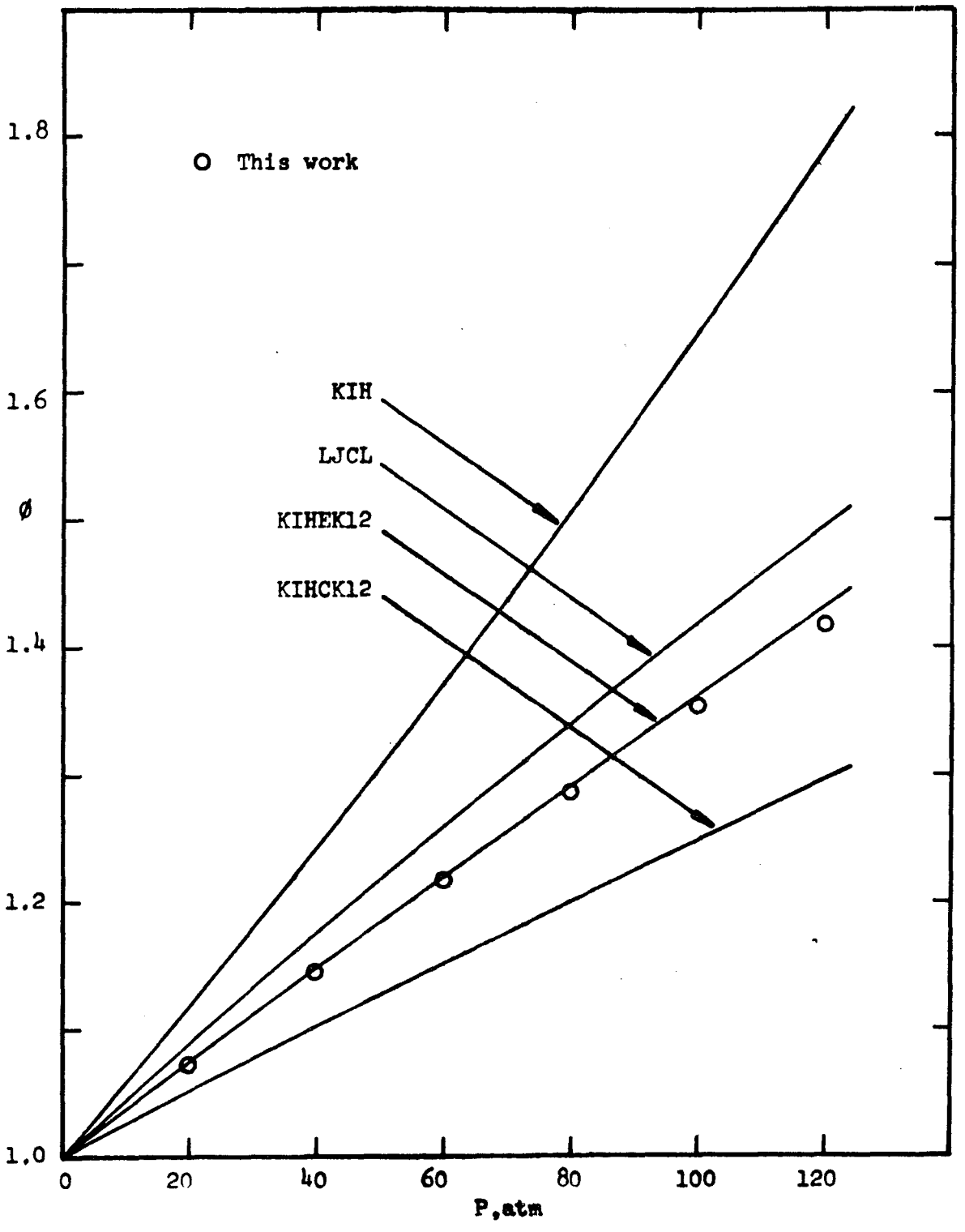

Figure 17. Theoretical and Experimental Enhancement Factors in the Helium-Chlorotrifluoromethane System at 145.21 K.

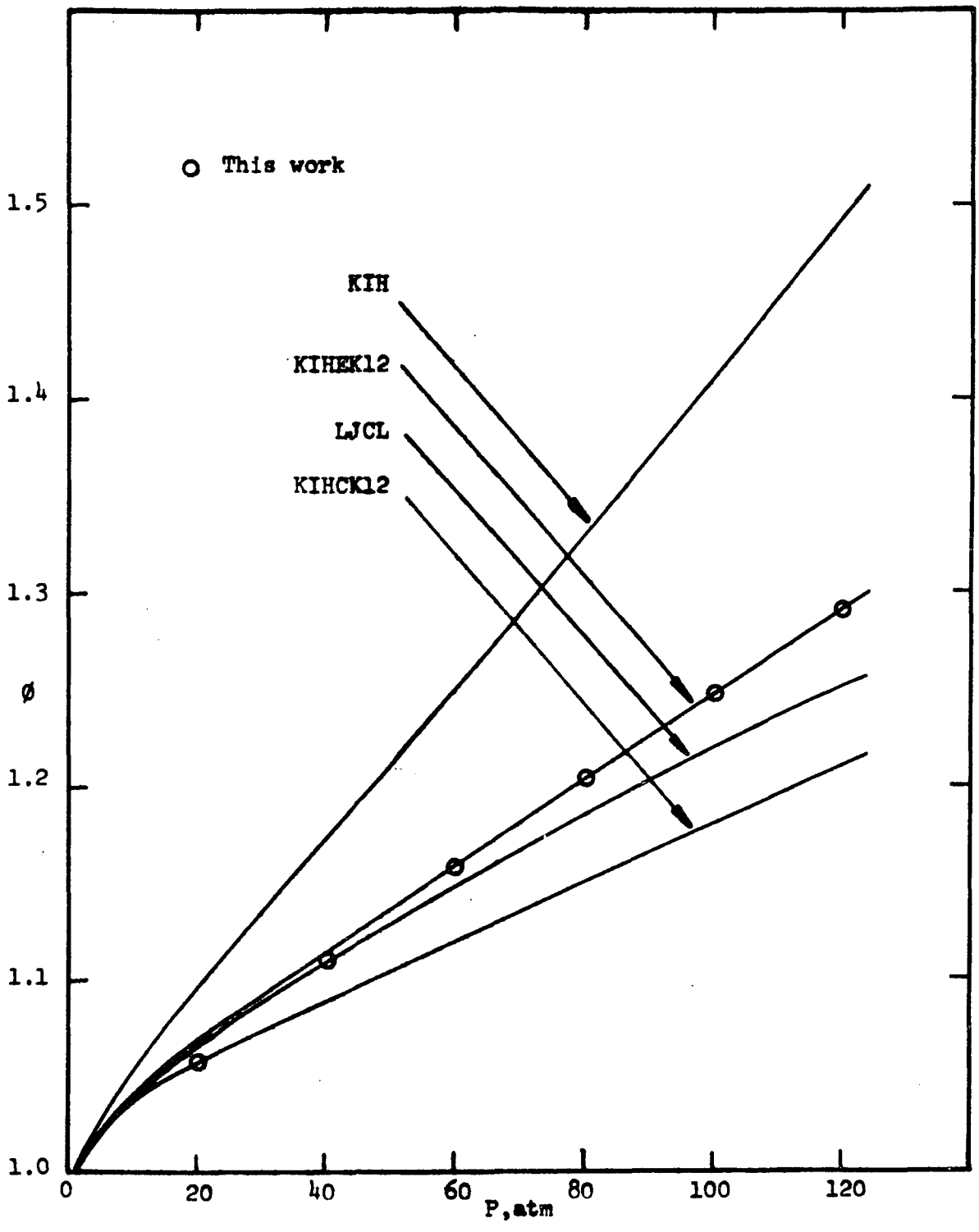

Figure 18. Theoretical and Experimental Enhancement Factors in the Helium-Chlorotrifluoromethane System at 180.02 K.

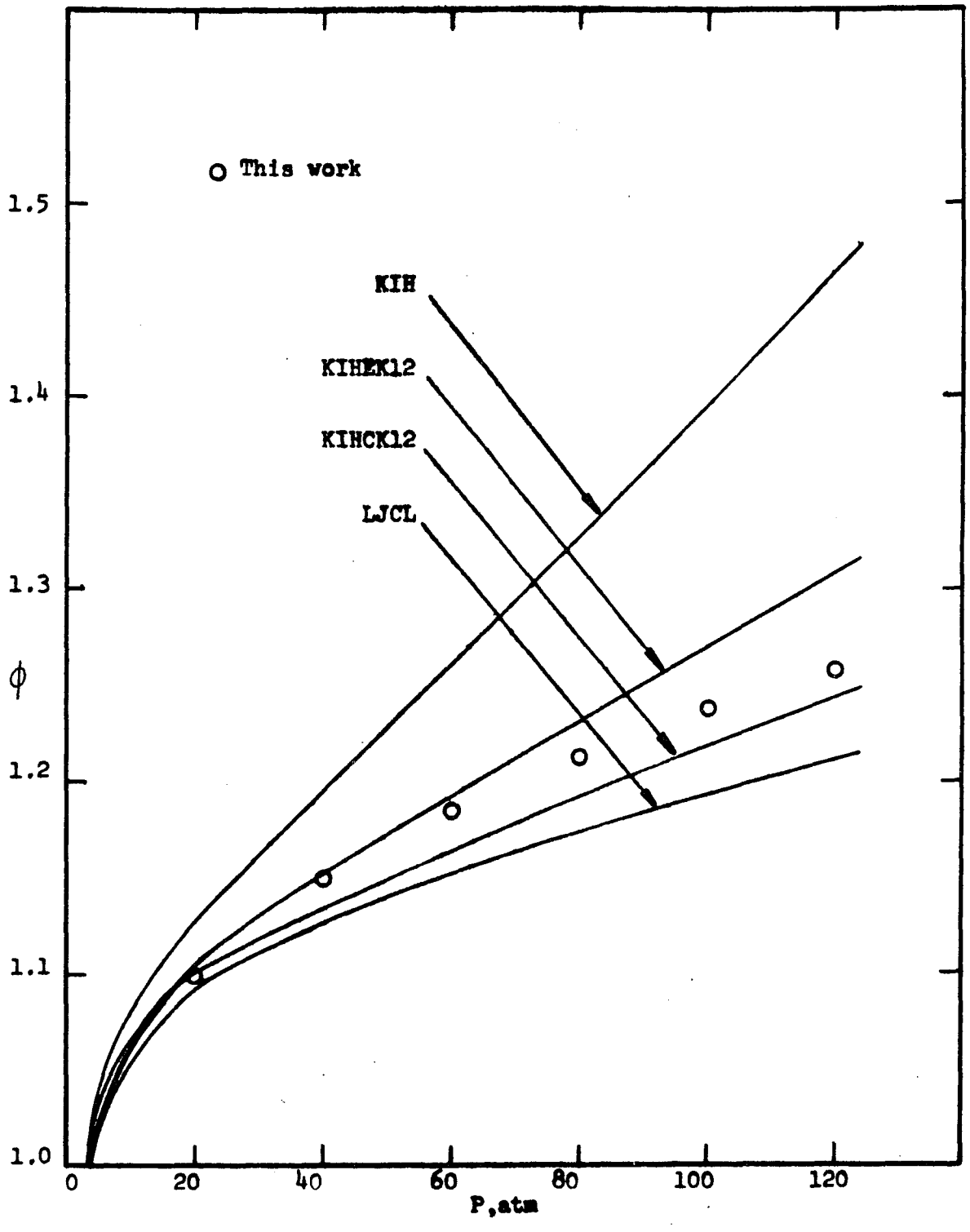

Figure 19. Theoretical and Experimental Enhancement Factors in the Helium-Chlorotrifluoromethane System at 211.06 K.

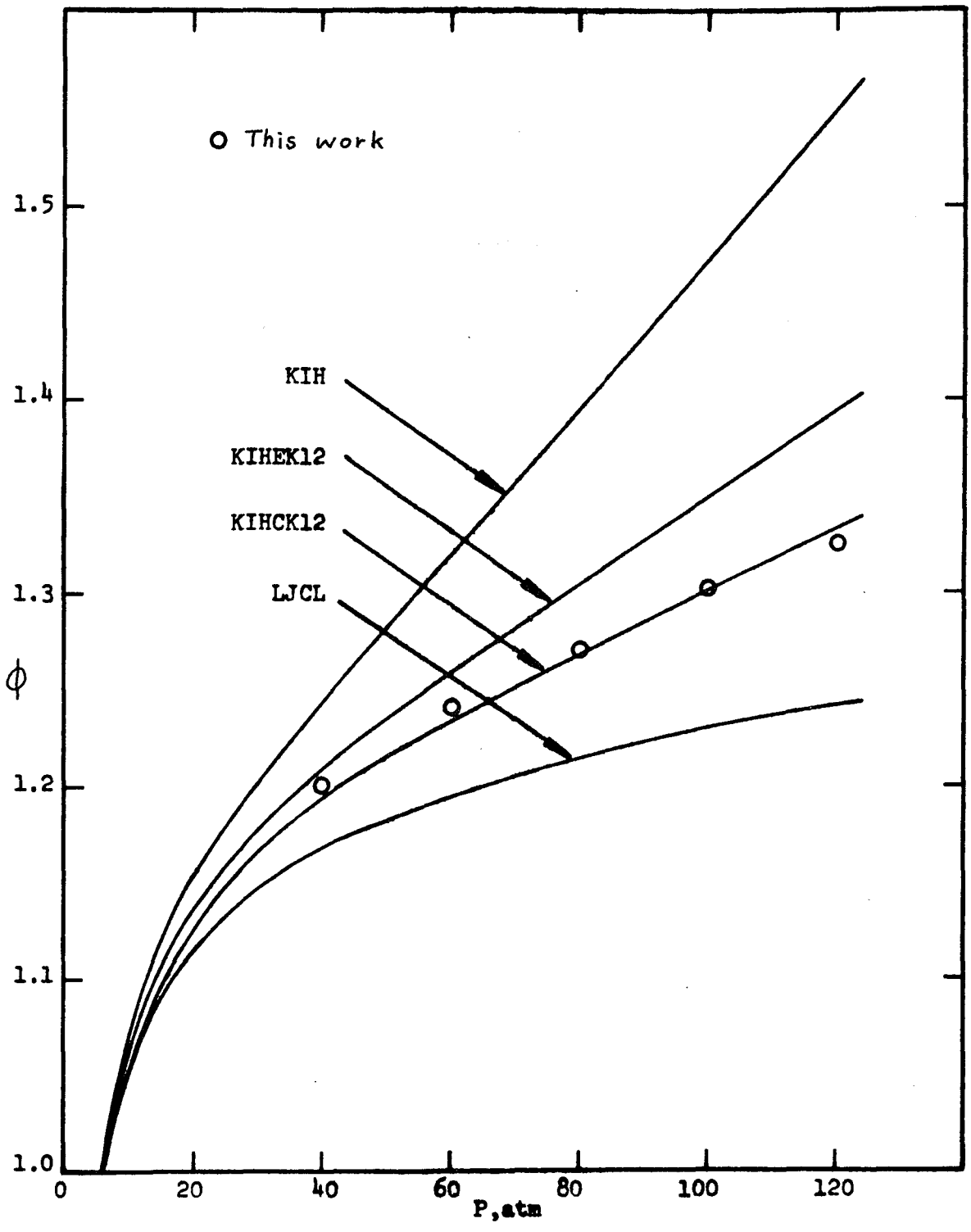

Figure 20. Theoretical and Experimental Enhancement Factors in the Helium-Chlorotrifluoromethane System at 231.08 K.

the low temperatures, the KIHEK12 and LJCL models predict the enhancement factors closest to the experimental values as shown in Figures 13 and 14, and the next best models are KIH and BWR (LORENTZ) whose predicted values are 4 to 8 percent off from the experimental enhancement factors. The BWR (LINEAR) and KIHCK12 models are less satisfactory, the predicted values differing from the experimental data by a maximum of 20 percent. The above trend still exists at the 147.10 K isotherm in Figure 15 though some change occurs as temperature increases. The highest isotherm of 173.02 K presented in Figure 16 shows that none of the theoretical models can predict values resonably close to the experimental enhancement factors. The KIHEK12, BWR (LINEAR), LJCL, and KIHCK12 models represent the experimental data within 6 percent. The predicted values using the KIH and BWR (LORENTZ) models are high by 10 and 15 percent, respectively.

Figure 17 through 20 show the four enhancement factor isotherms of 145.21, 180.02, 211.06, and 231.08 K for the helium-chlorotrifluoromethane system. Two lowest experimental isotherms of 145.21 and 180.02 K shown in Figure 17 and 18 are best represented by the KIHEK12 model, while the LJCL model predicts values which agree with experiment within 5 percent. The KIHCK12 and KIH models are less satisfactory in predicting the enhancement factors, their values differing by as much as 9 and 25 percent, respectively. Figure 19 shows that the enhancement factors predicted with the

KIHEK12, KIHCK12, and LJCL models are in good agreement with the experimental data within 4 percent at all points, but again the KIH model is the poorest one in predicting the enhancement factors at this isotherm of 211.06 K and differs by a maximum of 16 percent. The highest isotherm at 231.08 K is best represented by the KIHCK12 model as shown in Figure 20. The KIHEK12, LJCL, and KIH models predict enhancement factors which deviate by 5, 6, and 17 percent, respectively, from the experimental values.

In the prediction of enhancement factors at low pressures, where the third virial coefficients are insignificant, the B_{12} values play an important role within the same group of theoretical models such as KIH, KIHCK12, and KIHEK12 or BWR (LINEAR) and BWR (LORENTZ). Since the pure second virial coefficients are identical in this case, the effect of B_{12} on the enhancement factor can be seen directly by comparing the B_{12} curves in Figures 10 and 12 with the enhancement factor curves in Figures 13 through 20.

For both of the helium binary systems considered here, the KIH model predicts larger enhancement factors at all the temperatures than not only the other Kihara models, KIHCK12 and KIHEK12, but also BWR (LINEAR) and LJCL models. The predicted enhancement factors from the KIH model are also higher than those from the BWR (LORENTZ) model except at the highest temperature as shown in Figure 16. This can be expected since, first, the K_{12} factor is always positive and

this positive value of K_{12} increases the B_{12} values which contribute negatively to the enhancement factors, and second, B_{12} values of the KIH model are greater than those of the LJCL, BWR (LINEAR), and BWR (LORENTZ) models as shown in Figures 10 and 12 in this chapter. Here, one more comment has to be made on the enhancement factor equation. Since y_1 is much smaller than unity and V_m is very small compared with V_{o1} in Equation (IV-19), the effect of B_{12} on the enhancement factors at the low temperatures is much greater than B_{11} whose predicted values with the KIH, LJCL, and BWR models are quite different from one another at the low temperatures (see Figures 35 and 37 in Appendix H).

Unlike other helium binary gas mixtures, the K_{12} values calculated using Equation (V-5) are quite different from the experimentally determined K_{12} values. This difference produced a considerable difference in the predicted enhancement factors. From these results, it is concluded that the correlation for the K_{12} factor given by Hiza and Duncan[51] is inadequate for the helium-carbon tetrafluoride and helium-chlorotrifluoromethane systems.

Of all theoretical models considered, except the KIHEK12 model which has been adjusted to agree with the experimental enhancement factors, the LJCL model predicts most satisfactorily the enhancement factors for both systems, although the agreement of its predicted values with experimental data is poor at the highest isotherms. The agreement

of the B_{12} values predicted by the LJCL model with the experimental B_{12} values can easily account for this trend.

Mullins,[90] and Garber[37] have shown that the BWR (LINEAR) model gives better results than the BWR (LORENTS) for the prediction of enhancement factors for the hydrogen-argon, helium-ethane, -ethylene, -propane, and -propylene systems. Benedict, et al.[8] have also recommended the BWR (LINEAR) model for the prediction of the phase equilibrium. Both BWR (LINEAR) and BWR (LORENTZ) models were investigated for the calculation of the enhancement factors for the helium-carbon tetrafluoride system in this work. For this system it was found, on the contrary to the expectation, that the BWR (LORENTZ) model generally gave better agreement with the experimental enhancement factors than the BWR (LINEAR) model. Although no further consideration has been made on this subject, this is probably because of the unusual behavior of carbon tetrafluoride. The B_{12} values predicted by the BWR (LORENTZ) model are in much better agreement with the experimental B_{12} values than the BWR (LINEAR) model as shown in Figure 10.

The BWR third virial coefficients of carbon tetrafluoride calculated using Equation (IV-83) are presented with the experimental data in Figure 36 of Appendix H. The BWR parameters used here are extracted from the P-V-T data of carbon tetrafluoride[30] in the temperature region between 0°-350° C. These theoretical third virial coefficients in-

crease exponentially instead of decreasing as temperature decreases below 0° C. These calculated values do not agree even qualitatively with the experimental values which decrease with decreasing temperature below around 225 K. This has been also pointed out by Garber[37] in his study of the BWR equation for ethane, ethylene, propane, and propylene. This inconsistency clearly shows that the extrapolation of the BWR third virial coefficients to the lower temperatures is highly inadequate. Although the BWR third virial coefficients of carbon tetrafluoride are probably grossly in error at low temperatures, nevertheless the enhancement factors predicted using the BWR models are generally satisfactory. This is probably because in the temperature region considered in this work (106-173 K), the contribution of C_{111} (also C_{112} and C_{122}) values to the enhancement factors is negligible and some higher order volume terms in the BWR equation, Equation (IV-71), may be compensating for the large error in these predicted third virial coefficients.

Some investigators[37,46,51,111] have experimentally shown that the enhancement factors in the helium binary systems decrease along an isobar with increasing temperature and then increase with increasing temperature, thereby generating a minimum point in the enhancement factor isobars. Recently, Garber[37] has pointed out that this minimum in the enhancement factor isobars is rather general in the helium binary systems and seems to be unique to these systems. The

enhancement factor isobars shown in Figures 4 and 8 in Chapter III also show this minimum as can be expected. This phenomenon is more pronounced at the higher isobars where the third virial coefficients are important. Table 14 and 15 in Appendix G show that all theoretical models used exhibit this minimum in their isobars. In other words, the prediction of enhancement factors using these various theoretical models can be at least qualitatively satisfactory. It is quite natural to expect a maximum point in the helium binary enhancement factor isobars below the critical pressure, since the enhancement factor is unity when the total pressure of a binary system is equal to the vapor pressure of the condensible component. This maximum has been also demonstrated by Garber[37] using experimental and theoretical enhancement factor isobars of the helium-ethane system at 20 atmospheres. The theoretical models used by Garber were the KIH, LJCL, and BWR (LINEAR) models. Unfortunately, in this work this maximum could not be shown conclusively because the highest temperature covered may not have been high enough for the 20 atm enhancement factor isobar to exhibit a maximum. However, Figure 4 in Chapter III shows that the experimental 20 atm enhancement factor isobar in the helium carbon tetrafluoride system tend to bend downward at the highest temperature, barely showing a maximum.

From the enhancement factor calculation, the following

conclusions can be drawn. First, the theoretical model which can predict the B_{12} values accurately predicts generally the better enhancement factors. Second, accordingly, the KIHEK12 model is the best in predicting the enhancement factors in both helium binary systems considered here except at the highest isotherm in the helium-chlorotrifluoromethane system, where the predicted enhancement factors deviate from the experimental data by a maximum of 5 percent. The LJCL model is generally quite satisfactory in predicting the enhancement factors except at the highest isotherms where the calculated and experimental enhancement factors agree within 6 percent. Third, the correlation of Hiza and Duncan[51] has to be improved or new correlation is necessary for the correction factor, K_{12}, to the geometric mixing rule for the Kihara energy parameter for the helium-carbon tetrafluoride and helium-chlorotrifluoromethane systems.

CHAPTER VI

COMPARISON OF PREDICTED AND EXPERIMENTAL LIQUID PHASE EQUILIBRIUM DATA

Experimental Henry's Law Constant and Partial Molar Volume at Infinite Dilution

Introduction

The amount of gas which is dissolved in a liquid at a given temperature depends on the partial pressure of the gas in equilibrium with the liquid. For a binary gas-liquid phase equilibrium system where the solubility of the gas and total pressure are small, this relation can be written as

$$Py_2 = Hx_2 \qquad \text{(VI-1)}$$

which is widely known as the original Henry's law and is a special case of a more general thermodynamic formulation.

The conditions for the binary systems considered in this work are such that one component of a system (helium) is well above its critical temperature and the other component below its critical temperature, and that the two phases are in equilibrium. It is required from the latter that the chemical potential of the solute gas dissolved in the liquid phase be equal to the chemical potential of that species in the gas phase for a given temperature. This is the same

criterion for the phase equilibrium as described in Chapter IV. Thus,

$$\mu_2^G(P,T,y_2) = \mu_2^L(P,T,x_2) \qquad \text{(VI-2)}$$

The chemical potential of the component 2 in the liquid phase can be written as

$$\mu_2^L(P,T,x_2) = \mu_2^{*L}(P,T) + RT \ln (\gamma_2' x_2) \qquad \text{(VI-3)}$$

where $\gamma_2' \to 1$ as $x_2 \to 0$, while $P \to P_{o1}$

The standard state for the gase phase is chosen as an ideal gas at one atmosphere for convenience's sake. The chemical potential of the component 2 in the gas phase can now be expressed as

$$\mu_2^G(P,T,y_2) = \mu_2^o(P=1, T) + RT \ln \frac{f_2^G}{f_2^o} \qquad \text{(VI-4)}$$

where f_2^o is unity from the choice of the standard state. Substituting Equations (VI-3) and (VI-4) into Equation (VI-4), and defining

$$\ln H_2(P,T) = \frac{\mu_2^{*L}(P,T) - \mu_2^o(P=1,T)}{RT} \qquad \text{(VI-5)}$$

one obtains

$$\ln \frac{f_2^G(P,T,y_2)}{x_2} = \ln H_2(P,T) + \ln \gamma_2' \qquad \text{(VI-6)}$$

In Equation (VI-5), $H_2(P,T)$ is the thermodynamic Henry's law constant and has the units of atmospheres. H_2^{∞}, the Henry's law constant at infinite dilution, is the value of $H_2(P,T)$ in Equation (VI-5) in the limit as $x_2 \to 0$ and $P \to P_{o1}$ at a given temperature.

If Equation (VI-3) is differentiated with respect to pressure at constant temperature and composition, Equation (VI-7) can be obtained.

$$\left(\frac{\partial \mu_2^{L}}{\partial P}\right)_{T,x_2} = \bar{V}_2 = \left(\frac{\partial \mu_2^{*L}(P,T)}{\partial P}\right)_{T} + RT \left(\frac{\partial (\ell n\, \gamma_2')}{\partial P}\right)_{T,x_2} \qquad \text{(VI-7)}$$

Since the region of interest is near $x_2 = 0$, the last term in Equation (VI-7) can be set equal to zero. Thus,

$$\left(\frac{\partial \mu_2^{*L}(P,T)}{\partial P}\right)_{T} = \bar{V}_2^{\infty} \qquad \text{(VI-8)}$$

Differentiation of Equation (VI-5) with respect to pressure at constant temperature gives

$$\left(\frac{\partial \ell n\, H_2\,(P,T)}{\partial P}\right)_{T} = \frac{1}{RT}\left(\frac{\partial \mu_2^{*L}}{\partial P}\right)_{T} = \frac{\bar{V}_2^{\infty}}{RT} \qquad \text{(VI-9)}$$

Integrating Equation (VI-9), one obtains

$$\ell n\, H_2\,(P,T) = \ell n\, H_2^{\infty}\,(P_{o1},T) + \frac{1}{RT}\int_{P_{o1},T}^{P,T} \bar{V}_2^{\infty}\, dP \qquad \text{(VI-10)}$$

Subtitution of Equation (VI-10) into Equation (VI-6) gives

$$\ln \frac{f_2^G}{x_2} = \ln H_2^{\infty}(P_{o1},T) + \frac{1}{RT}\int_{P_{o1},T}^{P,T} \overline{V}_2^{\infty}\, dP + \ln \gamma_2' \qquad \text{(VI-11)}$$

This exact thermodynamic relation for the solubility x_2 of a gas in a binary liquid phase has been used by other investigators.[37,90,93,126]

If the change of $\overline{V}_2^{\infty}$ with pressure can be safely assumed to be negligible and the composition of the component 2 in the liquid phase, x_2, for all the systems considered in this work is never greater than 6 percent, so that the liquid phase can be assumed to be an ideal solution (i.e. $\gamma_2' = 1$), Equation (VI-11) can be reduced to the Krichevsky-Kasarnovsky equation.[73]

$$\ln \frac{f_2^G}{x_2} = \ln H_2^{\infty}(P_{o1},T) + \frac{\overline{V}_2^{\infty}(P - P_{o1})}{RT} \qquad \text{(VI-12)}$$

This is the working equation that has been used in this work. It may be noted that Equation (VI-12) reduces to Equation (VI-1) if the system pressure is low and the last term in Equation (VI-12) is neglected, that is, $P - P_{o1} \rightarrow 0$.

From Equation (VI-12), the values of H_2^{∞}, and $\overline{V}_2^{\infty}$ can be extracted using experimental phase equilibrium data and an equation of state model for the gas phase. Thus a plot of $\ln (f_2^G/x_2)$ versus $(P - P_{o1})$ should give a straight line whose

intercept at $(P - P_{o1}) = 0$ is equal to $\ell n\ H_2^\infty$ and whose slope is equal to $\bar{V}_2^\infty/(RT)$. The only unknown in the graphical evaluation of H_2^∞ and $\bar{V}_2^\infty$ values from Equation (VI-12) is the gas phase fugacity, f_2^G, since the values of x_2 have already been experimentally obtained for the helium binary systems considered here. Choosing the standard state for the gas phase as an ideal gas at one atmosphere, the following expression for f_2^G may be derived.

$$\ell n\ f_2^G = \frac{1}{RT} \int_V^\infty \left[\left(\frac{\partial P}{\partial n_2}\right)_{V,T,n_1} - \frac{RT}{V}\right] dV - \ell n\ \frac{V}{n_2 RT} \qquad \text{(VI-13)}$$

The evaluation f_2^G from this equation requires an equation of state for the gas mixture as well as the composition of the gas phase which has been experimentally determined for the systems of this work and whose smoothed values are presented in the form of the enhancement factor (and hence y_1) in Table 14 and 15 of Appendix G. The virial equation of state is used as an equation of state for the gas mixture since the necessary data for the virial equation of state have already been determined in Chapter V. Using Equation (IV-14), the integral in Equation (VI-13) can be evaluated. Thus, after some albegraic manipulation, Equation (IV-14) is obtained[37] from Equation (VI-13).

$$\ell n\ \frac{f_2^G}{x_2} = \frac{2(y_1 B_{12} + y_2 B_{22})}{V_m} + \frac{3(y_1^2 C_{112} + 2y_1 y_2 C_{122}}{2V_m^2} \qquad \text{(VI-14)}$$

(Continued)

$$\frac{+ y_2^2 C_{222})}{} + \ln \frac{y_2 RT}{x_2 V_m}$$

Since the virial coefficients used in evaluating Equation (VI-14) are not determined homogeneously but selected on the basis of the best representation to the experimental data, the values of these virial coefficients have to be specified here in detail. The virial equation of state truncated after the third virial coefficient was used for the evaluation of V_m. The values of x_2, y_1, and B_{12} used are those experimentally determined in this work; Tables 1 and 2 in Chapter V show the B_{12} values and the y_1 and x_2 values are given in Tables 14 and 15 in Appendix G. The values of C_{222} are presented in Figure 34 of Appendix H and all the other third virial coefficients were predicted using the method of Chueh and Prausnitz[18] whose parameters are given in Table 16 of Appendix H. The B_{11} and B_{22} values were estimated using the Kihara and Lennard-Jones parameters, respectively, given in Table 18 of Appendix H. The K_{12} values used for the evaluation of the interaction virial coefficients, C_{112} and C_{122}, were those extracted in this work and given in Table 3 of Chapter V.

There are several other methods for the extraction of the Henry's law constant from phase equilibrium data. One of these methods makes use of a pseudo Henry's law constant, $\overline{K}_2^{\infty}$, which is defined as

$$\overline{K}_2^{\infty} = \lim_{\substack{(P-P_{o1})\to 0 \\ x_2 \to 0}} \frac{P - P_{o1}}{x_2} \qquad \text{(VI-15)}$$

This method has been used by Mullins,[90] Hiza, et al.,[47,52,53] and Heck,[46] and Garber.[37] By plotting

$$\overline{K}_2 = \frac{P - P_{o1}}{x_2} \qquad \text{(VI-16)}$$

versus $(P - P_{o1})$ and extrapolating to $(P - P_{o1}) = 0$, the value of $\overline{K}_2^{\infty}$ can be obtained as an intercept. The evaluation of $\overline{K}_2^{\infty}$ from experimental data P, P_{o1}, and x_2 provides a very direct method for examining the internal consistency of the experimental data. It is referred to as the consistency method in this thesis. Since the evaluation of $\overline{K}_2^{\infty}$ values is simple and values of H_2^{∞} predicted using Equation (VI-12) agree very well with those of $\overline{K}_2^{\infty}$, this method has been also used in this work. It is interesting to note that if the total pressure P is small, Equation (VI-12) reduces to Equation (VI-15) as $P - P_{o1} \to 0$ while $x_2 \to 0$.

Recently, Solen, et al.[126] have also presented a method for the extraction of H_2^{∞}, but since the necessary parameters for this method for the systems considered here are not available, this method is not used in this work. Sinor, et al.[122] have used the same Krichevsky-Kasarnovsky equation (see Equation (VI-12)) as used in this work to

extract H_2^∞ and $\overline{V}_2^\infty$, but in the calculation of the fugacity of the gas, f_2^G, they assumed that the gas phase is an ideal solution, that is,

$$f_2^G = y_2 f_{(pure)}^G \qquad \text{(VI-17)}$$

based on the Lewis-Randall rule. This assumption is valid only when the value of y_1 is very close to zero so that the effects of B_{12}, C_{112}, and C_{122} on f_2^G in Equation (VI-14) can be safely neglected. Since the values of y_1 in the systems of this work are not so small, this method has not been used in this work either.

Using Equation (VI-12) and the consistency method, the Henry's law constants and $\overline{K}_2^\infty$ values are graphically extracted from the phase equilibrium data of this work for the helium-carbon tetrafluoride and helium-chlorotrifluoromethane systems. The results are presented in the following sections, together with the values of $\overline{V}_2^\infty$ extracted using Equation (VI-12). The smoothed values of H_2^∞ presented in the following tables were obtained from the smooth curve which represents the extracted values of H_2^∞ from Equation (VI-12). The extracted values of $\overline{V}_2^\infty$ in this work have been smoothed and these smoothed values are given in the following tables. Since no experimental H_2^∞ and $\overline{V}_2^\infty$ data were available for the systems of this work in the literature, no comparison could be made.

Experimental Values of H_2^∞ and $\overline{V}_2^\infty$ for the Helium-Carbon Tetrafluoride System

The phase equilibrium data for this system have been measured in this work and are the only available data. The temperature range of 106.01 to 173.02 K and pressures up to 120 atmospheres are covered in this work. The smoothed values of these data given in Table 14 of Appendix G are used for the extraction of H_2^∞ and $\overline{V}_2^\infty$.

Table 4. H_2^∞ and $\overline{V}_2^\infty$ for the Helium-Carbon Tetrafluoride System

T, K*	H_2^∞, atm		$\overline{V}_2^\infty$, cc/gm mole	
	From Equation (VI-12)	Smoothed	From Equation (VI-12)	Smoothed
106.01	11,830 ± 287	11,840	18.2 ± 1.5	17.9
117.33	7.723 ± 140	7,715	20.2 ± 1.5	18.9
132.18	4,949 ± 75	4,975	19.3 ± 1.5	20.6
147.10	3,308 ± 60	3,310	24.1 ± 1.7	23.1
162.03	2,336 ± 51	2,345	25.6 ± 2.1	26.6
173.02	1,812 ± 33	1,810	30.5 ± 2.1	30.3

* Corresponding vapor pressures are presented in Table 19.

The values of H_2^∞ obtained using Equation (VI-12) agree very well with those from the consistency method as shown in Figure 21. They are smoothed and these smoothed values are presented in Table 4 together with the $\overline{V}_2^\infty$ values.

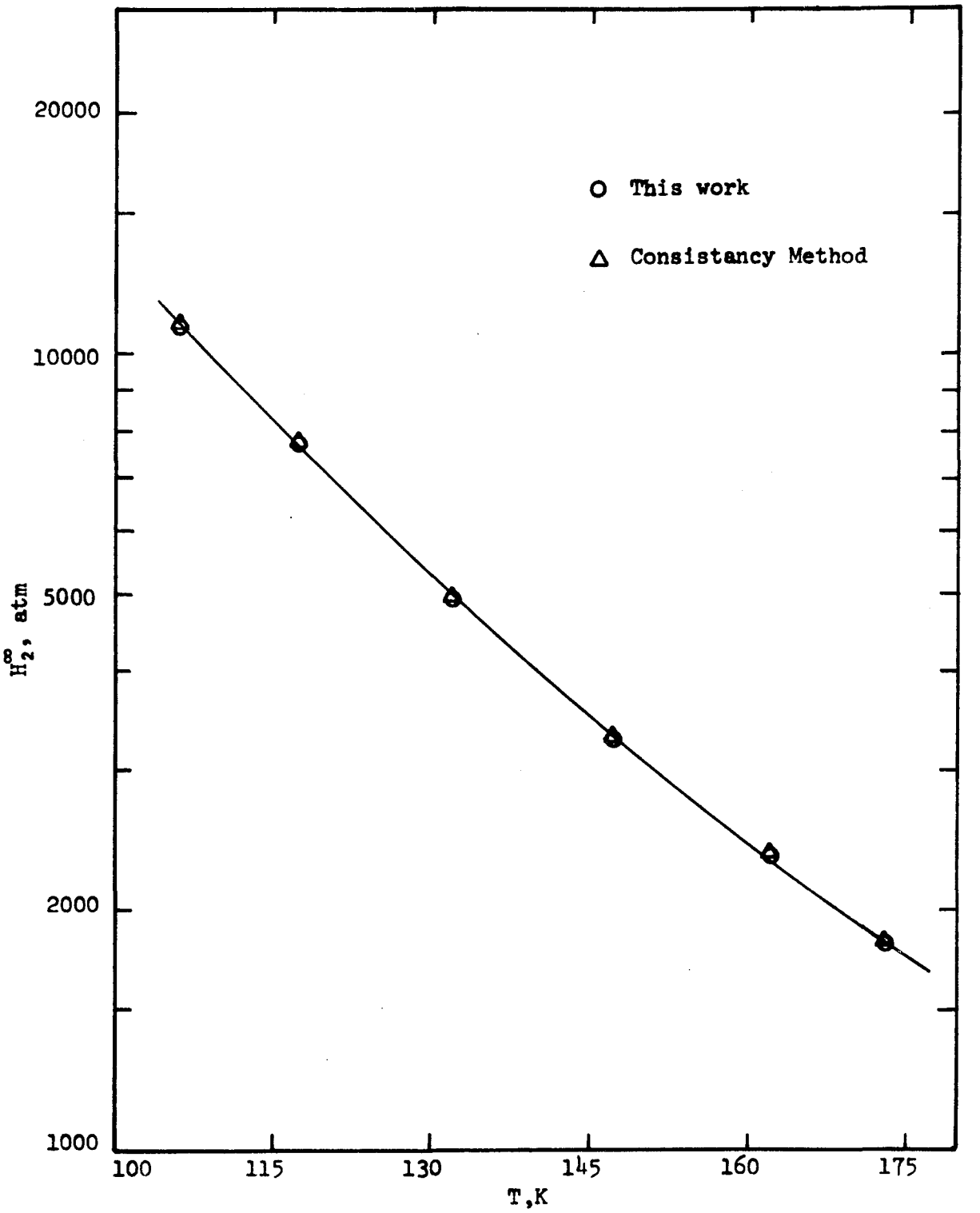

Figure 21. Experimentally Determined Henry's Law Constants for the Helium-Carbon Tetrafluoride System.

The error ranges shown in this table are determined by varying the input data of y_1 and x_2 by the corresponding experimental errors.

Experimental Values of H_2^∞ and $\overline{V}_2^\infty$ for the Helium-Chlorotrifluoromethane System

The H_2^∞ and $\overline{V}_2^\infty$ values for the helium-chlorotrifluoromethane system have been extracted from the smoothed phase equilibrium data of this work which are presented in Table 15 of Appendix G. These data have been obtained over the

Table 5. H_2^∞ and $\overline{V}_2^\infty$ for the Helium-Chlorotrifluoromethane System

T, K*	H_2^∞, atm		$\overline{V}_2^\infty$, cc/mole	
	From Equation(VI-12)	Smoothed	From Equation(VI-12)	Smoothed
145.21	10,037 ± 327	10,000	18.4 ± 3.2	17.9
163.01	6,516 ± 179	6,550	18.2 ± 3.6	19.3
180.02	4,537 ± 148	4,570	20.7 ± 3.9	21.1
196.01	3,314 ± 122	3,340	25.7 ± 4.8	23.3
211.06	2,599 ± 87	2,540	25.5 ± 4.8	26.5
221.27	2,191 ± 76	2,160	28.0 ± 5.0	29.3
231.08	1,808 ± 66	1,830	34.8 ± 6.0	33.2

* Corresponding vapor pressures are presented in Table 19.

temperature range of 145.21 to 231.08 K and pressures up to 120 atmospheres. Since no other phase equilibrium data

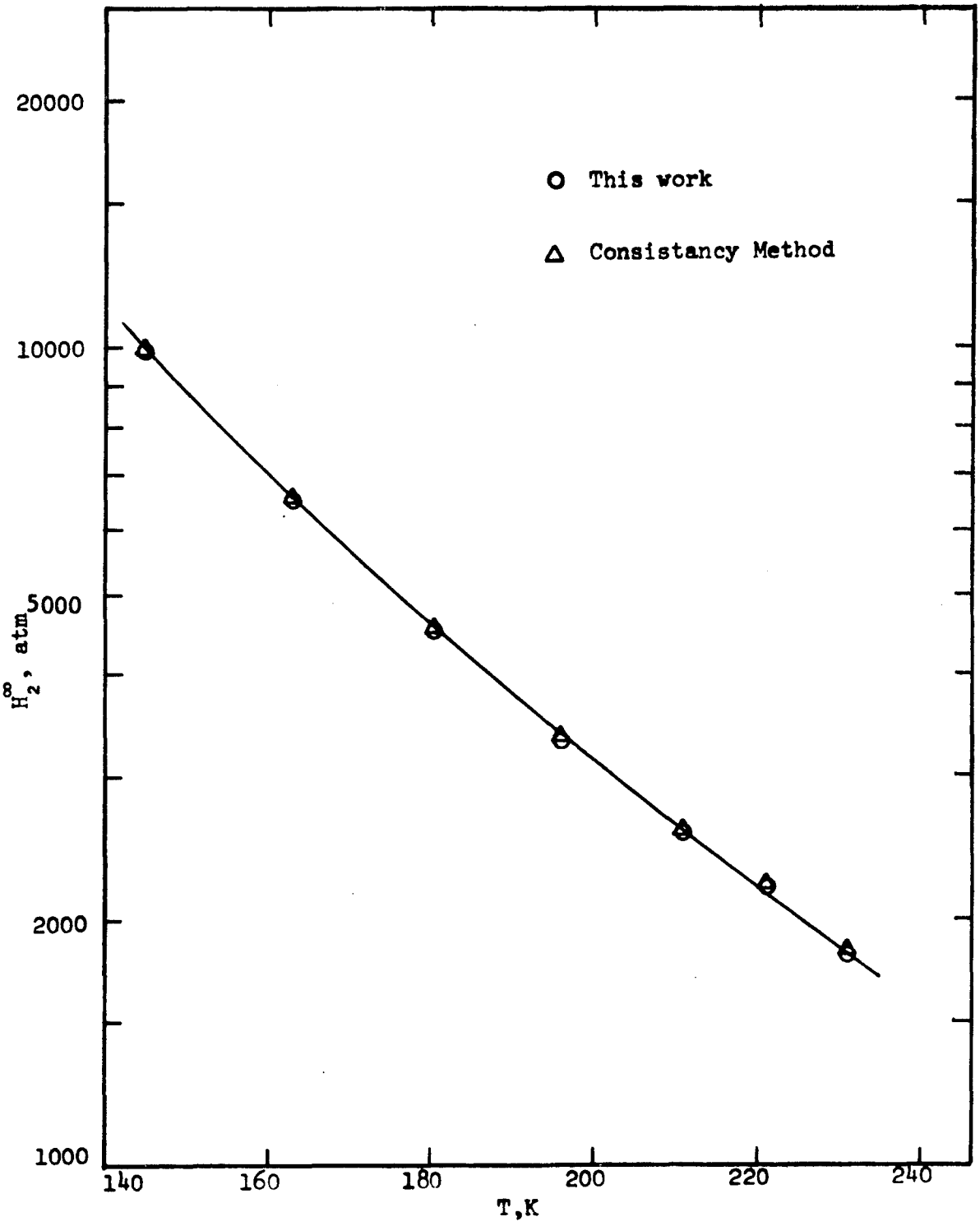

Figure 22. Experimentally Determined Henry's Law Constants for the Helium-Chlorotrifluoromethane System.

or the values of H_2^∞ and $\overline{V}_2^\infty$ were available for this system, no comparison could be made

The extracted values of H_2^∞ in this work are compared with those obtained from the consistency method in Figure 22 and their agreement is again very satisfactory. Table 5 show the calculated and smoothed values of H_2^∞ and $\overline{V}_2^\infty$ for this system as a function of temperature. The experimental error of ±3.5 percent of y_1 and ±2.0 percent of x_2 produced a maximum error of 3.5 percent in H_2^∞ and 18.5 percent in $\overline{V}_2^\infty$.

Discussion of Results

As can be seen in Figures 21 and 22, the values of H_2^∞ extracted using Equation (VI-12) are in excellent agreement with those obtained from the consistency method and the deviations are mostly less than one percent. This agreement can be naturally expected since the value of the term, $\overline{V}_2^\infty(P-P_{01})/RT$ in Equation (VI-12) is small compared with the other terms when total pressure, P, is not too large and the values of f_2^G differ only slightly from the values of $P - P_{01}$ in this case. Actually, Equation (VI-12) reduces to Equation (VI-15) (consistency method) as $P-P_{01} \to 0$ while $x_2 \to 0$ when P is small. Therefore, the values of H_2^∞ and $\overline{K}^\infty$ are getting closer to each other as the value of $P-P_{01}$ decreases and finally they become identical at $P - P_{01} = 0$ when P is small.

The range of percent error of $\overline{V}_2^\infty$ values is much greater than that of H_2^∞ values as can be seen in Tables 4

and 5. This is because in the systems of this work a small percent change of H_2^∞ values produces a large percent change in the slope of the $\ell n\ f_2^G/x_2$ versus $(P - P_{01})$ curve which determines the value of $\overline{V}_2^\infty$.

A good summary of the H_2^∞ and $\overline{V}_2^\infty$ values for the helium binary systems is given recently by Garber.[37] In his paper, he has compared the values of H_2^∞ and $\overline{V}_2^\infty$ for a number of binary systems at a reduced temperature of 0.75 and stated that no systematic trend could be found within the helium-hydrocarbon series. He has also pointed out that of all the helium binary systems studied the helium-nitrogen system gives the smallest H_2^∞ and $\overline{V}_2^\infty$ values, indicating the highest solubility of helium in the liquid nitrogen. In this work, the values of H_2^∞ in the helium-carbon tetrafluoride and helium-chlorotrifluoromethane systems have been found to be even smaller than those in the helium-nitrogen systems; the H_2^∞ value of $T_{R1} = 0.75$ for the helium-carbon tetrafluoride system is 1920 atm and that for the helium-chlorotrifluoromethane system 1960 atm, compared with the H_2^∞ value of 2120 atm for the helium-nitrogen system at the same reduced temperature. Although no attempt has been made to account for this high solubility of helium in the liquid carbon tetrafluoride and chlorotrifluoromethane, this is probably due to the anomalous solvent behavior of fluorochemicals. The values of $\overline{V}_2^\infty$ in the helium-hydrocarbon systems studied by Garber[37] are all above 30 cc/gm mole at

T_{R1} = 0.75, the smallest being 30.7 cc/gm mole in the helium-methane system. This value is comparable to the values of $\overline{V}_2^{\infty}$ in the helium-carbon tetrafluoride and helium-chlorotrifluoromethane systems, which are 27.8 and 31.1 cc/gm mole at T_{R1} = 0.75, respectively.

Theoretical Prediction of Henry's Law Constant and Partial Molar Volume at Infinite Dilution

Introduction

Many investigators have endeavored to describe the properties of a liquid phase as the solubility of gases in liquids have become increasingly important for both the theoretical understanding of the liquid state and solutions, and for practical applications. As a result, some remarkable advances have been made in the theory and empirical correlations during the last decade. Various theories of statistical mechanics of fluids have been developed and tested. Some are fundamental, being based on first principles, and some are semi-empirical or heuristic. However, no single theory has been applied satisfactorily to a variety of gas-liquid systems for the prediction of the gas solubilities in liquids.

An examination of the literature has revealed several good methods for the prediction of the solubility of gas in a liquid phase in terms of Henry's law constant, H_2^{∞}, and for the prediction of partial molar volume at infinite dilution, $\overline{V}_2^{\infty}$. Miller and Prausnitz,[88] using the free volume theory,[103],

[111] have presented a semi-empirical correlation for the prediction of the Henry's law constant for a high pressure system with one component well above its critical temperature. Only one empirical parameter, K_{12}, which has been discussed in Chapter V and is adjustable for the best agreement with the gas solubility data is included in their expression. Their results have shown that the agreement of predicted values of H_2^∞ with the experimental values of H_2^∞ is satisfactory. As they indicated, however, a change in K_{12} of 0.04 can change the predicted Henry's law constant by 20 to 30 percent. Since K_{12} is dependent on temperature, this method may cause large errors when applied over a wide temperature range.

Another method based on the scaled particle theory[106, 107] for the calculation of H_2^∞ and $\overline{V}_2^\infty$ has been presented by Pierotti[94,95] and used by Heck[46] and Garber.[37] This scaled particle theory based on first principles has been used in this method to treat a hard sphere model of gas solubility. Garber has sucessfully used this method for the helium binary systems and concluded that the values of H_2^∞ and $\overline{V}_2^\infty$ predicted are in satisfactory agreement with experimental data, and a slight modification of this method to fit the experimental data gives an excellent agreement between the predicted and experimental H_2^∞ values. Although this method appears to be one of the best methods available for the prediction of H_2^∞ and $\overline{V}_2^\infty$ values, the method employed by Pierotti,[94,95], Heck,[46]

and Garber[37] draws heavily on experimental data to determine the best values of the parameters needed in this method.

Very recently, Preston and Prausnitz[101] have shown a generalized thermodynamic expression for Henry's law constants based on the statistical mechanics of dilute liquid solutions. They have applied this correlation to obtain Henry's law constants in 60 nonpolar binary systems and the results were found to be quite satisfactory. But since their correlation is derived using the empirical two-parameter Strobridge equation of state, it may not be applied over a wide range of temperature as they recommended. Furthermore, it requires the experimental H_2^∞ data to extract the necessary parameters for the prediction of Henry's law constants, and these parameters have to be determined using the tidious graphical procedure.

Snider and Herrington[125] have developed a method for the calculation of the excess thermodynamic functions of binary liquid mixtures and also for the problem of the solubility of gases in liquids by applying the hard sphere model for fluids. This method has been used in the present work for the prediction of H_2^∞ and $\overline{V}_2^\infty$ values and is discussed in detail in the following sections.

Method of Snider and Herrington

This method which is based on first principles, is basically similar to that given by Pierotti[94,95,96] except that the equation of state for the hard sphere fluid

$$\frac{P}{\bar{\rho} kT} = \chi(\xi) \qquad \text{(VI-18)}$$

was used in Pierotti's method, where

$$\chi(\xi) = \frac{(1 + \xi + \xi^2)}{(1 - \xi)^3} \qquad \text{(VI-19)}$$

$$\xi = \frac{\pi \bar{\rho} r^3}{6} \qquad \text{(VI-20)}$$

and

$$\bar{\rho} = \frac{N_A}{v_{o1}} \qquad \text{(VI-21)}$$

Equation (VI-18), which is actually an approximation in cloased form for the equation of state for the hard-sphere fluid, was obtained first from the scaled particle theory[106] [107] and later from the solution of the Percus-Yevick equation for the hard sphere model.[133,137] Since this hard sphere model does not take into account configurational internal energy, it can not represent satisfactorily a real liquid.

Longuet-Higgins and Wisdom[78] have proposed a simple liquid model which has a finite configurational internal energy. By assuming a field of uniform and negative potential energy for a fluid of hard spheres, they have developed an equation of state for this model, which describes quite

well the thermodynamic properties of argon at its triple point. This equation is

$$\frac{P}{\bar{\rho}kT} = \chi(\xi) - \frac{a\bar{\rho}}{kT} \qquad \text{(VI-22)}$$

where a can be regarded as a measure of the strength of the attractive background potential. Equation (VI-22) has been successfully applied to the pure liquids of small, non-polar molecules. Snider and Herrington[125] have generalized this equation to the case of binary mixtures and calculated the excess thermodynamic functions of binary mixtures composed of simple molecules. The agreement of their results with experimental data appears to be quite satisfactory.

Snider and Herrington[125] have also applied this equation for the calculation of H_2^∞ and $\bar{V}_2^\infty$ values for a binary system in which component 1, a liquid solvent, is below its critical temperature and component 2, a gaseous solute, is well above its critical temperature. But, this case they concluded that the agreement with experiment was not good for the neon-argon system. Later, Staveley[127] pointed out that this disagreement was due to their choice of data for the neon-argon system and misinterpretation of these data. He has recalculated the solubility data for this system and proved that this method predicts excellent values of H_2^∞ and $\bar{V}_2^\infty$ for the systems shown in Table 9.

This method is described in detail in the following

section. The expressions[125] used in this method are:

$$\ln \frac{H_2^{\infty}}{\bar{\rho} kT} = - \ln (1 - \xi) + \xi\chi(\xi) \left(\frac{r_2}{r_1}\right)^3 + \frac{1}{2} \qquad \text{(VI-23)}$$

$$\times \left(\frac{3\xi}{1 - \xi}\right)^2 \left(\frac{r_2}{r_1}\right)^2 + \frac{3\xi}{1 - \xi} \left[\left(\frac{r_2}{r_1}\right)^2 + \frac{r_2}{r_1}\right] - \frac{2a_{12}\bar{\rho}}{kT}$$

$$\frac{\bar{\rho}\bar{V}_2^{\infty}}{N_A} = \frac{(1 - \xi)^4}{2\xi^3 + 4\xi^2 + 4\xi - 1} w \qquad \text{(VI-24)}$$

$$w = \left(\frac{\xi}{1 - \xi}\right) \left[\frac{(1 + 2\xi)^2}{(1 - \xi)^3} \left(\frac{r_2}{r_1}\right)^3 + 3 \frac{1 + 2\xi}{(1 - \xi)^2} \left(\frac{r_2}{r_1}\right)^2 \right. \qquad \text{(VI-25)}$$

$$\left. + \left(\frac{3}{1 - \xi}\right) \left(\frac{r_2}{r_1}\right) + 1 \right] - \frac{2a_{12}\bar{\rho}}{kT} + 1$$

The values of the hard sphere diameter r can be obtained from the boiling point data for pure components using either Equation (VI-26)[125] or (VI-27)[125,127]

$$\frac{\Delta H_v}{N_A kT} = \ln \frac{P_o}{\bar{\rho} kT} - \ln (1 - \xi) + \frac{3}{2}\xi \frac{2 - \xi}{(1 - \xi)^3} \qquad \text{(VI-26)}$$

$$\frac{\Delta H_v}{N_A kT} = \chi(\xi) + 1 - \frac{2P_o}{\bar{\rho} kT} \qquad \text{(VI-27)}$$

The last term in Equation (VI-27) is usually negligible except for very low-boiling liquids. Once the values of r

are determined, the values of parameter a can be calculated from Equation (VI-22) using the same boiling point data as was used in Equation (VI-26) or (VI-27). In order to determine the values of a_{12}, at least one experimental value of H_2^{∞} must be forced to agree with Equation (VI-23). Once the values of r and a_{12} are known, the values of H_2^{∞} and $\overline{V}_2^{\infty}$ are readily calculated using Equations (VI-23) and (VI-24).

Snider and Herrington[125] and Staveley[127] have used both Equations (VI-26) and (VI-27) to calculate the values of hard sphere diameter r and shown that there is not much difference between these two values. However, Staveley[127] pointed out in his paper that the value of r for helium calculated using Equation (VI-26) was 0.6 Å which seemed to be much too small, whereas that from Equation (VI-27) was 2.216 Å which is reasonable. Thus, the calculation of r values in this work is restricted to Equation (VI-27). The values of r and a evaluated for the helium-carbon tetrafluoride and helium-chlorotrifluoromethane systems using the boiling point data in Table 6 are presented in Table 7 together with the values of a_{12}. These a_{12} values have been extracted by least-square fitting the experimental H_2^{∞} data to Equation (VI-23). In this sense, the method of Snider and Herrington used in this work for the prediction of H_2^{∞} values can be said semi-empirical, though this method is firmly based on first principles. The experimental saturated liquid molar volumes given in Table 7 were used for the

Table 6. Boiling Point Data for Pure Components

	T (K)	ΔH_v (cal/gm mole)	P (atm)	v_{ol} (cc/gm mole)
Helium	4.215[22]	19.4[22]	1.0	32.05[61]
Carbon Tetrafluoride	145.12[119]	2823.6[123]	1.0	54.88[132]
Chlorotrifluoromethane	191.75[1]	3705.6*	1.0	68.67[1]

* Value taken from the Handbook of Physics and Chemistry, 52nd edition (1971).

Table 7. Parameters for the Method of Snider and Herrington

	r (Å)	$a_1 \times 10^{35}$ (erg cc/molecule)	$a_{12} \times 10^{37}$ (erg cc/molecule)
Helium	2.143		
Carbon Tetrafluoride	4.219	1.606	4.651
Chlorotrifluoromethane	4.542	2.635	3.106

evaluation $\bar{\rho}$ which is N_A/v_{01}.

Predicted Values of H_2^∞ and $\bar{V}_2^\infty$ for the Helium-Carbon Tetrafluoride System

Figure 23 shows a comparison of the calculated and experimental values of H_2^∞ for this system. The predicted values of H_2^∞ are lower than the smoothed experimental values of H_2^∞ given in Table 4 at the lowest temperature by about 20 percent and higher at the highest temperature by 50 percent of the experimental values, giving the best agreement at around 120 K. The smoothed experimental values of $\bar{V}_2^\infty$ presented in Table 4 are compared in Figure 24 with the predicted values of $\bar{V}_2^\infty$. In this case, the calculated values of $\bar{V}_2^\infty$ are consistently by 16 to 33 percent higher than the experimental values, the difference increasing with temperature. In both calculations, the values of r and a_{12} given in Table 7 were used.

Predicted Values of H_2^∞ and $\bar{V}_2^\infty$ for the Helium-Chlorotrifluoromethane System

In Figure 25, a comparison is made between the calculated values of H_2^∞ and smoothed experimental values of H_2^∞ taken from Table 5 for the helium-chlorotrifluoromethane system. As can be seen in this figure, the predicted H_2^∞ values are lower than the experimental data at the low temperatures and higher at the high temperatures. These calculated values of H_2^∞ differ from the experimental values by a

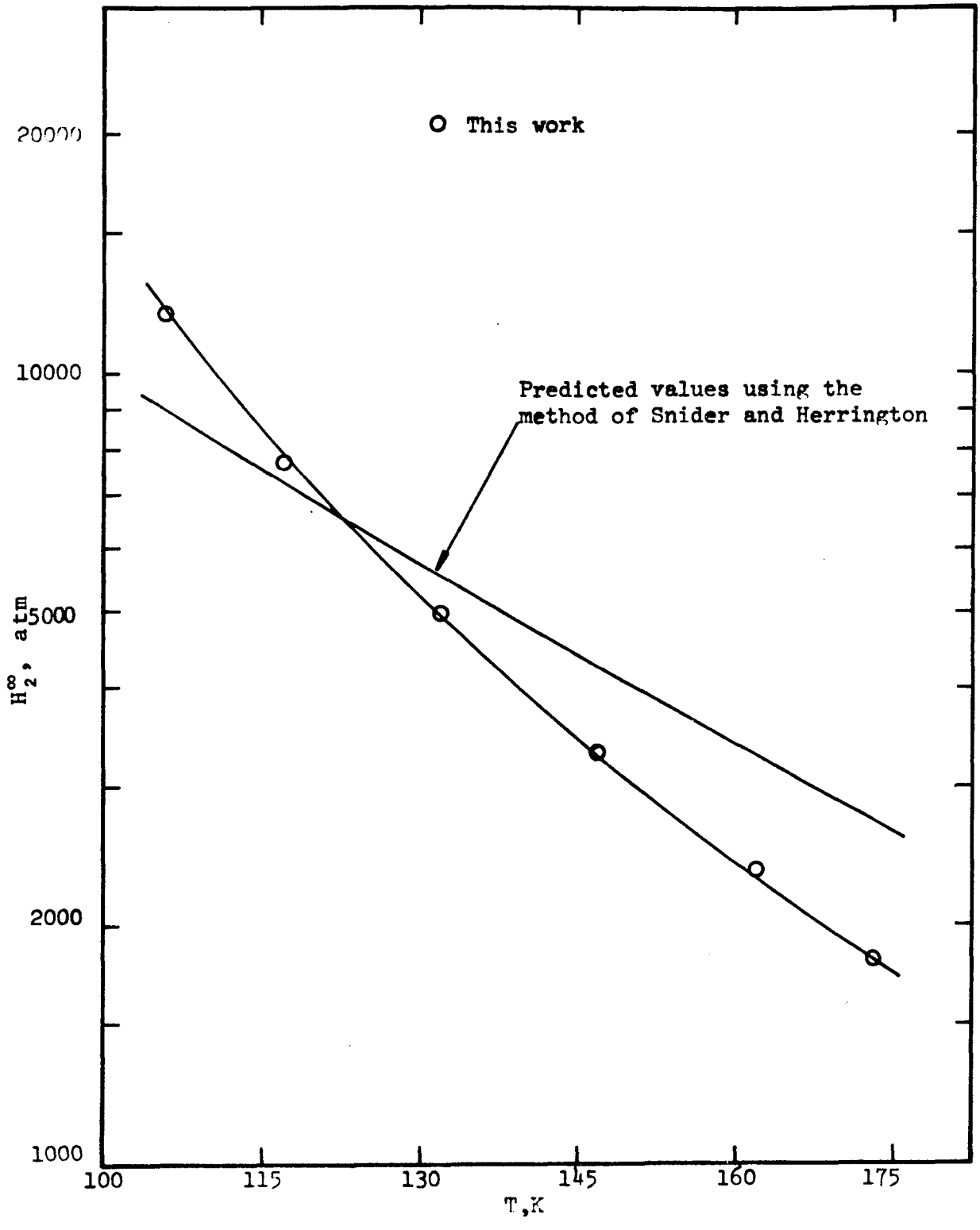

Figure 23. Comparison of Theoretical and Experimental H_2^∞ for the Helium-Carbon Tetrafluoride System.

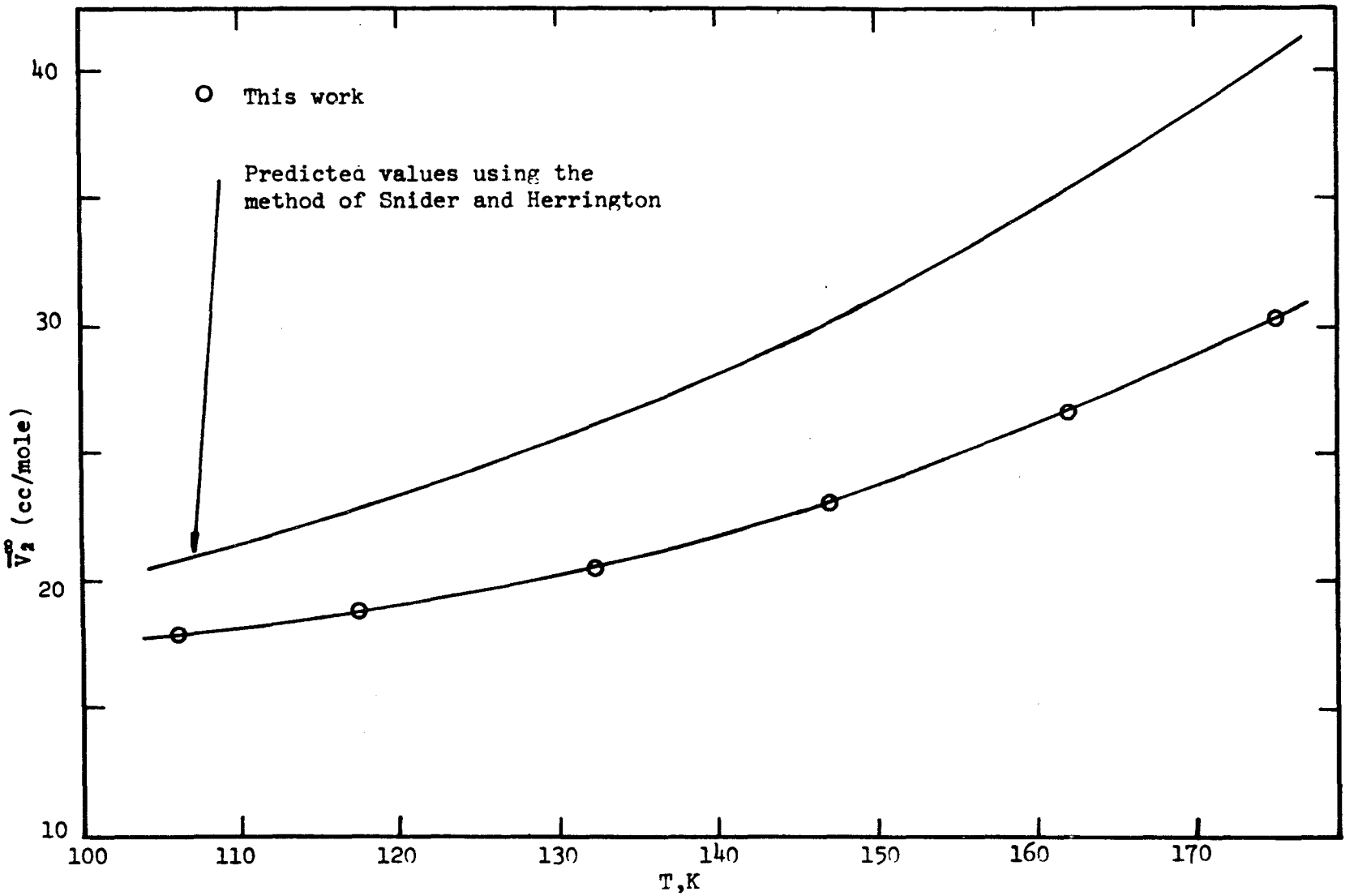

Figure 24. Comparison of Theoretical and Experimental $\overline{V}_2^\infty$ for the Helium-Carbon Tetrafluoride System.

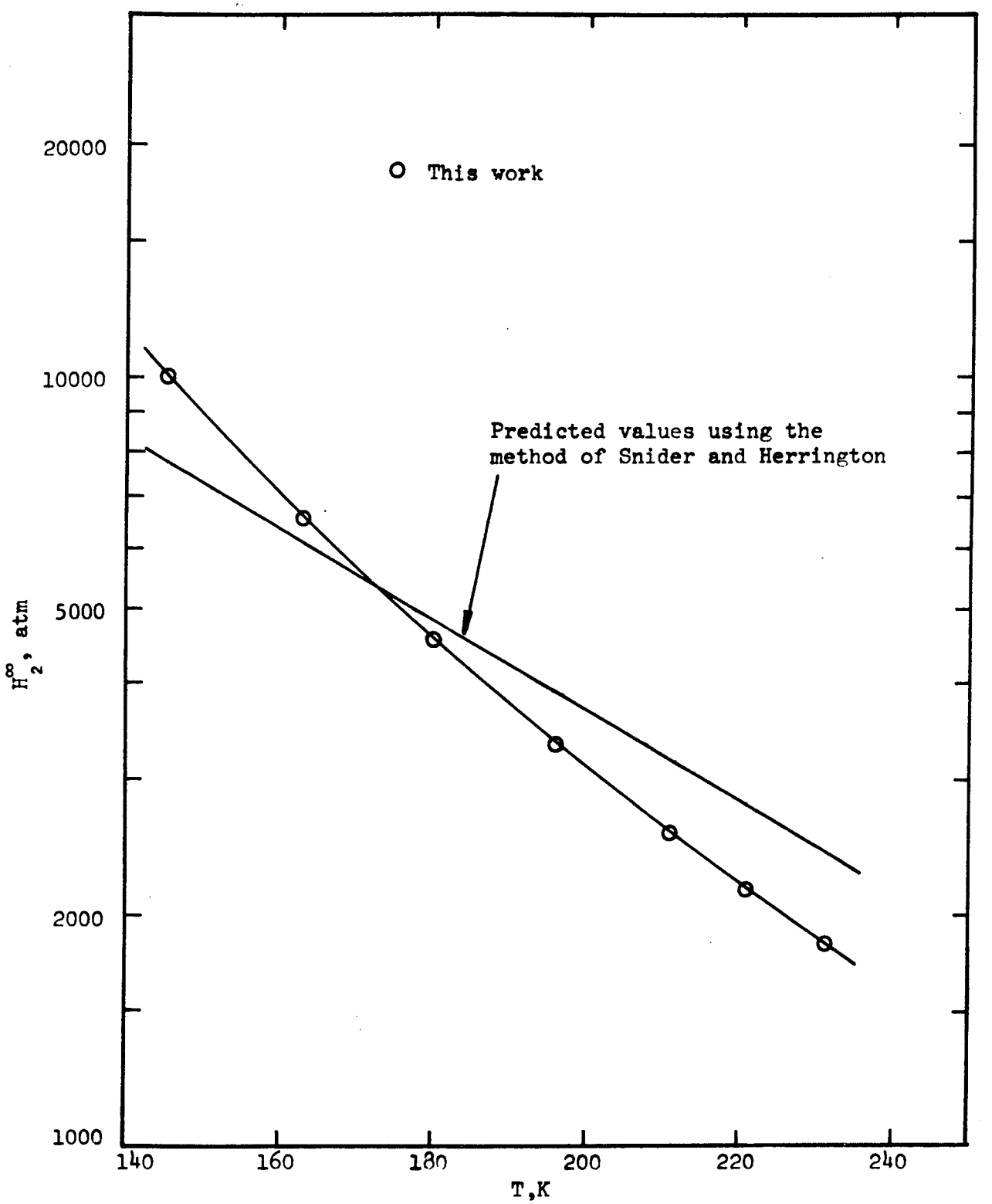

Figure 25. Comparison of Theoretical and Experimental H_2^∞ for the Helium-Chlorotrifluoromethane System.

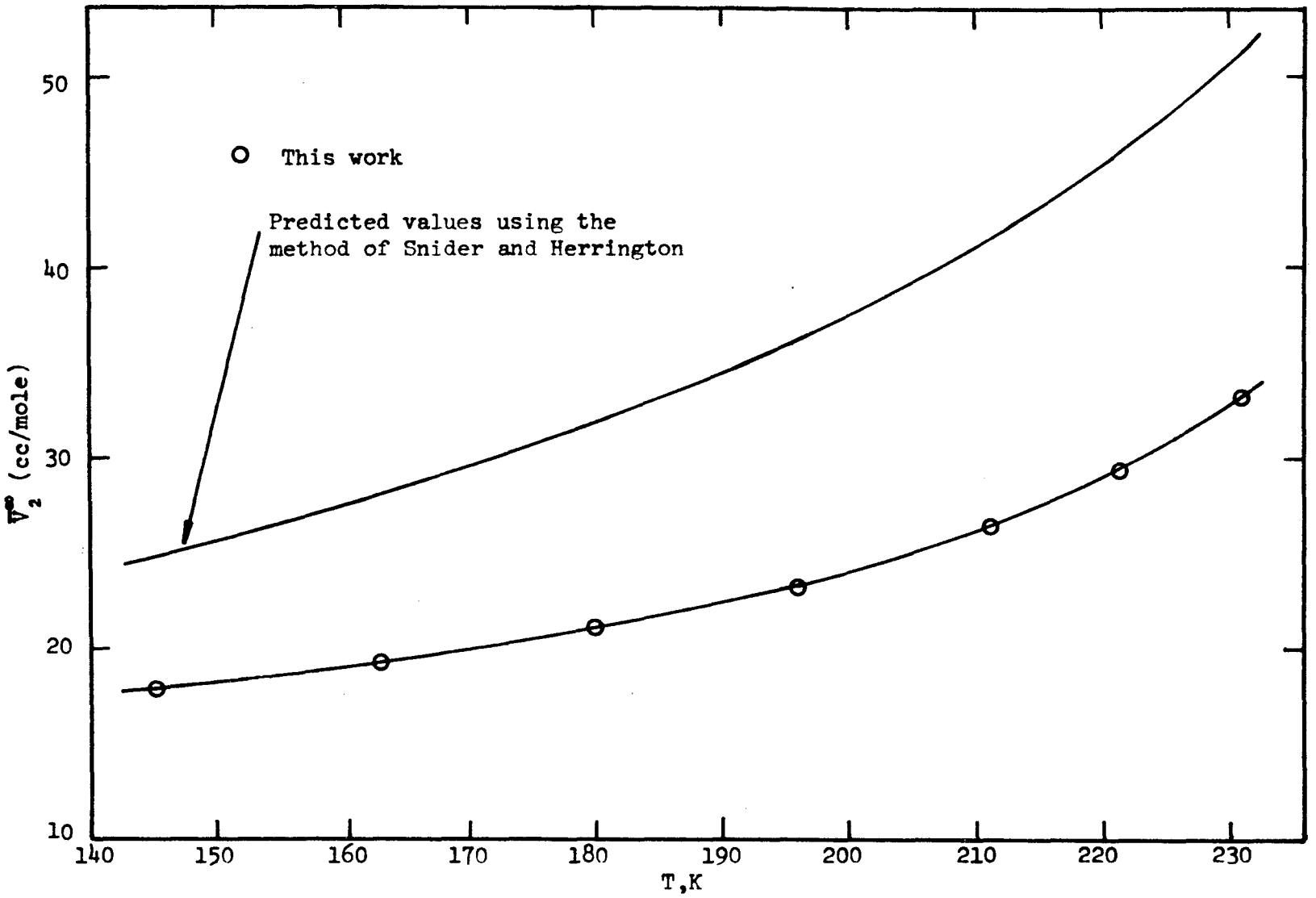

Figure 26. Comparison of Theoretical and Experimental $\bar{V}_2^\infty$ for the Helium-Chlorotrifluoromethane System.

maximum of 33 percent of the experimental values with the best agreement at around 170 K. The calculated values of $\overline{V}_2^{\infty}$ and the smoothed experimental values of $\overline{V}_2^{\infty}$ from Table 5 are shown in Figure 26. The agreement between the predicted and experimental $\overline{V}_2^{\infty}$ values for this system is in the range of 40 to 55 percent of the experimental values and the former is higher than the latter throughout the temperature range considered. In this calculation of H_2^{∞} and $\overline{V}_2^{\infty}$ values, use was made of the r and a_{12} values taken from Table 7.

Discussion of Results

Since the method is based on the equation of state for the hard sphere model, Equation (VI-22), Snider and Herrington[125] have tested this equation by calculating molar volumes of the pure components at the temperatures at which the mixtures were studied, using the parameters, r and a, extracted from the boiling point data of the pure components. Their results have shown that in most cases the calculated molar volumes were within five percent of the experimental values. As would be expected, the discrepancies between calculated and experimental values were greatest at the temperatures farthest from the boiling point.

This equation has also been tested in this work, and the molar volumes of carbon tetrafluoride and chlorotrifluoromethane are calculated at the temperature of interest using the values of r and a determined from the boiling point data and given in Table 7. These results are pre-

sented in Table 8 along with the experimental molar volumes. The same trend found by Snider and Herrington[125] is shown in these results. The closest agreements are shown at the temperatures near boiling point of the pure components and as temperature differs from the boiling point, the discrepancies between calculated and experimental molar volumes become more pronounced, giving a maximum of 2.6 percent difference for carbon tetrafluoride and 2.8 percent for the chlorotrifluoromethane. In other words, Equation (VI-22) is quite satisfactory in representing the pure liquid molar volumes of these components over the temperature region of this work.

Recently, Staveley[127] has applied the method of Snider and Herrington for the calculation of H_2^∞ and $\overline{V}_2^\infty$ for the systems of neon-argon, hydrogen-nitrogen, helium-methane, and helium-hydrogen. The values of r used in his calculations for the values of H_2^∞ and $\overline{V}_2^\infty$ were determined from both Equations (VI-26) and (VI-27), and accordingly two sets of each H_2^∞ and $\overline{V}_2^\infty$ values were obtained. These results are presented in Table 9. The values of a_{12} used in his work were obtained from Equation (VI-23) using an experimental value of H_2^∞ at one temperature, and with this a_{12} value, the values of H_2^∞ and $\overline{V}_2^\infty$ were predicted at one other temperature. For the molar volumes of the pure liquid necessary for the evaluation of Equations (VI-23) and (VI-24), Staveley used the calculated values from Equation (VI-22), not the

Table 8. Molar Volumes of the Pure Liquid Components at Saturation

Substance	T, K	V, cc/gm mole		Percent Difference
		Experimental	Calculated Using Equation (VI-22)	
Carbon Tetrafluoride[132]	106.01	48.69	47.42	2.6
	117.33	50.21	49.44	1.5
	132.18	52.43	52.26	0.3
	147.10	54.94	55.32	-0.7
	162.03	57.80	58.69	-1.5
	173.02	60.17	61.41	-2.1
Chlorotrifluoromethane	145.21	61.85	60.14	2.8
	163.01	64.20	63.22	1.5
	180.02	66.73	66.37	0.6
	196.01	69.41	69.54	-0.2
	211.06	72.32	72.77	-0.6
	221.27	74.56	75.13	-0.8
	231.08	76.99	77.52	-0.7

experimental values.

Although there are some minor differences between the method of Snider and Herrington used by Staveley[127] and that used in this work, these two methods are essentially identical. As can be seen in Table 9, the predicted values of H_2^∞ and $\overline{V}_2^\infty$ are in quite satisfactory agreement with the experimental values except for the helium-hydrogen system, for which the predicted H_2^∞ value seriously exceeds the experimental value. This is,as Staveley stated, probably due to the quantum effects for both components, which in turn suggest this method may not reliable for the binary systems in which both components exhibit quantum effects.

Table 9. Comparison of Predicted and Experimental H_2^∞ and $\overline{V}_2^\infty$ for Some Binary Systems

System	T (K)	H_2^∞ (exp) (atm)	H_2^∞ (calc) (atm) a	H_2^∞ (calc) (atm) b	$\overline{V}_2^\infty$ (exp) (cc/mole)	$\overline{V}_2^\infty$ (calc) (cc/mole) a	$\overline{V}_2^\infty$ (calc) (cc/mole) b
Neon-Argon	87.29	1086*[129]			20-30[130]	29	30
	115.8	651[129]	651	642	40-50[130]	51	53
Hydrogen-Nitrogen	77.35	454*[31]			35-45[83]	30	38
	90	345[31]	405	395		38	49
Helium-Methane	95	27239*[47]			26[121]		24.5
	125	6908[47]	6316		32[121]		41
Helium-Hydrogen	20.4	622*[131]					54.5
	15.25	1283[131]	3454				24

a Values evaluated using r values calculated from Equation (VI-26)

b Values evaluated using r values calculated from Equation (VI-27)

* Experimental H_2^∞ substituted in Equation (VI-23) to obtain a_{12}.

The results presented in Figures 23 through 26 show that this method generally represents the H_2^∞ and $\overline{V}_2^\infty$ values for the helium binary systems of this work with reasonable accuracy. The agreement between the predicted and experimental H_2^∞ values is best at temperatures 20 to 25 K below the normal boiling point of condensed components and as temperature decreases or increases from this point, the predicted values of H_2^∞ differ from the experimental values, showing a slight temperature dependency of a_{12} value. The a_{12} values extracted from the experimental data of H_2^∞ (see Table 9) were used to obtain $\overline{V}_2^\infty$ values from Equation (VI-24). These calculated $\overline{V}_2^\infty$ values agree with the experimental data within 16 to 55 percent of the experimental values, which bears out the validity of this method in predicting the values of H_2^∞ and $\overline{V}_2^\infty$ for the systems considered in this work.

As stated by Snider and Herrington,[125] although this method was originally developed to describe the thermodynamic properties of the binary mixtures whose components are small, nonpolar spherical molecules, this method has been successfully used in reproducing experimental values of various thermodynamic quantities for the binary systems whose liquid components consist of nonspherical molecules such as oxygen, nitrogen, and carbon monoxide. They pointed out that this is so because these molecules as liquids very nearly obey the same equation of state as do the liquified rare gases[41] and therefore can be treated as spherical molecules. They

also pointed out that their method could not predict satisfactorily the experimental results for the larger molecules such as carbon tetrachloride and neopentane despite of their high symmetries. O'Connell and Prausnitz[92] and Sherwood and Prausnitz[116] have shown that carbon tetrafluoride molecules can be treated as spherical molecules in the calculation of transport properties and second and third virial coefficients using Kihara potential. The nearly spherical or quasi-spherical nature of chlorotrifluoromethane molecules has been successfully used by Brandt[12] for the calculation of intermolecular force constants from polarizabilities. Also, carbon tetrafluoride and chlorotrifluoromethane molecules are not so large as to behave like carbon tetrachloride and neopentane. The above discussion, together with the fact that Equation (VI-22) represents quite satisfactorily the molar volumes of the liquid carbon tetrafluoride and chlorotrifluoromethane as shown in Table 8, strongly supports the use of the method of Snider and Herrington[125] for the calculation of the H_2^∞ and $\overline{V}_2^\infty$ values for the helium-carbon tetrafluoride and helium-chlorotrifluoromethane systems.

CHAPTER VII

CONCLUSIONS AND RECOMMENDATIONS

Conclusions

Equilibrium gas and liquid compositions for the helium-carbon tetrafluoride system have been measured at pressures up to 120 atmospheres with an interval of 20 atmospheres along six isotherms of 106.01, 117.33, 132.18, 147.10, 162.03, and 173.02 K. The estimated accuracy of the experimental gas and liquid phase equilibrium compositions is ±2 mole percent. Also measured are gas and liquid phase equilibrium compositions for the helium-chlorotrifluoromethane system at seven temperatures of 145.21, 163.01, 180.02, 196.01, 211.06, 221.27 and 231.08 K and pressures up to 120 atmospheres with an estimated accuracy of ±3.5 mole percent for the gas phase composition and ±2 mole percent for the liquid phase composition.

In constructing the chromatographic calibration curve, a gas imperfection correction of 1.1 mole percent was applied for the helium-chlorotrifluoromethane mixtures. For the helium-carbon tetrafluoride gas mixtures this correction was 0.4 mole percent. Therefore, it is apparent that the gas imperfection correction must be taken into account even at room temperature and pressure.

The Lennard-Jones and Kihara core potential parameters were extracted from the experimental second virial coefficient data of chlorotrifluoromethane. These results and the results of Sherwood and Prausnitz[116] showed that the Kihara core potential is superior to the Lennard-Jones potential in representing the second virial coefficients of carbon tetrafluoride and chlorotrifluoromethane. In the extraction of the Kihara parameters, the spherical core model was assumed for these molecules.

The theoretical models, LJCL, KIH, KIHCK12, KIHEK12, BWR (LORENTZ), and BWR (LINEAR) (see Chapter IV), have been used to extract the interaction second virial coefficient, B_{12}, from the phase equilibrium data obtained in this work for the helium-carbon tetrafluoride system and only four models, LJCL, KIH, KIHCK12, and KIHEK12 for the helium-chlorotrifluoromethane system. The B_{12} values extracted for the helium-chlorotrifluoromethane system are all positive and greater than those for the helium-carbon tetrafluoride system at the same reduced temperatures. The experimental B_{12} values for these systems, as expected, have shown a strong temperature dependency and theoretically predicted B_{12} values have also shown this trend. Of all the theoretical models, the KIHEK12 model has predicted the best B_{12} values for both systems considered. The agreement of the predicted values from LJCL model with the experimental B_{12} data was also quite satisfactory, a maximum discrepancy being

6 percent of the experimental value. No theoretical model was successful in predicting the B_{12} values in the temperature range of 300 to 770 K[59] for the helium-carbon tetrafluoride system.

The values of the correction factor, K_{12} (see Chapter IV), to the geometric mixing rule for the Kihara core model have been extracted from the experimental B_{12} data for the helium-carbon tetrafluoride and helium-chlorotrifluoromethane systems and compared with the calculated values of K_{12} using the correlation given by Hiza and Duncan.[51] Although several investigators[37,50,51] have shown that this correlation has predicted the K_{12} values in satisfactory agreement with experimental values for various binary systems, the same correlation was unable to predict the correct K_{12} values for the present systems. Accordingly, the B_{12} values predicted using K_{12} values from the correlation of Hiza and Duncan differ considerably from the B_{12} values extracted using the experimental K_{12} values. These experimental K_{12} values have also shown a slight temperature dependency.

The same theoretical models as used to compute the B_{12} values have been used to predict the enhancement factors for the helium-carbon tetrafluoride and helium-chlorotrifluoromethane systems. It is shown that the model which predicts the best B_{12} values also predicts the best enhancement factors. As expected, the enhancement factors calculated using the

KIHEK12 model were in the best agreement with the experimental data of this work. The LJCL model also predicted quite satisfactory values except at the highest temperatures considered for these systems. The enhancement factors predicted using the KIH model were generally much higher than the experimental data. The failure of the correlation given by Hiza and Duncan[51] to predict satisfactory K_{12} values resulted in poor agreement of the enhancement factors calculated using the KIHCK12 model with the experimental values. Benedict, et al.,[8] Mullins,[90] and Garber[37] have shown that the BWR (LINEAR) model is better than the BWR (LORENTZ) model in predicting phase equilibrium data. Contrary to this, for the helium-carbon tetrafluoride system it was found that the BWR (LORENTZ) model predicted enhancement factors which are in better agreement with experimental values than those predicted using the BWR (LINEAR) model. All theoretical enhancement factors as well as experimental enhancement factors showed a minimum in the enhancement factor versus temperature curves as has been observed for a number of other helium binary systems. This means that the predicted enhancement factors using the theoretical models used here are at least qualitatively correct.

The experimental H_2^{∞} and $\overline{V}_2^{\infty}$ values were extracted from the phase equilibrium data of this work for the helium-carbon tetrafluoride and helium-chlorotrifluoromethane systems using the Krichevsky-Ksarnovsky equation.[73] A theoretical predic-

tion of H_2^∞ and $\overline{V}_2^\infty$ values for these systems was made using the method of Snider and Herrington[125] based on hard-sphere model of fluid. These theoretical H_2^∞ and $\overline{V}_2^\infty$ values agreed with the experimental values within 55 percent of the experimental values. The predicted H_2^∞ values were higher than the experimental H_2^∞ values at higher temperatures and lower at lower temperatures, giving the best agreement in between. The theoretical $\overline{V}_2^\infty$ values were always higher than the experimental values throughout the temperature range considered. Considering the simplicity of this method, this method is excellent in representing H_2^∞ and $\overline{V}_2^\infty$ values for the binary systems of components whose molecules are small and either nonpolar or slightly polar.

Recommendations

Several recommendations for future work concerning to phase equilibria are summarized in the following.

1. It is recommended that the temperature range of this work be extended to higher temperatures so that a maximum on the experimental enhancement factor isobar curve at 20 atmospheres can be seen. For this purpose, it is necessary to install a recirculation system for the gas from the gas sample line to the lower inlet line leading to the equilibrium cell. The qualitative representation of the enhancement factors by the theoretical models used in this work can be checked on the ground of this maximu.

2. Sherwood and Prausnitz[116] have shown that the experimental second and third virial coefficient data of carbon tetrafluoride are best represented by the exp-6 potential. Hence, it is worth while testing this exp-6 potential for the prediction of phase equilibrium data for the helium-carbon tetrafluoride system.

3. The experimental values of the correction factor, K_{12}, for the geometric mixing rule applied for the mixture energy parameter of the Kihara core potential differs greatly from the K_{12} value calculated from the correlation of Hiza and Duncan[51] for the systems of this work. In this Kihara core potential model, the third virial coefficient of the condensed phase was calculated using the method of Chueh and Prausnitz[18] which sets all C_{111} values equal to zero in the temperature range of this work ($T_{R1} \leq 0.8$). As shown by Sherwood and Prausnitz,[115,116] the third virial coefficients predicted using the Kihara potential are in much better agreement with the experimental data than those predicted from the Lennard-Jones (6-12) potential for carbon tetrafluoride in the temperature range of 270 to 670 K. Thus, these Kihara third virial coefficients are recommended for the condensed component in the extraction of K_{12} value to see the dependency of K_{12} value on the C_{111} values and the difference between this K_{12} value and that calculated from the correlation of Hiza and Duncan. Neither of the Kihara potential nor the method of Chueh and Prausnitz[18] for the

calculation of C_{111} values can be said to be superior since no experimental third virial coefficient data in the temperature range of this work were available for carbon tetrafluoride and chlorotrifluoromethane.

4. Since there are no experimental virial coefficient data available for carbon tetrafluoride and chlorotrifluoromethane in the temperature range of this work, it is recommended that the second and third virial coefficients in this temperature range be extracted from the available P-V-T data or the equation of state which represents the P-V-T data for carbon tetrafluoride[16] and chlorotrifluoromethane.[1,32] These virial coefficients can be compared with those predicted from the Lennard-Jones potential, the Kihara core potential, and BWR equation of state.

5. Although there are no comments on the temperature dependency of the parameter a_{12} in the method of Snider and Herrington[125] for the prediction of H_{12}^{∞} and $\bar{V}_{12}^{\infty}$ values in the papers of Snider and Herrington[125] and Staveley,[127] this parameter appears to be slightly dependent upon temperature in this work. It would be interesting to apply this method to the various binary systems shown in Garber's thesis[37] and see if this a_{12} parameter is also dependent upon temperature in those systems.

6. Although the Pierotti method[94,95] requires more experimental data than the method of Snider and Herrington to determine the best values of the parameters needed for

the calculation of H_2^∞ and $\overline{V}_2^\infty$ values, it is worthwhile comparing these two methods. Of these parameters necessary for the Pierotti method, the hard sphere diameter of solvent molecule plays an important role in the prediction of H_2^∞ and $\overline{V}_2^\infty$ values. To extract this hard sphere diameter of solvent molecules for one binary system from experimental H_2^∞ values, it is necessary to have the experimental H_2^∞ value for another system with the same condensed component at the same temperature. Thus, the study of the phase equilibria in binary systems such as hydrogen-carbon tetrafluoride and hydrogen-chlorotrifluoromethane systems is recommended for this purpose.

APPENDICES

APPENDIX A

TEMPERATURE SCALE USED AND CORRECTIONS FOR PRESSURE GAUGES

A platinum resistance thermometer, Leeds and Northrup Company, Serial Number 1583528, previously used by Kirk,[68] Mullins,[90] Liu[77] and Garber[37] was used in all temperature measurements of the phase equilibria in this work and has been calibrated by the U.S. National Bureau of Standards on the International Practical Temperature Scale of 1948. All temperatures in this work were converted from IPTS-48 to IPTS-68 based on the paper of Barber[3] and are reported on the Kelvin scale, according to the following relation.

$$T(K) = 273.15 + t_{48}(°C) + (t_{68}(°C) - t_{48}(°C))$$

The two pressure gauges, low and high, used in this work were originally calibrated by Kirk[68] against a dead weight tester and recently have been recalibrated by Garber[37] using the vapor pressures of argon and carbon dioxide. As a quick check on these pressure gauges, the low and high pressure gauges were pressurized from 40 to 540 psi and depressurized from 540 to 0 psi, and the difference between the two gauge readings were recorded. The average difference of these readings was found to be 10.0 psi compared

with that of 9.7 psi found by Garber.[37] Neglecting this small difference between the two average values, Garber's[37] correction to both gauges were used in this work without further check, that is, an addition of 10 psi to high pressure gauge and 1 psi to the low pressure gauge.

APPENDIX B

HELIUM-PROPYLENE SYSTEM MEASUREMENTS

At the beginning of this research one of the isotherms of the helium-propylene system previously studied by Garber [37] was reproduced to check the operation of the phase equilibrium apparatus and to acquire some operating technique. Six equilibrium gas and liquid phase compositions at six different pressures at 200.01 K were measured. The results are shown in Figures 27 and 28 together with the data of Garber. [37] It can be seen that the experimental data so obtained agree within ±3 percent with the selected curve of Garber.

Garber's[37] calibration curve was also checked by running several gas mixtures on the 154D gas chromatograph. Those mixtures were made using the gas mixing burette built by Kirk. The agreement of these results with Garber's was within the experimental error claimed by Garber.

Both of these experiments confirmed that the phase equilibrium apparatus and gas mixing burette were not only working correctly but also the operating technique was satisfactory.

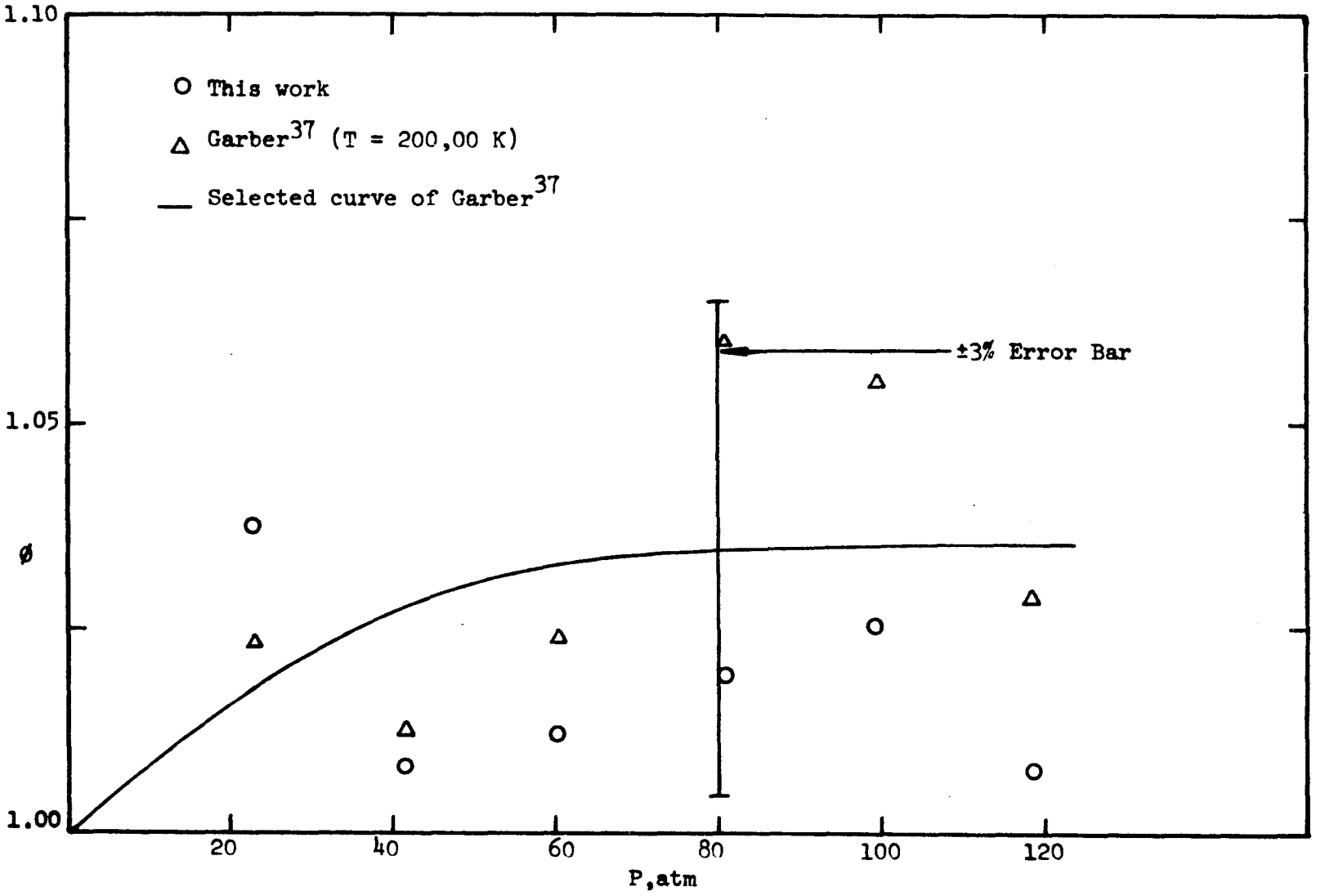

Figure 27. Experimental Enhancement Factors in the Helium-Propylene System at 200.01 K.

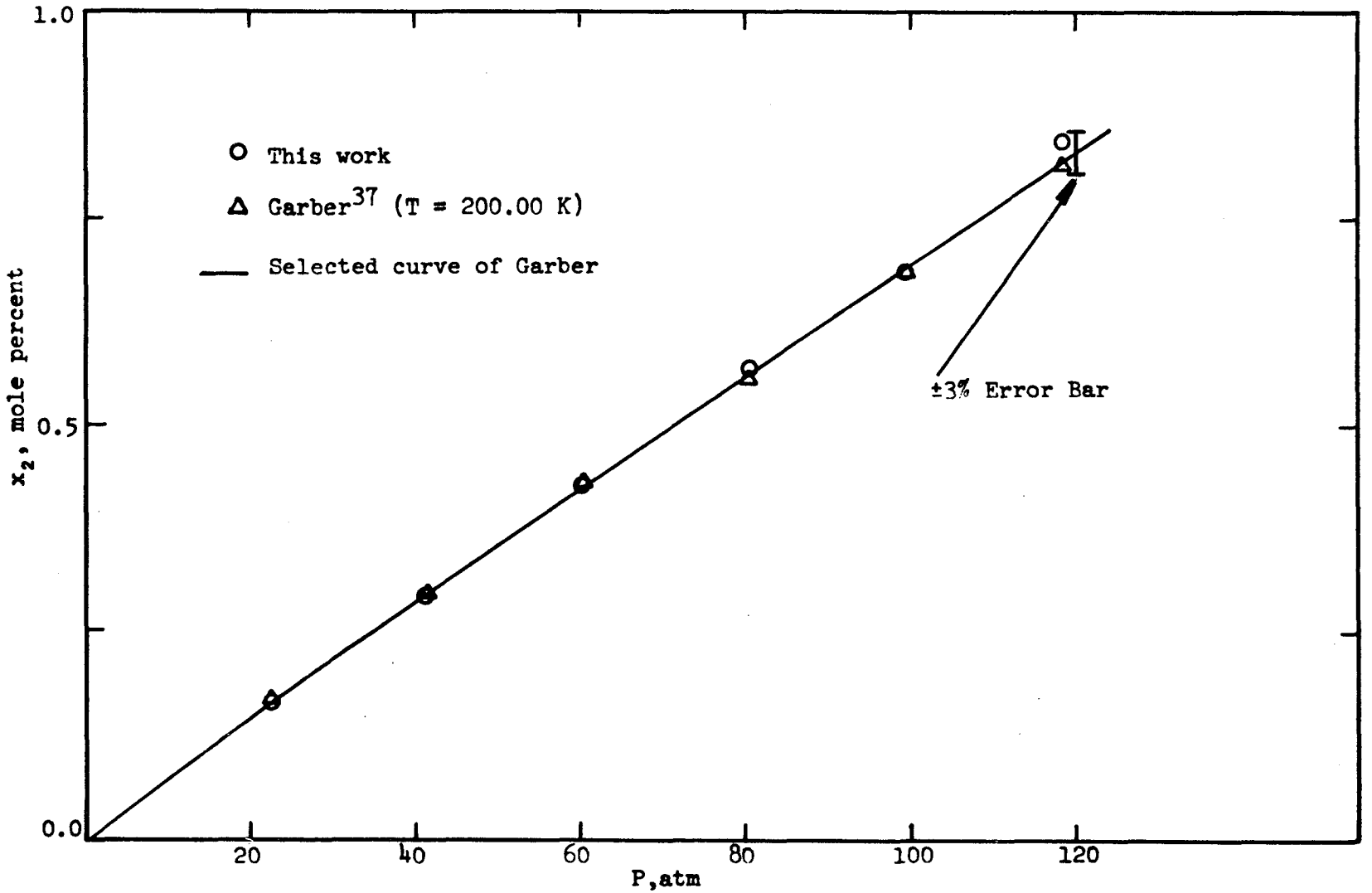

Figure 28. Experimental Solubility of Helium in Liquid Propylene at 200.01 K.

APPENDIX C

EXTRACTION OF KIHARA POTENTIAL PARAMETERS FROM EXPERIMENTAL SECOND VIRIAL COEFFICIENT DATA

Lack of the Kihara potential parameters for chlorotriluoromethane required that a least squares program be made for the extraction of these potential parameters from experimental second virial coefficient data.

In evaluating Kihara potential parameters from second virial coefficient data, the method described by Sherwood and Prausnitz[115] was closely followed. The basic idea is to determine the three potential parameters by automatic computation using the least squares criterion and minimizing the rms deviation between experimental and calculated second virial coefficients. The method is then as follows. Equation (IV-30) is first put into the following form assuming a spherical core of diameter $2a$ and using the relations $M_o = 4\pi a$, $S_o = 4\pi a^2$, $V_o = \frac{4}{3}\pi a^3$, and $\rho_o = 2^{\frac{1}{6}}(\sigma - 2a)$:

$$(B_K)_i = b_o \left[2^{\frac{1}{2}} F_3 + 3(2^{\frac{1}{3}})\, a^* F_2 + 3(2^{\frac{1}{6}})\, a^{*2} F_1 + a^{*3} \right] (1 + a^*)^{-3} \qquad \text{(C-1)}$$

where

$$a^* = \frac{2a}{\sigma - 2a} \tag{C-2}$$

$$b_o = \frac{2}{3}\pi N_A \sigma^3 \tag{C-3}$$

Defining

$$(B^*_K)_i = 2^{\frac{1}{2}} F_3 + 3(2^{\frac{1}{3}})\, a^* F_2 + 3(2^{\frac{1}{6}})\, a^{*2} F_1 + a^{*3} \tag{C-4}$$

and

$$(BB_K)_i = (B_K)_i\, (1 + a^*)^3 \tag{C-5}$$

Equation (C-1) becomes

$$(BB_K)_i = b_o\, (B^*_K)_i \tag{C-6}$$

Equations (C-1) and (C-6) have three adjustable parameters, a^*, U_o/k, and b_o. A least squares procedure used by Ziegler and Mullines[139] is applied to Equation (C-6) for a fixed value of a^*.

The residue is defined, after dropping the subscript K for convenience's sake, as

$$R_i = \overline{BB}_i - BB_i \tag{C-7}$$

where

$$\overline{BB}_i = \overline{B}_i \, (1 + a^*)^3 \tag{C-8}$$

and $\overline{B}_i$ is the experimental second virial coefficient at the temperature T_i.

Conditions of the least squares assumption for n data points are

$$\frac{\partial}{\partial b_o} \left(\sum_{i=1}^{n} R_i^2 \right) = 0 \tag{C-9}$$

and

$$\frac{\partial}{\partial (U_o/k)} \left(\sum_{i=1}^{n} R_i^2 \right) = 0 \tag{C-10}$$

Subsitituting Equation (C-7) into Equations (C-9) and (C-10), the following results are obtained. From Equation (C-9)

$$\frac{\partial}{\partial b_o} \left[\sum_{i=1}^{n} (\overline{BB}_i^2 - 2\overline{BB}_i BB_i + BB_i^2) \right] = 0 \tag{C-11}$$

$$\therefore \quad b_o = \frac{\sum_{i=1}^{n} \overline{BB}_i B_i^*}{\sum_{i=1}^{n} B_i^{*2}} \tag{C-12}$$

and similarly from Equation (C-10),

$$\sum_{j=1}^{n} (\overline{BB}_i - b_o B_i^*) \left[b_o \frac{\partial B_i^*}{\partial (U_o/k)} \right] = 0 \qquad \text{(C-13)}$$

Differentiation of Equation (C-4) with respect to U_o/k (see Equation (IV-31) for F_1, F_2, and F_3) gives

$$\frac{\partial B_i^*}{\partial (U_o/k)} = 2^{\frac{1}{2}} \left(\frac{U_o}{k}\right)^{-1} \sum_{i=o}^{n} \left[\left(\frac{6j+3}{12}\right) b_3^j \left(\frac{U_o}{kT_i}\right)^{\frac{6j+3}{12}} \right] + 3 \qquad \text{(C-14)}$$

$$\times (2^{\frac{1}{3}}) \left(\frac{U_o}{k}\right)^{-1} a^* \sum_{j=o}^{n} \left[\left(\frac{6j+2}{12}\right) b_2^j \left(\frac{U_o}{kT_i}\right)^{\frac{6j+2}{12}} \right]$$

$$+ 3(2^{\frac{1}{6}}) \left(\frac{U_o}{k}\right)^{-1} a^{*2} \sum_{j=o}^{n} \left[\left(\frac{6j+1}{12}\right) b_1^j \left(\frac{U_o}{kT}\right)^{\frac{6j+1}{12}} \right]$$

Defining G_i^* as

$$G_i^* = 2^{\frac{1}{2}} \sum_{j=o}^{n} \left[\left(\frac{6j+3}{12}\right) b_3^i \left(\frac{U_o}{kT_i}\right)^{\frac{6j+3}{12}} \right] + 3(2^{\frac{1}{3}}) \qquad \text{(C-15)}$$

$$\times a^* \sum_{j=o}^{n} \left[\left(\frac{6j+2}{12}\right) b_2^j \left(\frac{U_o}{kT_i}\right)^{\frac{6j+2}{12}} \right] + 3(2^{\frac{1}{6}})$$

$$\times a^{*2} \sum_{j=o}^{n} \left[\left(\frac{6j+1}{12}\right) b_1^j \left(\frac{U_o}{kT_i}\right)^{\frac{6j+1}{12}} \right]$$

The following equation is obtained

$$\frac{\partial B_i^*}{\partial (U_o/k)} = \left(\frac{U_o}{k}\right)^{-1} G_i^* \qquad \text{(C-16)}$$

$$b_o \sum_{i=1}^{n} B_i^{*2} = \sum_{i=1}^{n} \overline{BB}_i \, B_i^* \qquad \text{(C-17)}$$

Substitution of Equation (C-16) into Equation (C-13) gives

$$b_o \left(\frac{U_o}{k}\right)^{-1} \sum_{i=1}^{n} (\overline{BB}_i \, G_i^*) - b_o^2 \left(\frac{U_o}{k}\right)^{-1} \sum_{i=1}^{n} B_i^* \, G_i^* = 0 \qquad \text{(C-18)}$$

Simplifying Equation (C-18), multiplying both sides by $\sum_{i=1}^{n} B_i^{*2}$, and making use of Equation (C-17), the following equation is obtained.

$$\sum_{i=1}^{n} (B_i^* \, G_i^*) \sum_{i=1}^{n} (\overline{BB}_i \, B_i^*) - \sum_{i=1}^{n} (\overline{BB}_i \, G_i^*) \sum_{i=1}^{n} B_i^{*2} = 0 \qquad \text{(C-19)}$$

Equation (C-19) has only two parameters, U_o/k and a^*.

The three Kihara potential parameters were now evaluated as follows. For a fixed value of a^* a value of U_o/k is found by iterative solution of Equation (C-19). Equation (C-12) is then used to obtain a value of b_o corresponding to these values of a^* and U_o/k. The optimum set of values of a^*, U_o/k and b_o is now determined by varying a^* in discrete steps until the rms deviation between the calculated

and experimental second virial coefficients passes through a minimum.*

The computer program for carrying out the above procedure was tested by extracting the Kihara parameters for carbon tetrafluoride using the experimental second virial coefficient data of Douslin, et al.[30] The values of the parameters found were $a^* = 0.51$, $\sigma = 4.311$ Å and $U_o/k = 292.3$ K corresponding to an rms of 0.077 cc/mole. The values of U_o/k and b_o were found not to be very sensitive to the value of a^*. Using the same rivial coefficient data Sherwood and Prausnitz[115] reported values of $a^* = 0.50$, $\sigma = 4.319$ Å and $U_o/k = 289.7$ K.

---

* Sherwood and Prausnitz[115] remark that a well-defined single minimum is always obtained for the Kihara potential by this method. In the extraction of the Kihara parameters for chlorotrifluoromethane in the present work a^* was varied from 0.10 to 0.55 in increments of 0.01.

APPENDIX D

COMMENTS ON THE CALCULATION OF THE REDUCED VIRIAL COEFFICIENTS BASED ON LENNARD-JONES (6-12) POTENTIAL

The reduced classical virial coefficient functions for the Lennard-Jones (6-12) potential are discussed in detail by Hirschfelder, et al.[49] Since there are several different evaluations for the reduced virial coefficients, there has to be some remark in selecting them.

The reduced second virial coefficient, B^*_{CL}, is expressed as follows:

$$B^*_{CL}(T^*) = \sum_{j=o}^{\infty} b^{(j)} (T^*)^{-(1+2j)/4} \qquad (D\text{-}1)$$

Since the right hand side of the Equation (D-1) is the sum of an infinite series, for the practical purpose it is truncated after first forty-one terms. The first forty-one values of $b^{(j)}$ (see Equation (IV-27)) are given by Hirschfelder, et al.[49] and Kirk[68] has recomputed these values. These two sets of $b^{(j)}$ values agree well with each other except for the value of $b^{(16)}$ at which Kirk's claculation shows $-0.3386316 \times 10^{-5}$ compared to $-0.33872440 \times 10^{-5}$ computed by Hirschfelder, et al.[49] The $b^{(j)}$ values computed by Kirk have been used in this work.

The reduced third virial coefficient for the Lennard-Jones (6-12) potential has been evaluated by de Boer, et al.,[26] Montroll, et al.[89] and Bird, et al.[11] using their expressions for the third virial coefficient, and Kihara,[66] Bergeon,[10] and Rowlinson,et al.[110] by calculating $c^{(j)}$ values as shown in Equation (D-2). All of these are compared in Figure 29 except that calculated by Bergeon.[10]

De Boer, et al.[26] calculated the third virial coefficient by integrating graphically their expression derived from the pair distribution function, while Montroll, et al.[89] performed a numerical integration for their integrals which are mathematically equivalent to those of de Boer, et al.[26] The results of these two methods are somewhat different as shown in Figure 29. Bird, et al.[11] have evaluated their expression for the third virial coefficient with great accuracy by means of punched card techniques. This evaluation seemed to be most precise.

Kihara,[66] Rowlinson, et al.,[110] and Bergeon[10] used the same expression for the reduced third virial coefficient, namely,

$$C^*_{CL}(T^*) = \sum_{j=o}^{\infty} c^{(j)} (T^*)^{-(1+j)/2} \qquad \text{(D-2)}$$

In the calculation of $C^*_{CL}(T^*)$, Kihara evaluated the first eighteen values of $c^{(j)}$, Rowlinson the first twenty-one, and Bergeon the first six. $C^*_{CL}(T^*)$ values calculated using

Table 10. Comparison of $B^*_{CL}(T^*)$ and $C^*_{CL}(T^*)$ Values Calculated Using Kirk's $b^{(j)}$'s and Kihara's $c^{(j)}$'s, respectively.

Reduced Temperature (kT/e)	$B^*_{CL}(T^*)$ No. of Terms Used in Equation (D-1)	$B^*_{CL}(T^*)$ Percent Difference a	$B^*_{CL}(T^*)$ No. of Terms Used in Equation (D-2)	$B^*_{CL}(T^*)$ Percent Difference b
0.6	First 30	0.000000	First 17	3.549
	" 15	0.014907	" 15	13.526
0.8	" 30	0.000000	" 17	3.396
	" 15	0.002430	" 15	15.424
1.0	" 30	0.000000	" 17	0.939
	" 15	0.000595	" 15	4.930
1.2	" 30	0.000000	" 17	0.131
	" 15	0.000192	" 15	0.778
1.4	" 30	0.000000	" 17	0.034
	" 15	0.000074	" 15	0.226
1.6	" 30	0.000000	" 17	0.011
	" 15	0.000031	" 15	0.082

a Percent difference between the sums of the first forty-one terms and the given number of terms (based on the Kirk's $b^{(j)}$ values) in the second column.

b Percent difference between the sums of the first eighteen terms and the given number of terms (based on the Kihara's $c^{(j)}$ values) in the fourth column.

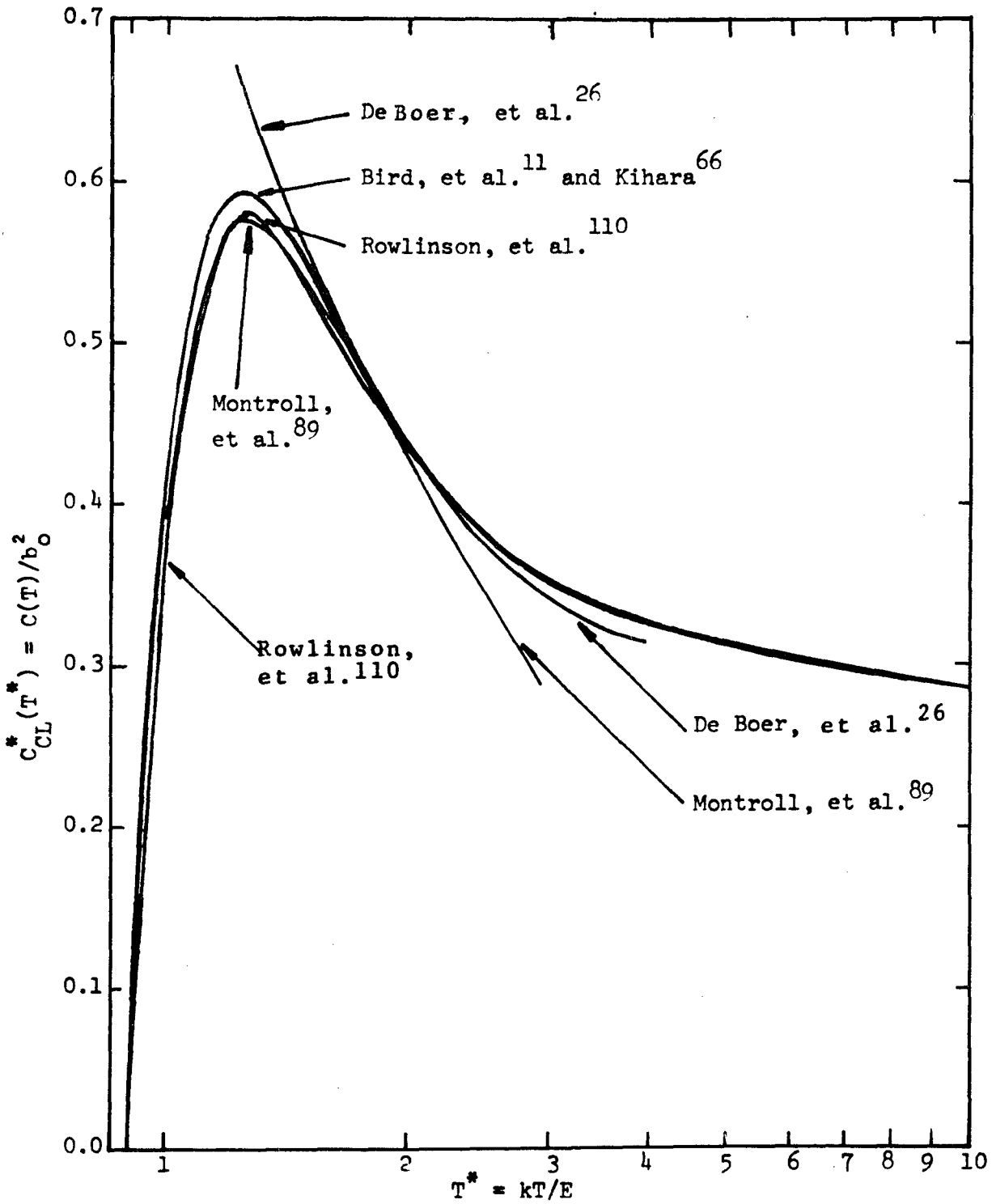

Figure 29. Comparison of Calculated Curves of the reduced Third Virial Coefficient by Different Investigators.

the Kihara's first eighteen values of $c^{(j)}$ are in excellent agreement with those calcuated by Bird, et al.[11] The first eighteen values of Kihara for $c^{(j)}$ were selected for use in this work and the remaining terms were truncated.

A comparison is made in Table 10 between the $B^*_{CL}(T^*)$ values used in the present work and $B^*_{CL}(T^*)$values calculated using the first 15 and 30 terms in the infinite series in Equation (D-1). As can be seen in Table 10, the sum of the first 15 terms represents the $B^*_{CL}(T^*)$ value of this work quite satisfactorily. A similar comparison is also shown in Table 10 for $C^*_{CL}(T^*)$.

APPENDIX E

CALIBRATION OF GAS CHROMATOGRAPHS

General

Two chromatographs, the Perkin-Elmer vapor fractometer 154B and 154D were used to analyse the gas and liquid compositions, and all of the chromatographic analyses were based on the peak heights.

Prior to starting the actual calibration, the approximate composition range of the equilibrium gas and liquid phases was determined to find the right column and reasonable conditions for the column. The approximate composition range of the gas phase was calculated using LJCL model (see Chapter IV) and assuming that the condensed phase is pure. For the liquid phase two experimental points, one each at the highest and lowest temperatures were actually run to determine the approximate composition range. A column and carrier gas were simultaneously determined by considering the required time for each anaysis, separation of the peaks (if there is mroe than one), stable base lines on both sides of the peak to be analysed and width and symmetry of the main peak. After the column was chosen, the variables such as detector voltage, recorder voltage, gas sample size, recorder chart speed, oven temperature and flow rate of the

carrier gas were adjusted so that the optimum condition for the calibration were obtained.

As a first step in the calibration, a standard bottle of approximate composition was made for each chromatograph attenuation switch used such that its peak height is about three-quarters of the width of the recorder chart paper. Initially, several peak heights for each standard bottle were measured in less than two hours so as to minimize the possible drifts in the chromatograph during these measurements. The average peak height of each standard bottle was later used to correct any drifts in the chromatograph during the calibration and the phase equilibrium measurements. The correction for the sample peak height was done by analysing the sample and the corresponding standard bottle one after the other and changing the sample peak height by a proportional amount to the ratio of the original peak height to the peak height of the standard bottle at the time of the analysis.

The samples of the gas mixtures with known compositions for the calibration were made using a gas mixing burette built by Kirk.[68] These samples contained two components, one to be analysed and a second. Nonideality of gases was taken into account for all gases in calculating the compositions of the samples by using the second virial coefficients. The calibration points were plotted h's vs

h·s/y on semi-log paper as shown in Figures 30, 31, and 32, where h is the corrected sample peak height, s is the factor of the attenuation switch, and y is the composition of the minor component of a sample. To determine the composition of the known sample during the gas-liquid runs, the corrected peak height of that unknown sample was multiplied by the corresponding attenuation factor and that product was read on the calibration curve which had been drawn through the calibration points by eye.

Analysis of Carbon Tetrafluoride in Helium

The calibration curve for the carbon tetrafluoride in helium in the gas phase was obtained using a 154D chromatograph and is shown in Figure 30. The composition range in the calibration was from 0.03 to 20 mole percent and to cover this, nine standard bottles were required.

Initially, three peak heights for each standard bottle were measured and the average value of these peak heights were used to correct any drifts in the chromatograph. All of these measurements were done in around two hours, and the net maximum correction for these peak heights to a datum temperature and pressure due to the change of ambient conditions during these measurements was less than ±0.035 mole percent which was neglected.

The room temperature and barometric pressure were recorded during gas mixing for the calibration. The gas

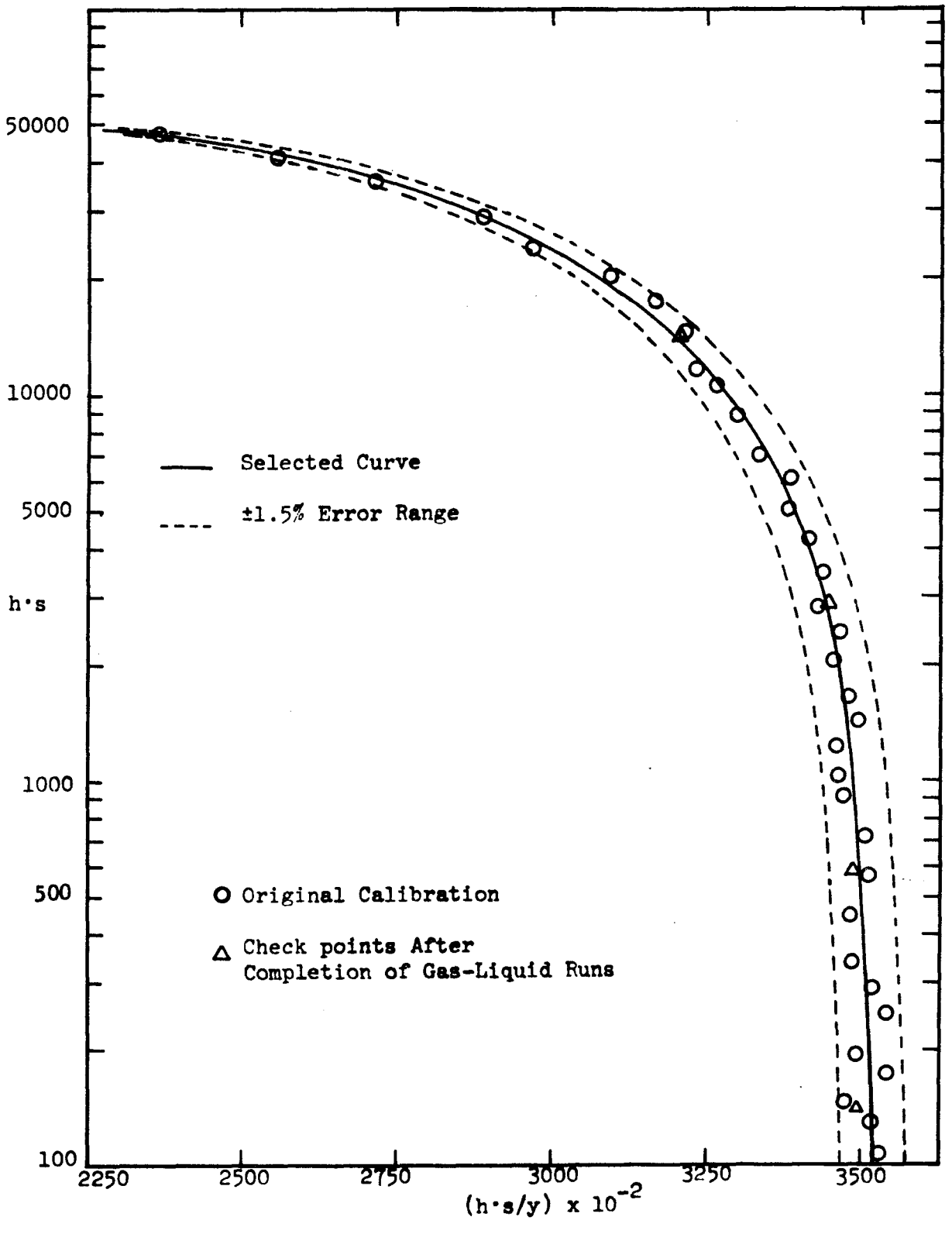

Figure 30. Calibration Curve of Carbon Tetrafluoride in Helium.

imperfection correction of 0.35 mole percent based on the average room temperature and barometric pressure during the calibration was made for the carbon tetrafluoride and 0.05 mole percent for the helium in calculating the composition of the gas mixture. A smooth curve was drawn through the calibration points and all points were within ±1.5 mole percent from this curve. After completion of the phase equilibrium measurements, four additional calibration points were made. These are shown in Figure 30.

The operating conditions of the 154D for this system are given in Table 11.

Analysis of Chlorotrifluoromethane in Helium

The composition range of the calibration of the chlorotrifluoromethane in the gas phase was around 0.04 to 23 mole percent and the calibration curve is shown in Figure 31. Nine standard bottles were required to cover this composition range. For the samples of the gas mixtures prepared by using the gas mixing burette, the correction of 1.06 mole percent for the gas imperfection based on the average room temperature and barometric pressure during the calibration was made for the chlorotrifluoromethane and 0.05 mole percent for the helium in calculating the composition of the samples.

The uncertainty of the calibration curve was about ±3 mole percent throughout the composition range and was again proved by making three additional points after comple-

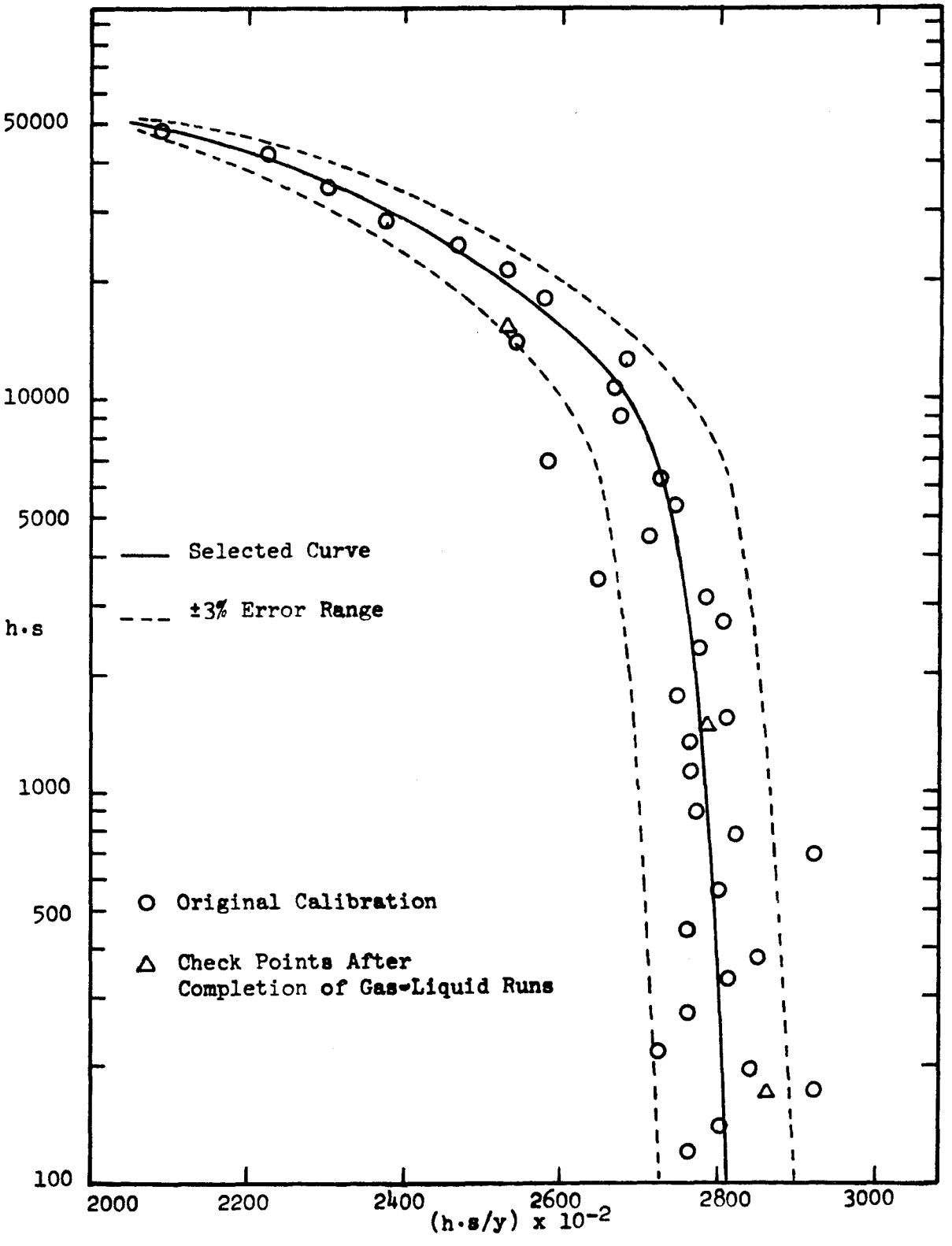

Figure 31. Calibration Curve of Chlorotrifluoromethane in Helium.

tion of the gas-liquid runs. The 154D chromatograph was used for this analysis and its operating conditions are given in Table 11.

Analysis of Helium in Carbon Tetrafluoride and Chlorotrifluoromethane

For this analysis the 154B chromatograph was used and its operating conditions are given in Table 11. As the purpose was to analyse the helium composition in both systems, only one calibration curve was made in the composition range of approximately 0.16 to 6.9 mole percent of helium in carbon tetrafluoride and seven standard bottles were required to cover this composition range. The gas mixtures were also prepared using the gas mixing burette and the same amount of gas imperfection correction for both components as stated earlier was made in the calculation of the composition of the samples. The calibration curve is shown in Figure 32 together with ±1.5 mole percent error range and six additional calibration points, three after completion of the phase equilibrium measurements in the helium-carbon tetrafluoride system and three after completion of the helium-chlorotrifluoromethane system.

To separate helium from carbon tetrafluoride and or chlorotrifluoromethane wide enough to have a stable base line after the helium peak, it was necessary to install a seven feet of silica gel (30/60 mesh) column externally

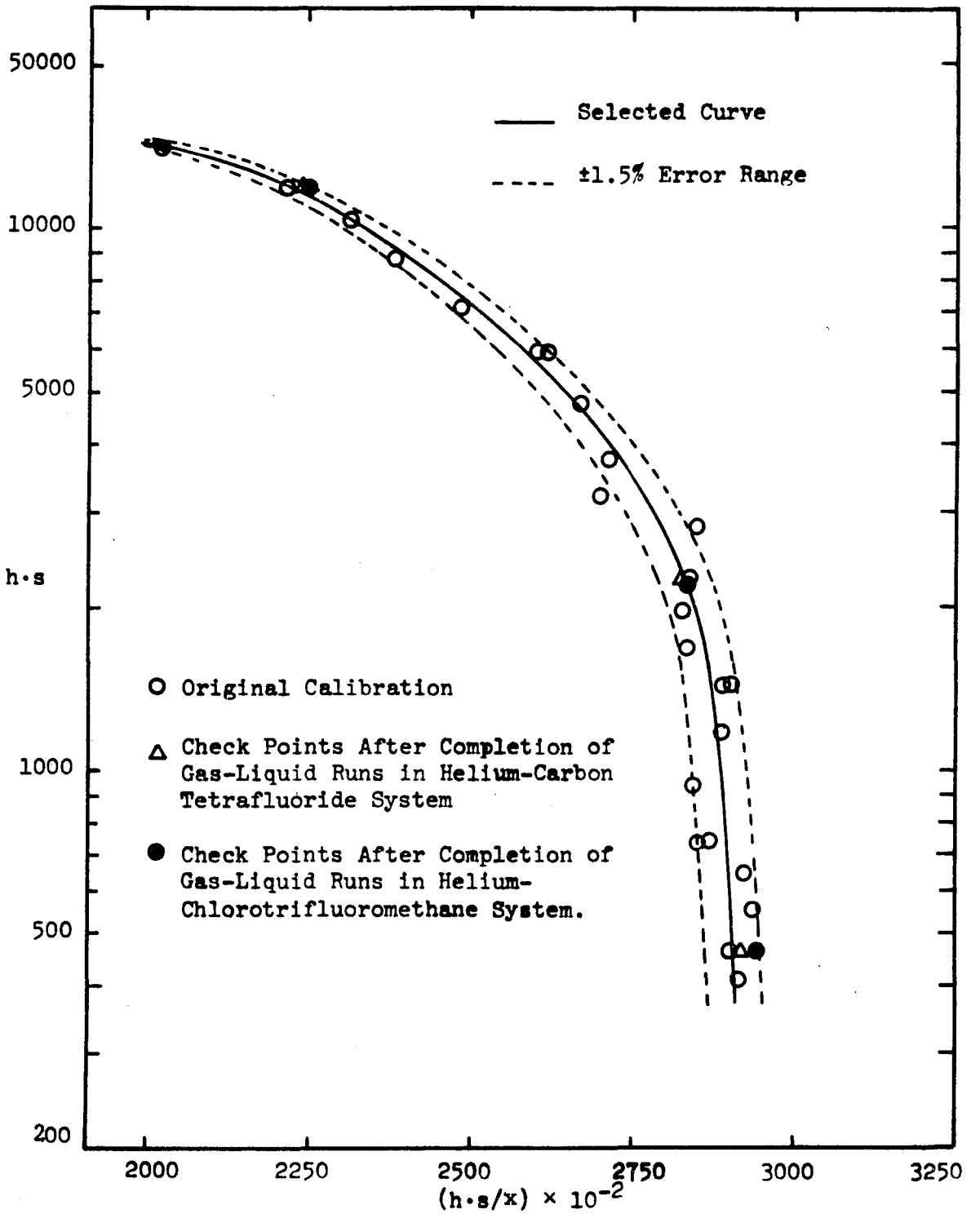

Figure 32. Calibration Curve of Helium in Carbon Tetrafluoride and Chlorotrifluoromethane.

Table 11. Operating Conditions of Chromatograph

	Systems of Analysis		
	He in CF_4	CF_4 in He	$CClF_3$ in He
Chromatograph	154B	154D	154D
Perkin-Elmer Column Type	Molecular Sieve 5A	Silica Gel	Silica Gel
Carrier Gas	Argon	Helium	Helium
Length, meter	1	1	1
Sample Size, cc	10	16.4	16.4
Oven Temperature, C	30	33	90
Pressure inside Column, psig	15	6.5	11.5
Flow Rate, cc/min at Room T and P	127	116	173
Detector Voltage mv at Shunt	58.50	4.65	4.65
Recorder Voltage at Shunt	5.70	2.00*	0.45*
Chart Speed, inches/min	1.5	1.5	1.5

* These voltages caused a deflection of 95 divisions on the recorder chart.

between the sample valve and the main column in the oven. Extreme care was taken not to introduce any trace of the chlorotrifluoromethane into the main column during the experiment because it is permanently adsorbed on the molecular sieve 5A.

APPENDIX F

SUMMARY OF EXPERIMENTAL PHASE EQUILIBRIUM DATA FOR THE HELIUM-CARBON TETRAFLUORIDE AND HELIUM-CHLOROTRIFLUOROMETHANE SYSTEMS

In Tables 12 and 13 the complete experimental data of phase equilibria for the helium-carbon tetrafluoride and helium-chlorotrifluoromethane systems are shown and these tables present the compositions of the gas and liquid phase, together with the corresponding temperatures and pressures. Six isotherms for the helium-carbon tetrafluoride system in the temperature range from approximately 106 to 173 K and seven isotherms for the helium-chlorotrifluoromethane system ranging from around 145 to 231 K were measured. The data are presented in the order in which they were measured.

The samples are designated by four characters mixing letters and numbers in the first column in the tables. The first letter G or L represents the gas phase or liquid phase, the first number designates the sequential pressure setting, the second letter indicates the isotherm investigated and the second number is assigned sequentially to the samples taken at each pressure point.

All temperatures are in the IPTS-68 (see Appendix A) and the conversion factor of 14.696 was used to convert pressures in psia to those in atmospheres. The temperature

assigned to the gas and liquid samples was the average of the maximum and minimum temperatures indicated by the platinum resistance thermometer during the analysis of the gas and liquid samples at each pressure setting, and is shown together with the drifts. The temperature (indicated by the platinum resistance thermometer) control of the equilibrium cell was always maintained within ±0.02 K and the maximum of the temperature gradients along the cell was 0.03 K in the helium-carbon tetrafluoride system and 0.02 K in the helium-chlorotrifluoromethane system. These differences were neglected in assigning the equilibrium temperatures to the gas and liquid samples since these small temperature gradients change the enhancement factors less than 0.2 percent and the liquid compositions less than only 0.1 percent.

The uncertainty of gas phase equilibrium data for the helium-carbon tetrafluoride system is estimated to be within ±2.0 percent of the experimental values and ±3.5 percent for the helium-chlorotrifluoromethane system. Liquid phase equilibrium data for both of these systems have the experimental uncertainty of ±2.0 percent. Since the experimental uncertainties are such as given above, the last number in the numerical values of ϕ and x_2 in Tables 12 and 13 is meaningless but included for the purpose of internal consistency in the numerical calculation.

The normal flow rate used throughout these experimental measurements was 100 cc/hr at the cell temperature and pressure except in the case of the specified measurements.

Table 12. Experimental Gas and Liquid Phase Equilibrium Compositions in the Helium-Carbon Tetrafluoride System

Sample No.	T, K	P, atm	P_{o1}, atm	$100y_1$ mole %	ϕ	$100x_2$ mole %
G1A6	106.005	120.39	0.01926	0.03282	2.051	
G1A7	±0.010	120.39	0.01926	0.03278	2.049	
G1A8		120.39	0.01926	0.03273	2.045	
Selected	106.01	120.39			2.048	
G2A3*	106.004	120.39	0.01926	0.03278	2.049	
G2A4*	±0.001	120.39	0.01926	0.03259	2.037	
Selected	106.00	120.39			2.043	
G3A3**	106.002	120.39	0.01925	0.03291	2.059	
G3A4**	±0.001	120.39	0.01925	0.03284	2.054	
L1A1**		120.39				0.9316
L1A2**		120.39				0.9476
Selected	106.00	120.39			2.057	0.9396
G4A3	106.012	99.71	0.01928	0.03559	1.840	
G4A4	±0.003	99.71	0.01928	0.03567	1.844	
G4A5		99.71	0.01928	0.03582	1.852	
L2A1		99.71				0.7787
L2A2		99.71				0.7797
Selected	106.01	99.71			1.845	0.7792
G5A4	106.004	80.05	0.01926	0.04208	1.749	
G5A5	±0.000	80.05	0.01926	0.04206	1.748	
G5A6		80.05	0.01926	0.04202	1.746	
L3A2		80.05				0.6511
L3A3		80.05				0.6521
Selected	106.00	80.05			1.748	0.6516
G6A3	106.008	59.70	0.01927	0.04909	1.521	
G6A4	±0.005	59.70	0.01927	0.04911	1.521	
G6A5		59.70	0.01927	0.04941	1.531	
L4A2		59.70				0.4888
L4A3		59.70				0.4895
Selected	106.01	59.70			1.524	0.4892

Table 12. (Continued)

Sample No.	T,K	P,atm	P_{o1},atm	$100y_1$ mole %	ϕ	$100x_2$ mole %
G7A3	106.000	39.86	0.01925	0.06400	1.325	
G7A4	±0.005	39.86	0.01925	0.06346	1.314	
G7A5		39.86	0.01925	0.06419	1.329	
L5A1		39.86				0.3245
L5A2		39.86				0.3235
Selected	106.00	39.86			1.323	0.3240
G8A4	106.003	19.92	0.01926	0.1121	1.160	
G8A5	±0.009	19.92	0.01926	0.1123	1.162	
G8A6		19.92	0.01926	0.1114	1.152	
L6A1		19.92				0.1644
L6A2		19.92				0.1652
L6A3		19.92				0.1657
Selected	106.00	19.92			1.157	0.1651
G1B3	117.323	19.85	0.08271	0.4727	1.134	
G1B4	±0.014	19.85	0.08271	0.4730	1.135	
G1B5		19.85	0.08271	0.4750	1.140	
L1B1		19.85				0.2526
L1B2		19.85				0.2530
Selected	117.32	19.85			1.137	0.2528
G2B3**	117.336	19.85	0.08283	0.4743	1.137	
G2B4**	±0.002	19.85	0.08283	0.4737	1.135	
G2B5**		19.85	0.08283	0.4735	1.135	
Selected	117.34	19.85			1.135	
G3B3*	117.344	19.93	0.08291	0.4731	1.137	
G3B4*	±0.015	19.93	0.08291	0.4729	1.137	
G3B5*		19.93	0.08291	0.4735	1.138	
Selected	117.34	19.93			1.137	
G4B5***	117.325	19.80	0.08273	0.4713	1.128	
G4B6***	±0.011	19.80	0.08273	0.4724	1.131	
G4B7***		19.80	0.08273	0.4686	1.122	
L2B1***		19.80				0.2519
L2B2***		19.80				0.2497
Selected	117.33	19.80			1.127	0.2508

Table 12. (Continued)

Sample No.	T,K	P,atm	P_{o1},atm	$100y_1$ mole %	Ø	$100x_2$ mole %
G5B3	117.334	40.44	0.08281	0.2575	1.257	
G5B4	±0.011	40.44	0.08281	0.2569	1.255	
G5B5		40.44	0.08281	0.2570	1.255	
L3B1		40.44				0.5055
L3B2		40.44				0.5067
Selected	117.33	40.44			1.255	0.5061
G6B3	117.334	59.73	0.08281	0.1937	1.397	
G6B4	±0.019	59.73	0.08281	0.1926	1.389	
G6B5		59.73	0.08281	0.1931	1.393	
L4B1		59.73				0.7225
L4B2		59.73				0.7252
Selected	117.33	59.73			1.393	0.7238
G7B5	117.330	80.01	0.08278	0.1590	1.537	
G7B6	±0.011	80.01	0.08278	0.1596	1.543	
G7B7		80.01	0.08278	0.1586	1.533	
L5B1		80.01				0.9753
L5B2		80.01				0.9779
Selected	117.33	80.01			1.538	0.9766
G8B4	117.353	100.02	0.08299	0.1378	1.661	
G8B5	±0.005	100.02	0.08299	0.1374	1.656	
G8B6		100.02	0.08299	0.1378	1.661	
L6B1		100.02				1.166
L6B2		100.02				1.163
Selected	117.35	100.02			1.658	1.165
G9B3	117.315	119.95	0.08264	0.1258	1.826	
G9B4	±0.013	119.95	0.08264	0.1249	1.813	
G9B5		119.95	0.08264	0.1261	1.830	
L7B1		119.95				1.398
L7B2		119.95				1.399
Selected	117.32	119.95			1.823	1.399
G10B3**	117.358	119.95	0.08304	0.1259	1.819	
G10B4**	±0.001	119.95	0.08304	0.1259	1.817	
G10B5**		119.95	0.08304	0.1259	1.819	
Selected	117.36	119.95			1.819	

Table 12. (Continued)

Sample No.	T,K	P,atm	P_{o1},atm	$100y_1$ mole %	ϕ	$100x_2$ mole %
G1C3	132.178	120.19	0.3636	0.4879	1.613	
G1C4	±0.013	120.19	0.3636	0.4884	1.614	
G1C5		120.19	0.3636	0.4885	1.615	
L1C1		120.19				2.296
L1C2		120.19				2.289
Selected	132.18	120.19			1.614	2.293
G2C4	132.175	99.95	0.3635	0.5469	1.504	
G2C5	±0.010	99.95	0.3635	0.5461	1.501	
G2C6		99.95	0.3635	0.5485	1.508	
L2C1		99.95				1.886
L2C2		99.95				1.895
Selected	132.18	99.95			1.504	1.891
G3C3	132.178	79.94	0.3636	0.6368	1.400	
G3C4	±0.01	79.94	0.3636	0.6360	1.398	
G3C5		79.94	0.3636	0.6378	1.402	
L3C1		79.94				1.490
L3C2		79.94				1.509
Selected	132.18	79.94			1.400	1.500
G4C3	132.171	60.00	0.3634	0.7942	1.311	
G4C4	±0.013	60.00	0.3634	0.7933	1.310	
G4C5		60.00	0.3634	0.7937	1.310	
L4C1		60.00				1.167
L4C2		60.00				1.182
Selected	132.17	60.00			1.310	1.174
G5C3	132.186	40.20	0.3639	1.100	1.215	
G5C4	±0.010	40.20	0.3639	1.098	1.213	
G5C5		40.20	0.3639	1.100	1.215	
L5C1		40.20				0.7746
L5C2		40.20				0.7727
Selected	132.19	40.20			1.215	0.7736
G6C4	132.177	20.08	0.3636	2.011	1.111	
G6C5	±0.013	20.08	0.3636	2.019	1.115	
G6C6		20.08	0.3636	2.011	1.111	
L6C1		20.08				0.3887
L6C2		20.08				0.3891
Selected	132.18	20.08			1.112	0.3889

Table 12. (Continued)

Sample No.	T,K	P,atm	P_{o1},atm	$100y_1$ mole %	Ø	$100x_2$ mole %
G1D5	147.101	20.12	1.148	6.420	1.126	
G1D6	±0.011	20.12	1.148	6.415	1.125	
G1D7		20.12	1.148	6.429	1.127	
L1D1		20.12				0.5656
L1D2		20.12				0.5585
Selected	147.10	20.12			1.126	0.5620
G2D3	147.097	40.20	1.147	3.425	1.200	
G2D4	±0.015	40.20	1.147	3.418	1.198	
G2D5		40.20	1.147	3.430	1.202	
L2D1		40.20				1.141
L2D2		40.20				1.139
Selected	147.10	40.20			1.200	1.140
G3D3	147.092	59.90	1.147	2.445	1.277	
G3D4	±0.006	59.90	1.147	2.451	1.280	
G3D5		59.90	1.147	2.436	1.272	
L3D1		59.90				1.683
L3D2		59.90				1.686
Selected	147.09	59.90			1.277	1.685
G4D3	147.108	80.45	1.148	1.923	1.347	
G4D4	±0.003	80.45	1.148	1.923	1.347	
G4D5		80.45	1.148	1.922	1.347	
L4D1		80.45				2.269
L4D2		80.45				2.263
Selected	147.11	80.45			1.347	2.266
G5D3	147.097	99.98	1.147	1.654	1.441	
G5D4	±0.007	99.98	1.147	1.656	1.443	
G5D5		99.98	1.147	1.655	1.442	
L5D1		99.98				2.682
G5D2		99.98				2.663
Selected	147.10	99.98			1.442	2.673
G6D3	147.095	120.06	1.147	1.454	1.522	
G6D4	±0.009	120.06	1.147	1.456	1.524	
G6D5		120.06	1.147	1.454	1.522	
L6D1		120.06				3.172
L6D2		120.06				3.146
Selected	147.10	120.06			1.523	3.159

Table 12. (Continued)

Sample No.	T,K	P,atm	P_{o_1},atm	$100y_1$ mole %	ϕ	$100x_2$ mole %
G1E6	162.022	120.19	2.864	3.544	1.487	
G1E7	±0.009	120.19	2.864	3.531	1.482	
G1E8		120.19	2.864	3.556	1.493	
L1E1		120.19				4.484
L1E2		120.19				4.469
Selected	162.02	120.19			1.487	4.477
G2E3	162.019	100.12	2.863	4.023	1.407	
G2E4	±0.003	100.12	2.863	4.028	1.409	
G2E5		100.12	2.863	4.048	1.416	
L2E1		100.12				3.736
L2E2		100.12				3.742
Selected	162.02	100.12			1.410	3.739
G3E7	162.030	80.59	2.865	4.794	1.349	
G3E8	±0.012	80.59	2.865	4.808	1.352	
G3E9		80.59	2.865	4.813	1.354	
L3E1		80.59				3.020
L3E2		80.59				3.020
Selected	162.03	80.59			1.352	3.020
G4E4	162.022	60.00	2.864	6.115	1.281	
G4E5	±0.004	60.00	2.864	6.146	1.288	
G4E6		60.00	2.864	6.104	1.280	
L4E1		60.00				2.349
L4E2		60.00				2.347
Selected	162.02	60.00			1.283	2.348
G5E4	162.022	40.03	2.864	8.600	1.202	
G5E5	±0.005	40.03	2.864	8.587	1.200	
G5E6		40.03	2.864	8.625	1.206	
L5E1		40.03				1.500
L5E2		40.03				1.502
Selected	162.02	40.03			1.203	1.501
G6E3	162.033	20.42	2.865	15.72	1.120	
G6E4	±0.016	20.42	2.865	15.79	1.125	
G6E5		20.42	2.865	15.77	1.124	
L6E1		20.42				0.7058
L6E2		20.42				0.7143
Selected	162.03	20.42			1.123	0.7103

Table 12. (Concluded)

Sample No.	T,K	P,atm	P_{o1},atm	$100y_1$ mole %	ϕ	$100x_2$ mole %
G1F6	173.018	120.09	5.028	6.323	1.510	
G1F7	±0.008	120.09	5.028	6.281	1.500	
G1F8		120.09	5.028	6.310	1.507	
L1F1		120.09				5.317
L1F2		120.09				5.309
Selected	173.02	120.09			1.506	5.313
G2F3	173.023	100.18	5.030	7.233	1.441	
G2F4	±0.001	100.18	5.030	7.240	1.442	
G2F5		100.18	5.030	7.204	1.435	
L2F1		100.18				4.665
L2F2		100.18				4.676
Selected	173.02	100.18			1.439	4.670
G3F6	173.021	80.31	5.029	8.569	1.368	
G3F7	±0.010	80.31	5.029	8.569	1.368	
G3F8		80.31	5.029	8.544	1.364	
L3F1		80.31				3.781
L3F2		80.31				3.793
Selected	173.02	80.31			1.367	3.787
G4F3	173.019	59.69	5.029	10.90	1.294	
G4F4	±0.001	59.69	5.029	10.92	1.296	
G4F5		59.69	5.029	10.89	1.293	
L4F1		59.69				2.732
L4F2		59.69				2.755
Selected	173.02	59.69			1.294	2.743
G5F3	173.019	40.23	5.029	15.12	1.210	
G5F4	±0.006	40.23	5.029	15.13	1.210	
G5F5		40.23	5.029	15.14	1.211	
L5F2		40.23				1.847
L5F3		40.23				1.839
Selected	173.02	40.23			1.210	1.843

* Flow rate was half the normal flow rate.

** Flow rate was twice the normal flow rate.

*** Temperature was lowered from 132.18 K

Table 13. Experimental Gas and Liquid Phase Equilibrium Compositions in the Helium-Chlorotrifluoromethane System.

Sample No.	T,K	P,atm	P_{o1},atm	$100y_1$ mole %	ϕ	$100x_2$ mole %
G1A3	145.215	120.13	0.03245	0.03808	1.410	
G1A4	±0.017	120.13	0.03245	0.03750	1.388	
G1A5		120.13	0.03245	0.03738	1.384	
G1A6		120.13	0.03245	0.03795	1.405	
G1A7		120.13	0.03245	0.03833	1.419	
L1A1		120.13				1.134
L1A2		120.13				1.128
Selected	145.22	120.13			1.401	1.131
G2A3**	145.206	120.13	0.03242	0.03701	1.371	
G2A4**	±0.01	120.13	0.03242	0.03726	1.381	
G2A5**		120.13	0.03242	0.03737	1.385	
Selected	145.21	120.13			1.379	
G3A3*	145.227	120.13	0.03249	0.03750	1.387	
G3A4*	±0.006	120.13	0.03249	0.03760	1.390	
G3A5*		120.13	0.03249	0.03821	1.413	
Selected	145.23	120.13			1.397	
G4A6	145.206	100.12	0.03242	0.04485	1.385	
G4A7	±0.01	100.12	0.03242	0.04435	1.370	
G4A8		100.12	0.03242	0.04406	1.361	
L2A2		100.12				0.9446
L2A3		100.12				0.9395
Selected	145.21	100.12			1.372	0.9420
G5A3	145.223	80.01	0.03248	0.05266	1.297	
G5A4	±0.003	80.01	0.03248	0.05387	1.302	
G5A5		80.01	0.03248	0.05237	1.290	
L3A1		80.01				0.7582
L3A2		80.01				0.7569
Selected	145.22				1.296	0.7576

Table 13. (Continued)

Sample No.	T,K	P,atm	P_{o_1},atm	$100y_1$ mole %	ϕ	$100x_2$ mole %
G6A3	145.217	59.97	0.03246	0.06673	1.233	
G6A4	±0.012	59.97	0.03246	0.06629	1.225	
G6A5		59.97	0.03246	0.06599	1.219	
G6A6		59.97	0.03246	0.06683	1.235	
L4A1		59.97				0.5951
L4A2		59.97				0.5916
Selected	145.22	59.97			1.228	0.5934
G7A3	145.218	40.17	0.03246	0.09024	1.117	
G7A4	±0.012	40.17	0.03246	0.09080	1.124	
G7A5		40.17	0.03246	0.09021	1.116	
L5A1		40.17				0.3956
L5A2		40.17				0.3962
Selected	145.22	40.17			1.119	0.3959
G8A3	145.212	20.15	0.03244	0.1737	1.079	
G8A4	±0.014	20.15	0.03244	0.1738	1.080	
G8A5		20.15	0.03244	0.1736	1.078	
L6A1		20.15				0.2033
L6A2		20.15				0.2025
Selected	145.21	20.15			1.079	0.2029
G9A3***	145.226	20.14	0.03249	0.1729	1.072	
G9A4***	±0.000	20.14	0.03249	0.1726	1.070	
Selected	145.23	20.14			1.071	
G10A3*	145.226	20.17	0.03249	0.1736	1.078	
G10A4*	±0.002	20.17	0.03249	0.1750	1.086	
Selected	145.23	20.17			1.082	
G1B4	163.010	20.13	0.1574	0.8274	1.059	
G1B5	±0.012	20.13	0.1574	0.8357	1.069	
G1B6		20.13	0.1574	0.8329	1.065	
L1B1		20.13				0.3062
L1B2		20.13				0.3054
Selected	163.01	20.13			1.064	0.3058

Table 13. (Continued)

Sample No.	T,K	P,atm	P_{o1},atm	$100y_1$ mole %	ϕ	$100x_2$ mole %
G2B4	163.022	39.68	0.1575	0.4384	1.104	
G2B5	±0.005	39.68	0.1575	0.4388	1.105	
G2B6		39.68	0.1575	0.4382	1.105	
L2B1		39.68				0.5934
L2B2		39.68				0.5851
Selected	163.02	39.68			1.104	0.5892
G3B4	163.010	60.09	0.1574	0.2998	1.145	
G3B5	±0.008	60.09	0.1574	0.2985	1.140	
G3B6		60.09	0.1574	0.2994	1.143	
L3B1		60.09				0.8959
L3B2		60.09				0.8976
Selected	163.01	60.09			1.142	0.8968
G4B3	163.005	79.84	0.1573	0.2450	1.244	
G4B4	±0.009	79.84	0.1573	0.2447	1.242	
G4B5		79.84	0.1573	0.2435	1.236	
L4B1		79.84				1.199
L4B2		79.84				1.208
Selected	163.01	79.84			1.240	1.204
G5B4	163.013	100.05	0.1574	0.2040	1.297	
G5B5	±0.010	100.05	0.1574	0.2022	1.285	
G5B6		100.05	0.1574	0.2026	1.288	
L5B1		100.05				1.447
L5B2		100.05				1.451
Selected	163.01	100.05			1.291	1.449
G6B3	163.003	120.05	0.1573	1.734	1.323	
G6B4	±0.008	120.05	0.1573	1.728	1.319	
G6B5		120.05	0.1573	1.737	1.326	
L6B1		120.05				1.736
L6B2		120.05				1.755
Selected	163.00	120.05			1.323	1.746
G1C4	180.022	120.07	0.5102	0.5473	1.288	
G1C5	±0.015	120.07	0.5102	0.5483	1.290	
G1C6		120.07	0.5102	0.5460	1.285	

Table 13. (Continued)

Sample No.	T,K	P,atm	P_{o1},atm	$100y_1$ mole %	ϕ	$100x_2$ mole %
L1C1		120.07				2.562
L1C2		120.07				2.501
L1C3		120.07				2.530
Selected	180.02	120.07			1.288	2.531
G2C3	180.026	100.40	0.5103	0.6387	1.257	
G2C4	±0.017	100.40	0.5103	0.6388	1.257	
G2C5		100.40	0.5103	0.6355	1.250	
L2C1		100.40				2.102
L2C2		100.40				2.111
Selected	180.03	100.40			1.254	2.107
G3C3	180.020	80.06	0.5101	0.7614	1.195	
G3C4	±0.015	80.06	0.5101	0.7599	1.193	
G3C5		80.06	0.5101	0.7531	1.182	
G3C6		80.06	0.5101	0.7500	1.177	
L3C1		80.06				1.652
L3C2		80.06				1.684
Selected	180.02	80.06			1.187	1.668
G4C5	180.006	60.19	0.5103	0.9869	1.164	
G4C6	±0.013	60.19	0.5103	0.9881	1.165	
G4C7		60.19	0.5103	0.9920	1.170	
L4C1		60.19				1.260
L4C2		60.19				1.265
Selected	180.01	60.19			1.167	1.263
G5C3	180.005	40.05	0.5103	1.388	1.089	
G5C4	±0.007	40.05	0.5103	1.393	1.093	
G5C5		40.05	0.5103	1.385	1.087	
L5C1		40.05				0.8631
L5C2		40.05				0.8634
Selected	180.01	40.05			1.090	0.8633
G6C3	180.019	20.24	0.5101	2.595	1.030	
G6C4	±0.012	20.24	0.5101	2.617	1.038	
G6C5		20.24	0.5101	2.601	1.032	
L6C1		20.24				0.4301
L6C2		20.24				0.4358
Selected	180.02	20.24			1.033	0.4329

Table 13. (Continued)

Sample No.	T,K	P,atm	P_{o1},atm	$100y_1$ mole %	Ø	$100x_2$ mole %
G1D3	196.009	20.18	1.249	6.590	1.065	
G1D4	±0.014	20.18	1.249	6.549	1.058	
G1D5		20.18	1.249	6.588	1.064	
L1D1		20.18				0.5874
L1D2		20.18				0.5773
Selected	196.01	20.18			1.062	0.5824
G2D4	196.002	39.93	1.248	3.506	1.122	
G2D5	±0.013	39.93	1.248	3.482	1.114	
G2D6		39.93	1.248	3.491	1.117	
L2D1		39.93				1.152
L2D2		39.93				1.160
Selected	196.00	39.93			1.118	1.157
G3D4	195.999	60.07	1.248	2.441	1.175	
G3D5	±0.011	60.07	1.248	2.441	1.175	
G3D6		60.07	1.248	2.445	1.177	
Selected	196.00	60.07			1.176	
G4D4	196.006	79.83	1.248	1.901	1.216	
G4D5	±0.007	79.83	1.248	1.892	1.210	
G4D6		79.83	1.248	1.911	1.222	
L4D1		79.83				2.280
L4D2		79.83				2.262
L4D3		79.83				2.267
Selected	196.01	79.83			1.216	2.270
G5D4	196.000	100.32	1.248	1.514	1.217	
G5D5	±0.012	100.32	1.248	1.511	1.215	
G5D6		100.32	1.248	1.532	1.231	
G5D7		100.32	1.248	1.514	1.217	
L5D1		100.32				2.659
L5D2		100.32				2.657
Selected	196.00	100.32			1.220	2.658
G6D3	196.004	120.08	1.248	1.307	1.258	
G6D4	±0.014	120.08	1.248	1.314	1.264	
G6D5		120.08	1.248	1.308	1.259	
L6D1		120.08				3.195
L6D2		120.08				3.180
Selected	196.00	120.08			1.260	3.187

Table 13. (Continued)

Sample No.	T,K	P,atm	P_{o1},atm	$100y_1$ mole %	ϕ	$100x_2$ mole %
G1E3	211.063	120.46	2.526	2.594	1.237	
G1E4	±0.005	120.46	2.526	2.585	1.233	
G1E5		120.46	2.526	2.572	1.227	
L1E1		120.46				4.128
L1E2		120.46				4.097
Selected	211.06	120.46			1.232	4.112
G2E4	211.065	100.04	2.526	3.113	1.233	
G2E5	±0.001	100.04	2.526	3.089	1.223	
G2E6		100.04	2.526	3.096	1.226	
L2E1		100.04				3.453
L2E2		100.04				3.433
Selected	211.07	100.04			1.227	3.443
G3E4	211.059	79.89	2.526	3.866	1.223	
G3E5	±0.015	79.89	2.526	3.847	1.217	
G3E6		79.89	2.526	3.868	1.223	
L3E1		79.89				2.760
L3E2		79.89				2.740
Selected	211.06	79.89			1.221	2.750
G4E4	211.055	60.16	2.525	5.054	1.204	
G4E5	±0.011	60.16	2.525	5.077	1.210	
G4E6		60.16	2.525	5.049	1.203	
L4E1		60.16				2.181
L4E2		60.16				2.184
Selected	211.06	60.16			1.206	2.183
G5E3	211.065	40.16	2.526	7.241	1.151	
G5E4	±0.012	40.16	2.526	7.285	1.158	
G5E5		40.16	2.526	7.251	1.153	
L5E1		40.16				1.407
L5E2		40.16				1.429
Selected	211.07	40.16			1.154	1.418
G6E4	211.062	20.32	2.526	13.60	1.094	
G6E5	±0.014	20.32	2.526	13.84	1.113	
G6E6		20.32	2.526	13.71	1.103	
G6E7		20.32	2.526	13.73	1.104	

Table 13. (Continued)

Sample No.	T,K	P,atm	P_{o1},atm	$100y_1$ mole %	ϕ	$100x_2$ mole %
L6E1		20.32				0.6759
L6E2		20.32				0.6730
Selected	211.06	20.32			1.104	0.6745
G1F3	221.271	20.17	3.838	22.24	1.169	
G1F4	±0.018	20.17	3.838	22.23	1.168	
G1F5		20.17	3.838	22.27	1.170	
L1F1		20.17				0.7373
L1F2		20.17				0.7541
Selected	221.27	20.17			1.169	0.7457
G2F3	221.278	40.18	3.839	11.31	1.184	
G2F4	±0.01	40.18	3.839	11.29	1.182	
G2F5		40.18	3.839	11.28	1.181	
Selected	221.28	40.18			1.182	
G3F4	221.269	60.01	3.837	7.510	1.175	
G3F5	±0.012	60.01	3.837	7.582	1.185	
C3F6		60.01	3.837	7.590	1.187	
Selected	221.27	60.01			1.183	
G4F4	221.266	80.02	3.837	5.743	1.198	
G4F5	±0.009	80.02	3.837	5.719	1.193	
G4F6		80.02	3.837	5.705	1.190	
L2F1		80.02				3.139
L2F2		80.02				3.203
Selected	221.27	80.02			1.193	3.171
G5F4	221.271	100.06	3.838	4.915	1.281	
G5G5	±0.010	100.06	3.838	4.902	1.278	
G5F6		100.06	3.838	4.884	1.273	
L3F1		100.06				4.034
L3F2		100.06				4.036
Selected	221.27	100.06			1.277	4.035
G6F3	221.269	119.99	3.838	4.193	1.311	
G6F4	±0.018	119.99	3.838	4.169	1.303	
G6F5		119.99	3.838	4.203	1.314	
G6F6		119.99	3.838	4.182	1.307	

Table 13. (Continued)

Sample No.	T,K	P,atm	P_{o1},atm	$100y_1$ mole %	ø	$100x_2$ mole %
L4F1		119.99				4.796
L4F2		119.99				4.753
Selected	221.27	119.99			1.309	4.774
G1G5	231.079	120.40	5.525	5.966	1.300	
G1G6	±0.022	120.40	5.525	5.940	1.294	
G1G7		120.40	5.525	5.944	1.295	
L1G1		120.40				5.492
L1G2		120.40				5.521
Selected	231.08	120.40			1.297	5.506
G2G3	231.085	100.08	5.526	7.049	1.277	
G2G4	±0.006	100.08	5.526	7.045	1.276	
G2G5		100.08	5.526	7.046	1.276	
L2G1		100.08				4.568
L2G2		100.08				4.624
Selected	231.09	100.08			1.276	4.596
G3G3	231.071	80.17	5.523	8.841	1.283	
G3G4	±0.011	80.17	5.523	8.872	1.288	
G3G5		80.17	5.523	8.821	1.280	
L3G1		80.17				3.671
L3G2		80.17				3.725
Selected	231.07	80.17			1.284	3.698
G4G3	231.081	59.93	5.525	11.62	1.260	
G4G4	±0.007	59.93	5.525	11.60	1.258	
G4G5		59.93	5.525	11.64	1.263	
Selected	231.08	59.93			1.260	
G5G5	231.073	40.16	5.524	16.60	1.207	
G5G6	±0.016	40.16	5.524	16.62	1.208	
G5G7		40.16	5.524	16.58	1.205	
L4G1		40.16				1.838
L4G2		40.16				1.861
Selected	231.07	40.16			1.207	1.849

Table 13. (Concluded)

* Flow rate was half the normal flow rate.

** Flow rate was twice the normal flow rate.

APPENDIX G

SMOOTHED EXPERIMENTAL AND THEORETICAL ENHANCEMENT FACTORS, AND SMOOTHED EXPERIMENTAL SOLUBILITY OF HELIUM

The graphically smoothed experimental enhancement factors and liquid phase compositions of the helium-carbon tetrafluoride and helium-chlorotrifluoromethane systems in this work are presented in Table 14 and 15 together with the theoretically predicted enhancement factors. No other available experimental data have been found for these systems.

Six models were used to predict the enhancement factors of the helium-carbon tetrafluoride system. They were the Lennard-Jones (6-12) classical (LJCL), the Kihara core model (KIH), the Kihara core model with the K_{12} factor calculated from the correlation of Hiza and Duncan (KIHCK12), the Kihara core model with the experimentally determined K_{12} factor (KIHEK12), the BWR equation with $(B_o)_{12}$ calculated using the linear average (BWR(LINEAR)), and the BWR equation using the Lorentz average for the calculation of $(B_o)_{12}$ (BWR (LORENTZ)). For the prediction of the enhancement factors of the helium-chlorotrifluoromethane system, only the four models, LJCL, KIH, KIHCK12 and KIHEK12, were tested since the BWR constants for the chlorotrifluoromethane were not available.

Table 14. Smoothed Experimental and Theoretical Enhancement Factors of Carbon Tetrafluoride in Helium, and the Smoothed Experimental Solubility of Helium in Liquid Carbon Tetrafluoride.

P atm	ø exp	ø LJCL	ø KIH	ø KIHCK12	ø KIHEK12	ø BWR(a)	ø BWR(b)	$100x_2$
			····· 106.01 K ·····					
20	1.175	1.156	1.177	1.103	1.159	1.136	1.110	0.1650
40	1.350	1.320	1.367	1.206	1.327	1.275	1.219	0.3269
60	1.527	1.493	1.571	1.311	1.506	1.422	1.330	0.4870
80	1.710	1.676	1.795	1.417	1.696	1.575	1.445	0.6452
100	1.888	1.867	2.033	1.525	1.898	1.736	1.562	0.7919
120	2.067	2.068	2.288	1.636	2.112	1.903	1.682	0.9253
			····· 117.33 K ·····					
20	1.128	1.123	1.142	1.085	1.128	1.116	1.092	0.2535
40	1.259	1.246	1.288	1.165	1.257	1.225	1.174	0.5000
60	1.393	1.374	1.442	1.245	1.392	1.337	1.257	0.7370
80	1.529	1.505	1.604	1.325	1.532	1.452	1.340	0.9660
100	1.669	1.640	1.775	1.407	1.679	1.570	1.423	1.181
120	1.813	1.778	1.955	1.489	1.832	1.692	1.508	1.392
			····· 132.18 K ·····					
20	1.110	1.102	1.122	1.079	1.112	1.116	1.095	0.3875
40	1.211	1.193	1.232	1.140	1.210	1.203	1.158	0.7700
60	1.313	1.285	1.347	1.201	1.310	1.291	1.219	1.155
80	1.411	1.377	1.465	1.261	1.414	1.380	1.280	1.521
100	1.505	1.471	1.589	1.322	1.520	1.470	1.341	1.894
120	1.606	1.565	1.716	1.383	1.629	1.561	1.400	2.264
			····· 147.10 K ·····					
20	1.117	1.102	1.125	1.092	1.117	1.143	1.123	0.5540
40	1.200	1.175	1.217	1.144	1.199	1.222	1.178	1.120
60	1.279	1.246	1.310	1.194	1.282	1.300	1.230	1.672
80	1.356	1.317	1.407	1.244	1.366	1.378	1.281	2.223
100	1.431	1.389	1.507	1.294	1.453	1.457	1.331	2.714
120	1.508	1.461	1.611	1.346	1.542	1.537	1.380	3.136
			····· 162.03 K ·····					
20	1.116	1.118	1.145	1.121	1.139	1.188	1.171	0.7140
40	1.205	1.184	1.234	1.174	1.219	1.277	1.234	1.520

Table 14. (Concluded)

P atm	ø exp	ø LJCL	ø KIH	ø KIHCK12	ø KIHEK12	ø BWR(a)	ø BWR(b)	$100x_2$
60	1.280	1.246	1.321	1.223	1.296	1.358	1.286	2.311
80	1.349	1.306	1.410	1.270	1.375	1.439	1.336	3.035
100	1.416	1.365	1.502	1.317	1.455	1.520	1.384	3.740
120	1.483	1.424	1.597	1.363	1.537	1.600	1.429	4.442
····· 173.02 K ·····								
40	1.207	1.205	1.264	1.213	1.252	1.337	1.294	1.837
60	1.291	1.266	1.358	1.268	1.336	1.436	1.359	2.793
80	1.371	1.324	1.452	1.320	1.419	1.531	1.416	3.730
100	1.443	1.380	1.550	1.370	1.504	1.626	1.470	4.639
120	1.498	1.437	1.655	1.423	1.595	1.725	1.523	5.367

a LORENTZ

b LINEAR

Table 15. Smoothed Experimental and Theoretical Enhancement Factors of Chlorotrifluoromethane in Helium, and the Smoothed Experimental Solubility of Helium in Liquid Chlorotrifluoromethane.

P atm	ø exp	ø LJCL	ø KIH	ø KIHCK12	ø KIHEK12	$100x_2$
		····· 145.21 K ·····				
20	1.073	1.089	1.119	1.053	1.073	0.1967
40	1.146	1.173	1.241	1.103	1.144	0.3967
60	1.219	1.257	1.370	1.152	1.215	0.5835
80	1.288	1.338	1.505	1.201	1.287	0.7600
100	1.355	1.418	1.646	1.249	1.359	0.9336
120	1.417	1.495	1.794	1.297	1.433	1.122
		····· 163.01 K ·····				
20	1.056	1.069	1.099	1.049	1.064	0.3035
40	1.113	1.127	1.192	1.088	1.119	0.6000
60	1.169	1.183	1.288	1.125	1.173	0.8970
80	1.226	1.237	1.387	1.162	1.227	1.190
100	1.284	1.288	1.489	1.199	1.281	1.471
120	1.338	1.336	1.595	1.235	1.336	1.746
		····· 180.02 K ·····				
20	1.058	1.066	1.096	1.057	1.069	0.4230
40	1.110	1.109	1.172	1.089	1.114	0.8465
60	1.158	1.149	1.250	1.120	1.158	1.265
80	1.204	1.186	1.330	1.151	1.203	1.682
100	1.248	1.221	1.411	1.181	1.247	2.100
120	1.291	1.253	1.494	1.210	1.291	2.520
		····· 196.01 K ·····				
20	1.070	1.175	1.107	1.075	1.085	0.5550
40	1.123	1.110	1.175	1.105	1.126	1.133
60	1.167	1.141	1.243	1.133	1.166	1.690*
80	1.204	1.169	1.313	1.161	1.205	2.225
100	1.236	1.195	1.384	1.188	1.245	2.725
120	1.263	1.218	1.458	1.216	1.284	3.190
		····· 211.06 K ·····				
20	1.100	1.095	1.127	1.101	1.109	0.6520

Table 15. (Concluded)

P atm	ϕ exp	ϕ LJCL	ϕ KIH	ϕ KIHCK12	ϕ KIHEK12	$100x_2$
40	1.150	1.127	1.194	1.134	1.152	1.411
60	1.185	1.152	1.260	1.163	1.192	2.117
80	1.213	1.175	1.327	1.191	1.230	2.800
100	1.237	1.194	1.394	1.218	1.269	3.462
120	1.257	1.212	1.464	1.244	1.307	4.088
		····· 221.27 K ·····				
20	1.135	1.111	1.142	1.121	1.127	0.7310
40	1.173	1.146	1.217	1.163	1.179	1.571*
60	1.204	1.171	1.285	1.195	1.221	2.403*
80	1.229	1.191	1.353	1.224	1.262	3.229
100	1.251	1.207	1.423	1.252	1.301	4.033
120	1.272	1.221	1.494	1.281	1.341	4.769
		····· 231.08 K ·····				
40	1.203	1.169	1.242	1.194	1.208	1.852
60	1.241	1.195	1.319	1.233	1.258	2.785*
80	1.273	1.214	1.394	1.268	1.305	3.715
100	1.302	1.230	1.470	1.301	1.349	4.628
120	1.326	1.242	1.550	1.333	1.394	5.463

* Interpolated values

APPENDIX H

SELECTION OF PHYSICAL PROPERTY DATA FOR PURE COMPONENTS

To predict the theoretical enhancement factors and extract the experimental values of B_{12}, Henry's law constant, and partial molar volume from phase equilibrium data, the following physical property data for pure components were needed.

1. The Lennard-Jones (6-12) classical and the Kihara core model potential parameters for all components.
2. Second and third virial coefficient data for all components.
3. Benedict-Webb-Rubin constants for all components.
4. Vapor pressure as a function of temperature for the condensed component.
5. Critical constants and saturated molar volume to calculate the compressibility of the saturated liquid and the molar volume of the compressed liquid for the condensed component.

The physical property data used in this work were selected after comparing and analysing all available values in the literature.

The experimental second and third virial coefficient data were collected and their agreement with the calculated

second and third virial coefficients using the available potential function parameters were tested. If the fit was poor, or there were no available parameters, a least squares computer program described in Appendix C in this work for the Kihara parameters or written by Mullines[90] for the Lennard-Jones parameters was used to extract new parameters from the experimental second virial coefficients. Unfortunately experimental second and third virial coefficient data for condensible components which fully covers the temperature range of this work could not be found. Where there were no experimental second and third virial coefficient data available, the theoretically extrapolated values based on the potential function were used to predict the enhancement factors and to extract the interaction second virial coefficients and Henry's law constants. As for the third virial coefficient, a detailed discussion has been given in Chapter IV. In the calculation of C_{111} using the method of Chueh and Prausnitz[18] whose parameters are presented in Table 16, the limitation suggested by Chueh and Prausnitz[18] that this method should not be used below $T_{R1} < 0.8$ was strictly followed by setting C_{111} equal to zero for $T_{R1} < 0.8$ shown in Figures 34, 36 and 38. All potential function parameters used to compute the second and third virial coefficients are presented in Table 17.

The eight-parameter BWR equation of state originally developed for the light hydrocarbons was used in predicting

the enhancement factors for the helium-carbon tetrafluoride system. The helium parameters for the BWR equation of state were taken from the thesis of Heck[46] who obtained these parameters from private communications with R. N. Herring (1966). This set contained a temperature dependent value of γ. No information was available as to how these parameters were obtained, but the P-V-T data of helium down to 50 K could be calculated with those parameters within about one percent by Heck.[46] Douslin, et al.[30] extracted the BWR constants from their P-V-T data of carbon tetrafluoride in the temperature range of 0 to 350 °C and these were used in this work. No BWR parameters were available for chlorotrifluoromethane. The second and third virial coefficients of the BWR equation calculated using Equations (IV-82) and (IV-83), are presented in Figures 34 and 36. All BWR constants used in this work are given in Table 17.

The best available experimental data of vapor pressure and saturated molar volume for the condensed phases were selected from the literature and the equations representing these data as a function of temperature were used in this work. These data are discussed more fully later in this appendix.

Critical constants of the condensed components are shown in Table 18. The experimental data for the molar volumes of the compressed liquid for the condensed components studied in this work could not be found in the literature

and so, a generalized correlation for the compressibilities of normal liquids presented in a recent paper by Chueh and Prausnitz[21] was used in this work to estimate the molar volumes of the compressed liquids as described in Chapter IV. This is one of the best available methods and holds for the interval $0.4 \leq T_R \leq 0.98$. The compressibility factors of saturated liquid calculated using this method for the carbon tetrafluoride and chlorotrifluoromethane are presented in Table 17.

Table 16. Input Parameters for the Calculation of Third Virial Coefficients Using the Method of Chueh and Prausnitz.[18]

Component	T_c (K)	V_c (cc/gm mole)	d_1	d_{12}	M_{12}
Helium	10.47[18]	37.5[18]	0.0[18]		
Carbon Tetrafluoride	227.53[16]	140.65[16]	0.8(a)	0.4	7.657
Chlorotrifluoromethane	302.00[1]	180.81[1]	0.6(b)	0.3	7.710

a This value was estimated by plotting the third virial coefficient data from the papers of Douslin, et al.[30] and Lange and Stein[75] on the reduced curve presented by Churh and Prausnitz.[18]

b The value obtained using the same method as above except that the third virial coefficients data from the paper of Michels, et al.[87] were used.

Table 17. Intermolecular Potential Parameters and BWR Parameters.

Parameter	He	CF_4	$CClF_3$
LJCL (6-12)			
e/k, K	6.96 (90)	151.5 (115)	185.8 (This Work)
b_o, cc/gm mole	22.9	134.7	220.2
KIHARA			
U_o/k, K	9.927 (100)	289.7 (115)	404.4 (This Work)
ρ_o, Å	2.921	3.232	3.367
M_o, Å	0.0	9.048	10.21
S_o, Å^2	0.0	6.514	8.302
V_o, Å^3	0.0	1.564	2.250
M (a)	4.0026	88.005	104.47
BWR			
liter-atm-K-gm mole	He (46)	CF_4 (30)	
A_o	1.308895(-2)*	1.86000	
B_o	1.226171(-2)	5.52000(-2)	
C_o	4.802198	1.54500(5)	
a	5.759319(-4)	3.98530(-1)	
b	3.352402(-4)	1.21147(-2)	
c	2.440703(-1)	2.43300(4)	
α	2.592255(-5)	2.50000(-4)	
γ	**	1.25000(-2)	

a Molecular weight calculated by adding the atomic weights of the constituents based on the 1961 Table of International Atomic weights.

Table 17. (Continued)

* Number in parentheses indicates powers of 10.

** Value of γ is a function of temperature = $3.850179 \times 10^{-3} - 2.332414 \times 10^{-5}T - 7.228731 \times 10^{-8}T^2 + 6.765171 \times 10^{-10}T^3$.

Table 18. Compressibility Factors of Saturated Liquid Estimated Using the Generalized Correlation Given by Chueh and Prausnitz,[21] and the Critical Constants.

Component	T_c (K)	P_c (atm)	V_c (cc/gm mole)	T (K)	$\beta_T^S \times 10^4$ (atm^{-1})
Carbon Tetrafluoride	227.53(16)	36.96(16)	140.65(16)	106.01	1.111
				117.33	1.324
				132.18	1.772
				147.10	2.469
				162.03	3.573
				173.02	4.902
Chlorotrifluoromethane	302.00(1)	38.19(1)	180.81(1)	145.21	1.137
				163.01	1.432
				180.02	1.863
				196.01	2.443
				211.06	3.224
				221.27	3.968
				231.08	4.954

HELIUM

A good comparison of the experimental second and third virial coefficient data for helium with the theoretical second virial coefficients calculated using the KIH, LJCL, and BWR models and the theoretical third virial coefficients calculated using the LJCL model and the method of Chueh and Prausnitz[18] is given recently by Garber.[37] These data are shown in Figures 33 and 34.

Figure 33 shows the experimental second virial coefficient data for helium with the theoretically calculated values. The LJCL parameters selected for helium are those determined by Mullins[90] who fitted the second virial coefficient data of White, et al.[138] using a least square procedure. Kihara core parameters used in this work were determined by Prausnitz and Myers[100] and include the first two translational quantum corrections. It can be seen in the figure that the agreement of the calculated values with the experimental second virial coefficient data of Keesom,[60] White, et al.,[138] Canfield, et al,[15] and Hoover, et al.[55] are very good except those predicted with the BWR parameters.[46]

The experimental third virial coefficient data of helium of Keesom,[60] White, et al.,[138] Canfield, et al.,[15] and Hoover, et al.[55] are shown in Figure 34 together with the values predicted using various theoretical models. Figure 34 also shows the selected curve for the experimental third virial coefficients of helium drawn smoothly

through the experimental data which fully cover the temperature range of this work. All potential function parameters for helium together with those of the BWR equation of state used in this work are presented in Table 18.

Carbon Tetrafluoride

Douslin, et al.,[30] MacCormack and Schneider,[79] Hamann, et al.,[44] Lange and Stein,[75] and Kalfoglou and Miller[59] have measured the second virial coefficients of carbon tetrafluoride in the temperature range of 200 K to 630 K which is above that of this work. No experimental second virial coefficient data were available in the literature in the temperature range of 106 to 173 K. Two sets of LJCL and Kihara core parameters were available, one extracted by Douslin, et al.[30] and the other by Sherwood and Prausnitz[115] using the P-V-T data of Douslin, et al.[30] in the temperature range of 0 to 350 °C. Because the parameters of Sherwood and Prausnitz[115] gave better agreement with the experimental second virial coefficient data in the lower region of the temperature, the extrapolated values of the second virial coefficients computed using these potential parameters were used down to 106 K to predict the theoretical enhancement factors. As shown in Figure 35 the three-parameter potential Kihara core model is better in predicting the second virial coefficients than the two-parameter potential Lennard-Jones (6-12) model as Sherwood and Prausnitz[115] have pointed out. The

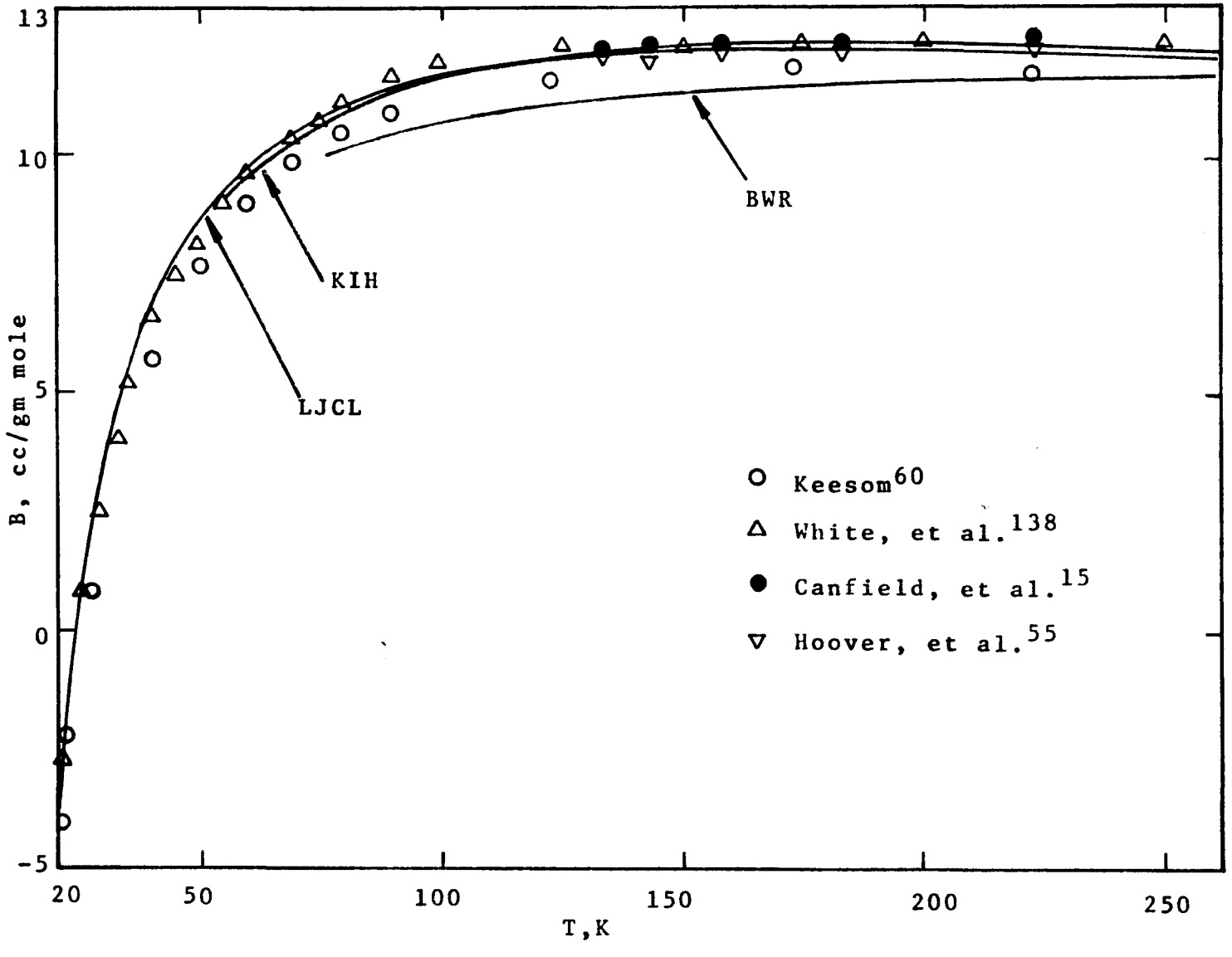

Figure 33. Second Virial Coefficient of Helium

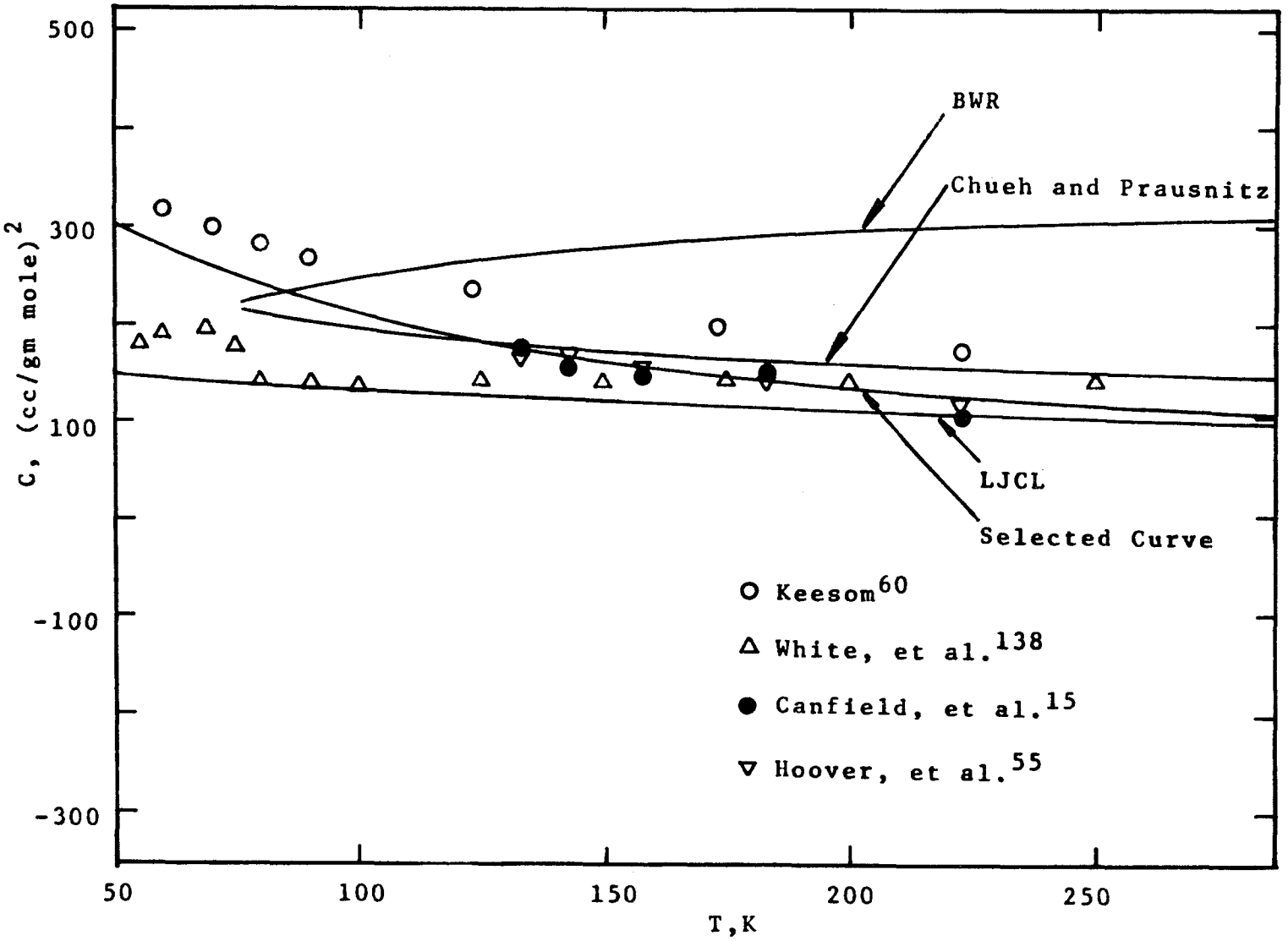

Figure 34. Third Virial Coefficient of Helium.

BWR parameters for carbon tetrafluoride were determined by Douslin, et al.[30] from the same P-V-T data mentioned above and the BWR equation of state with these parameters tends to predict the second virial coefficients which are believed to be too low at the lower temperatures as shown in Figure 35.

In Figure 36, the experimental third virial coefficient data of Douslin, et al.,[30] Lange and Stein,[75] and MacCormack, et al.[79] are compared with the theoretically predicted values for carbon tetrafluoride. The LJCL and BWR models all fail to predict the correct third virial coefficients. However the method of Chueh and Prausnitz[18] predicts quite satisfactory values for $T_R \geq 0.8$. No experimental third virial coefficient data were available below 200 K.

Extensive measurements for the vapor pressure of carbon tetrafluoride below one atmosphere were made by Menzel and Mohry,[86] Chari,[16] Simon, et al.,[119] and Smith and Pace[123] and above one atmosphere by Chari[16] whose data appeared to be exclusive. Of these, the equation representing the experimental data of Simon, et al.[119] was chosen for use in the temperature range of this work since it not only fit the experimental data of Simon, et al.[119] below one atmosphere but also agrees with the data of Chari[16] within 0.5 percent above one atmosphere up to 5 atmospheres. The equation is given below.

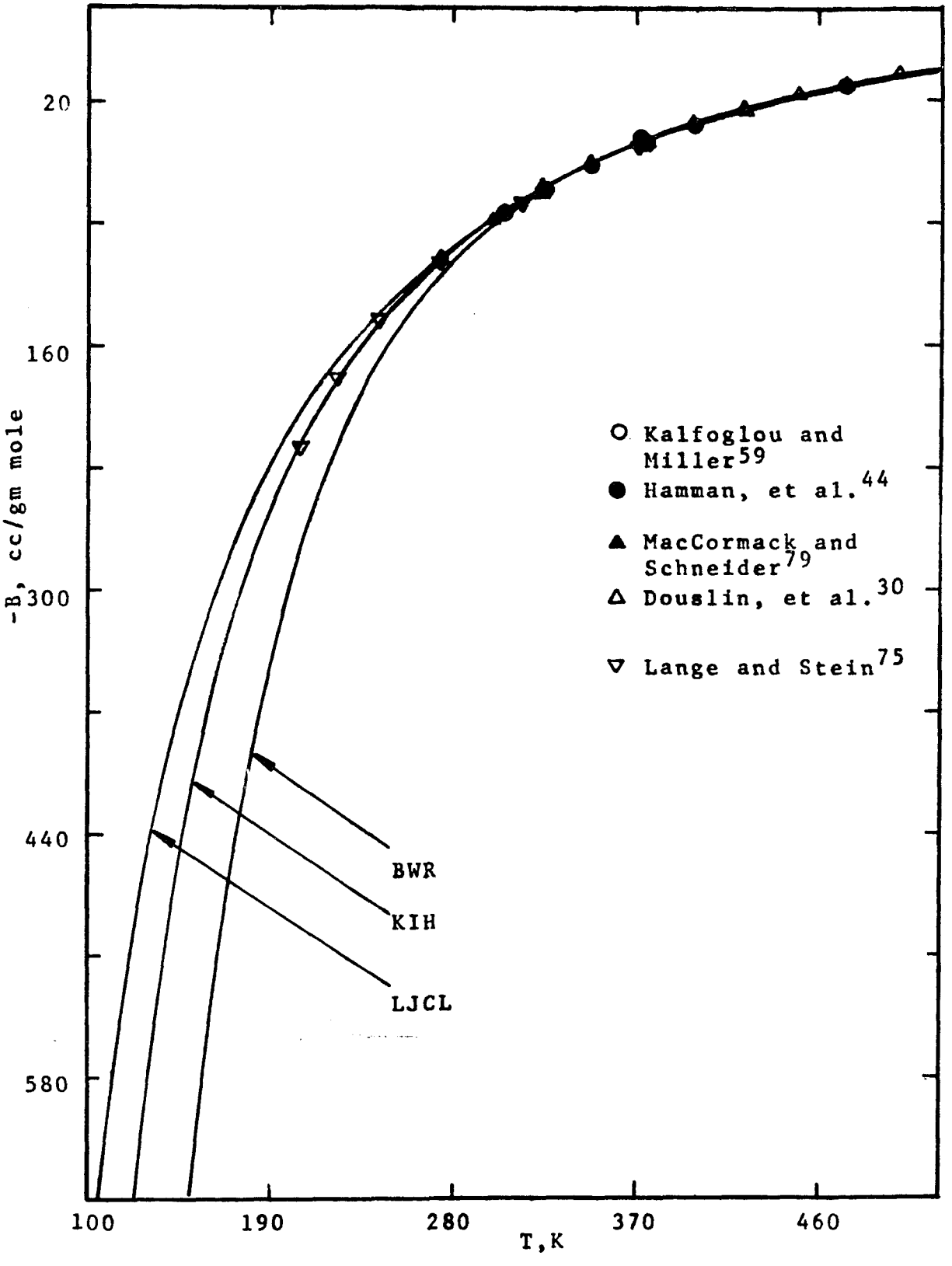

Figure 35. Second Virial Coefficient of Carbon Tetrafluoride.

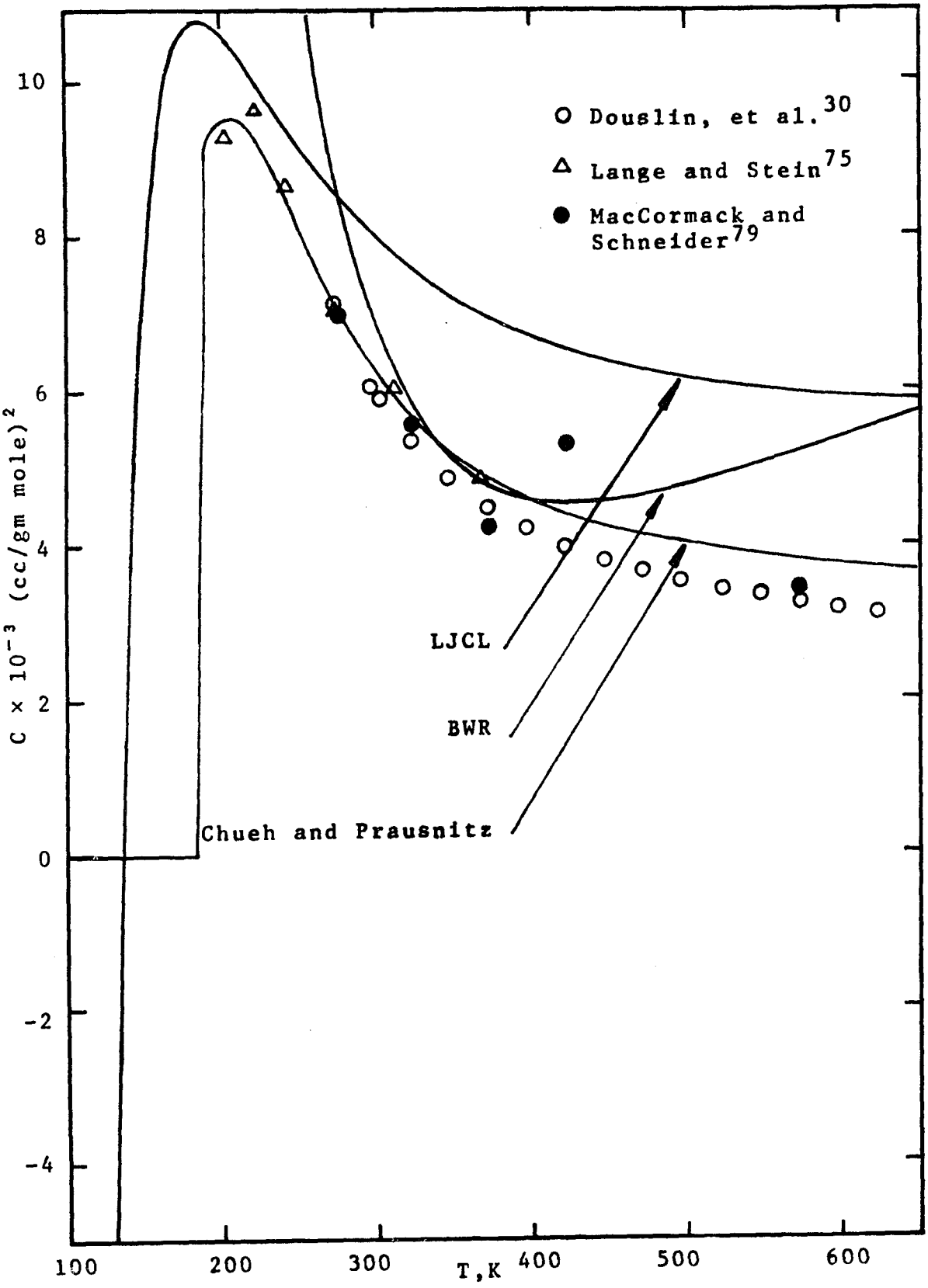

Figure 36. Third Virial Coefficient of Carbon Tetrafluoride.

$$\log P \text{ (torr)} = 6.8368405 - 511.69474/(T - 15.7744) \qquad \text{(H-1)}$$

The temperature scale used in this equation by Simon, et al.[119] was not clear on which scale it was based except that the platinum resistance thermometer used for the temperature measurements in his work was calibrated by the U.S. National Bureau of Standards, but the most likely temperature scale was probably the IPTS-48. The author of the present work used this temperature scale in the above equation. The vapor pressures of carbon tetrafluoride used in this work were calculated using Equation (H-1) and corrected to IPTS-68. They are presented in Table 19.

Several investigators[131,72,16] have measured the saturated molar volumes of carbon tetrafluoride. Of these, the experimental measurements of Terry, et al.[131] were most extensive and covered the entire temperature range of this work. The equation given by Terry, et al.[131] which represents their experimental data with average deviation of 0.017 cm^3/gm mole is:

$$v(cm^3/gm \text{ mole}) = 46.9166 + 1.26579 \times 10^{-1} \qquad \text{(H-2)}$$

$$\times (T - 89.569) - 0.0400011 \times 10^{-3} (T - 89.569)^2$$

$$+ 2.32262 \times 10^{-5} (T - 89.569)^3 - 2.71815 \times 10^{-7}$$

$$\times (T - 89.569)^4 + 1.47465 \times 10^{-9} (T - 89.569)^5$$

Table 19. Vapor Pressures of Carbon Tetrafluoride and Chlorotrifluoromethane.

Substance	T,K	P_{of}, atm
Carbon Tetrafluoride	106.01	0.01926[119]
	117.33	0.08276
	132.18	0.3636
	147.10	1.147
	162.03	2.865
	173.02	5.029
Chlorotrifluoromethane	145.21	0.03245[1]
	163.01	0.1574
	180.02	0.5103
	196.01	1.248
	211.06	2.526
	221.27	3.837
	231.08	5.525

Terry, et al.[132] used the IPTS-48 in deriving Equation (H-2). Table 8 shows the saturated liquid molar volumes of carbon tetrafluoride used in this work and these were calculated using Equation (H-2).

The critical constants of carbon tetrafluoride used are those determined by Chari[16] and presented in Table 18 together with the compressibility factors of liquid carbon tetrafluoride at saturation calculated using the generalized correlation for the compressibilities of normal liquids given by Chueh and Prausnitz.[21]

Chlorotrifluoromethane

Kunz and Kapner,[74] Hajjar and MacWood,[42,43] and Michels, et al.[87] have determined the experimental second

virial coefficients of chlorotrifluoromethane. Their values are shown in Figure 37, together with those calculated using the Kihara core and Lennard-Jones (6-12) models. Two sets of the Lennard-Jones potential parameters for chlorotrifluoromethane were presented in the papers of Hajjar and Macwood [42] and Brandt[12] who obtained his parameters in a communication with Auer.[2] The second virial coefficients calculated using these two sets of parameters do not agree satisfactorily with the available experimental data.[74,87,42,43] New Lennard-Jones parameters were extracted in the present work from the experimental second virial coefficient data of Kunz and Kapner,[74] and Michels, et al.[87] using a least squares program written by Mullins.[90,139] These parameters are given in Table 18. No Kihara parameters were available in the literature. From the data of Kunz and Kapner[74] and Michels, et al. [87] the Kihara potential parameters were extracted using a least squares program made in this work (see Appendix C). These extracted parameters are presented in Table 18.

The only available experimental third virial coefficient data for chlorotrifluoromethane were those determined by Michels, et al.[87] and are compared with the values predicted by the LJCL (6-12) model and the method of Chueh and Prausnitz.[18]

The BWR constants for halogen substituted hydrocarbons were scarce and no BWR data were available for chlorotrifluoromethane; therefore the BWR equation of state was

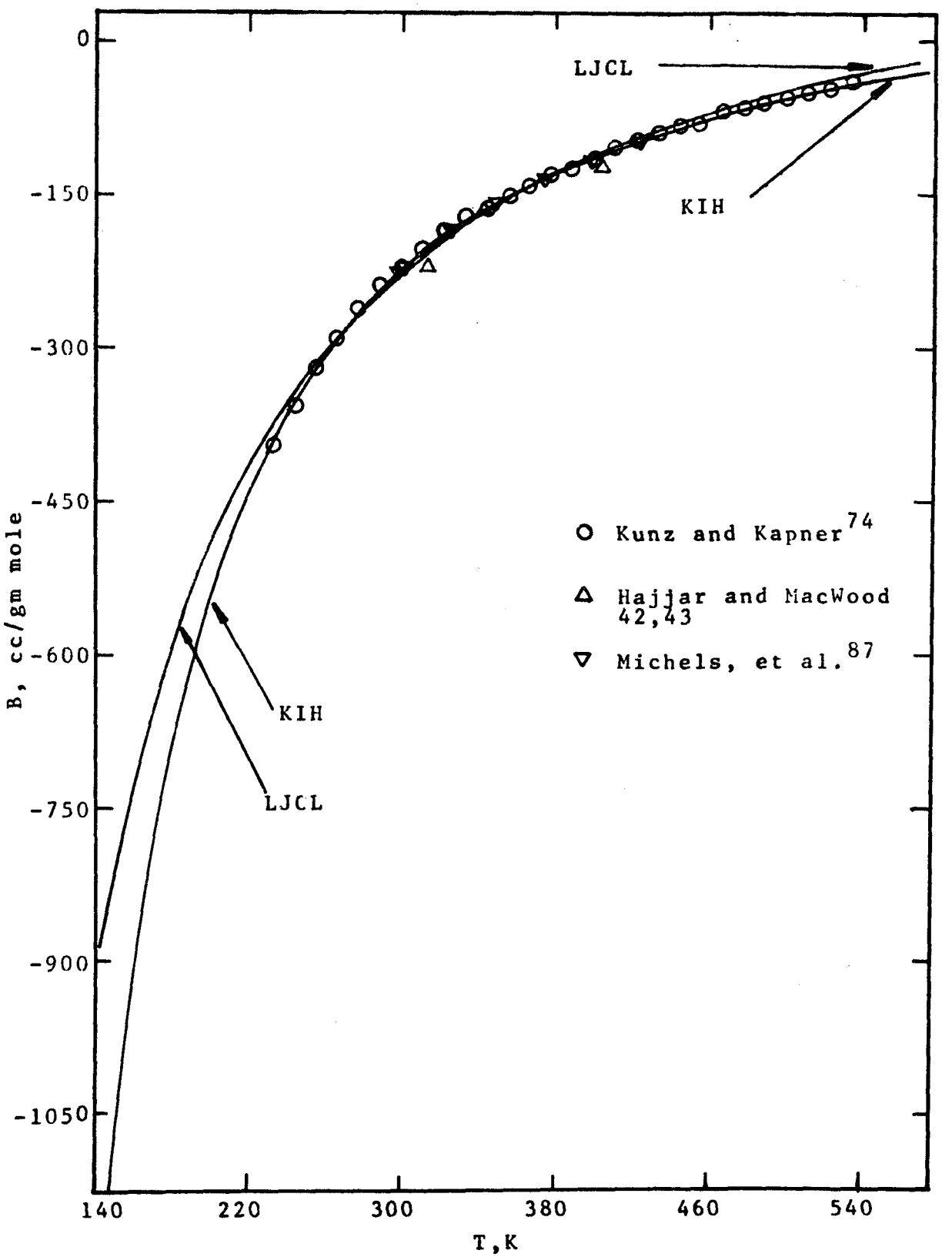

Figure 37. Second Virial Coefficient of Chlorotrifluoromethane.

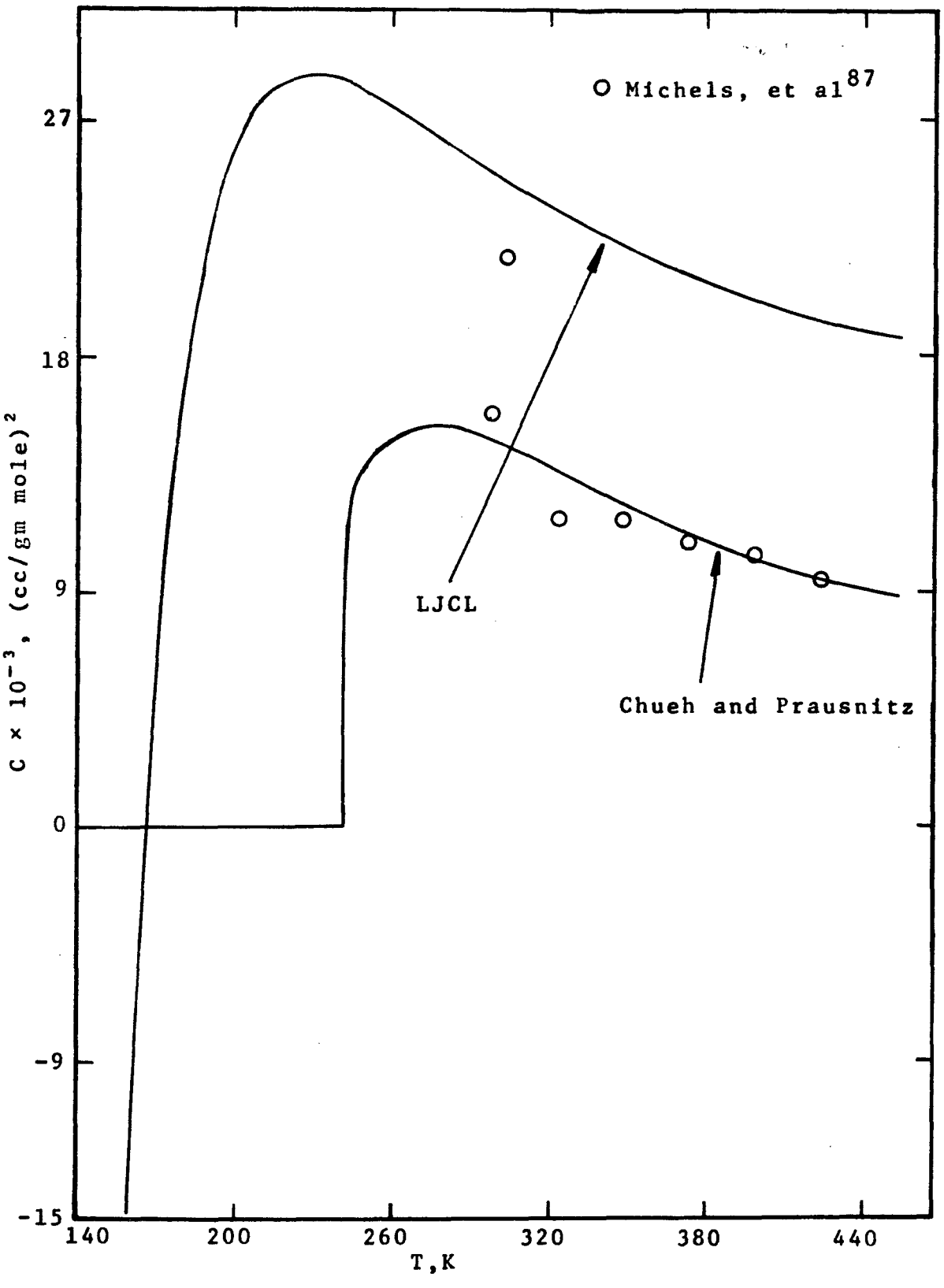

Figure 38. Third Virial Coefficient of Chlorotrifluoromethane.

not tested for the helium-chlorotrifluoromethane system.

The experimental vapor pressure data for chlorotrifluoromethane have been presented in several papers, and of these the data presented by Albright and Martin[1] have been selected since they not only cover the entire temperature range of this work but also their agreement with other data is satisfactory. The equation given by Albright and Martin[1] which represents these data within 0.08 percent from 144 K to 247 K and was used in this work is given as

$$\log P = 36.76130 - 2623.988/T - 11.80586 \log T + 5.71495 \times 10^{-3} T \qquad \text{(H-3)}$$

where P is psi and T is °R. It is not clear which temperature scale the investigator used. The IPTS-48 was used for Equation (H-3) in this work. The vapor pressures of chlorotrifluoromethane used in this work were calculated using Equation (H-3) after correction to IPTS-68. They are presented in Table 19.

The density data of saturated liquid chlorotrifluoromethane were obtained from the papers of Albright and Martin,[1] Fiske,[35] and E. I. du Pont de Nemours & Co.[32] These data agree closely with one another. The equation given by Albright and Martin[1] which fits their experimental data within 0.09 percent for the entire temperature range of this work was selected and is shown as follows:

$$d = 36.07 + 0.01566\,(83.93 - t) + 1.110 \qquad \text{(H-4)}$$

$$\times\,(83.93 - t)^{\frac{1}{2}} + 6.665\,(83.93 - t)^{\frac{1}{3}} + 3.245$$

$$\times\,10^{-5}\,(83.93 - t)^{2}$$

In Equation (H-4), d indicates density in pounds per cubic foot and t temperature in °F. The saturated liquid densities of chlorotrifluoromethane used in this work were calculated from Equation (H-4) and are shown in Table 8.

The critical constants of chlorotrifluoromethane used in this work also are those determined by Albright and Martin[1] and are presented in Table 18 together with the compressibility factors of saturated liquid chlorotrifluoromethane evaluated using the generalized correlation of Chueh and Prausnitz.[21]

APPENDIX I

PURITY OF GASES USED

The argon which was used in the helium-propylene and helium-carbon tetrafluoride systems was the same that was purchased by Garber[37] from the Air Products Company and had a quoted purity of 99.99 percent. The purity of propylene used in this work was approximately verified to be 99.99 percent pure by Garber and the gas was obtained from Phillips Petroleum Company. Helium with a quoted purity of 99.997 percent was obtained from the Air Reduction Company and used in this work. The argon for the helium-chlorotrifluoromethane system was purchased from the American Cryogenics, Inc. and its quoted purity was 99.999 percent.

Carbon tetrafluoride (Freon 14) and chlorotrifluoromethane (Freon 13) used in this work were supplied by E. I. du Pont de Nemours & Company, Inc. with a claimed purity of 99.9 percent. Their purities were approximately checked by using two chromatographs, 154B for carbon tetrafluoride and 154D for chlorotrifluoromethane and the impurity was found to be mainly air. The peak area method was used to calculate the approximate composition of the impurity.

All gases were used without further purification.

BIBLIOGRAPHY

1. Albright, L. F. and Martin, J. J., "Thermodynamic Properties of Chlorotrifluoromethane," Industrial and Engineering Chemistry 44, 188-198 (1952).

2. Auer, W., Physikalisch-Chemisches Institute, University of Heidelberg.

3. Barber, C. R., "The International Practical Temperature Scale of 1968," Metrologia 5, No. 2, 35-44 (1969).

4. Barrick, P. L., Heck, C. K., and MacKendrick, R. F., "Liquid Vapor Equilibria of the Helium-Carbon Dioxide System," Journal of Chemical and Engineering Data 13, 352-353 (1968).

5. Beattie, J. A. and Bridgeman, O. C., "A New Equation of State for Fluids," Proceedings of the American Academy of Arts and Sciences 63, 230-308 (1928).

6. Beattie, J. A. and Stockmayer, W. H., "The Thermodynamics and Statistical Mechanics of Real Gases, "A Treatise on Physical Chemistry 2, States of Matter, 3rd edition, D. Van Nostrand Company, New York, New York (1951).

7. Benedict, M., Webb, G. B., and Rubin, L. C., "An Empirical Equation for Thermodynamic Properties of Light Hydrocarbons and Their Mixtures," Journal of Chemical Physics 8, 334-345 (1940).

8. Benedict, M., Webb, G. B., and Rubin, L. C., "An Empirical Equation for Thermodynamic Properties of Light Hydrocarbons and Their Mixtures. II. Mixtures of Methane, Ethane, Propane and n-Butane," Journal of Chemical Physics 10, 747-758 (1942).

9. Benedict, M., Webb, G. B., and Rubin, L. C., "An Empirical Equation for Thermodynamic Properties of Light Hydrocarbons and Their Mixtures," Chemical Engineering Progress 47, No. 8, 419, 422 (1951).

10. Bergeon, M. R., "Le Troisie'me Coefficient du Viriel Pour un Potentiel Intermole'culaire avec Force Re'pulsive en r^{-a}," Acade'mie des Sciences. Comptes Rendus (Paris) 234B, 1039-1041 (1952).

11. Bird, R. B., Spotz, E. L., and Hirschfelder, J. O., "The Third Virial Coefficient for Non-Polar Gases," Journal of Chemical Physics 18, 1395-1402 (1950).

12. Brandt, W., "Calculation of Intermolecular Force Constants from Polarizabilities," Journal of Chemical Physics 24, 501-506 (1956).

13. Burnett, E. S., "Compressibility Determination Without Volume Measurements," Journal of Applied Mechanics 3, A136-140 (1936).

14. Buzyna, G., Macriss, R. A., and Ellington, R. T., "Vapor Liquid Equilibrium in the Helium-Nitrogen System," Chemical Engineering Progress Symposium Series No. 44, 101-111 (1963).

15. Canfield, F. B., Leland, T. W., and Kobayashi, R., "Volumetric Behavior of Gas Mixtures at Low Temperatures by the Burnett Method: Helium-Nitrogen System, 0 to -140°C," Advances in Cryogenic Engineering 8, 146-157 (1963).

16. Chari, N. C. S., Thermodynamic Properties of Carbon Tetrafluoride, Sc. D. Thesis, University of Michigan (1960).

17. Chiu, C. -h. and Canfield, F. B., "Thermodynamic Analysis of Vapor-Liquid and Vapor-Solid Equilibria Data to Obtain Interaction Second Virial Coefficients," Advances in Cryogenic Engineering 12, 741-753 (1967).

18. Chueh, P. L. and Prausnitz, J. M., "Third Virial Coefficients of Nonpolar Gases and Their Mixtures," American Institute of Chemical Engineers Journal 13, No. 5, 896-902 (1967).

19. Chueh, P. L. and Prausnitz, J. M., "Vapor-Liquid Equilibria at High Pressures. Vapor-Phase Fugacity Coefficients in Nonpolar and Quantum Gas Mixtures," Industrial and Engineering Chemistry Fundamentals 6, No. 4, 492-498 (1967).

20. Chueh, P. L. and Prausnitz, J. M., "Vapor-Liquid Equilibria at High Pressures. Calculation of Partial Molar Volumes in Nonpolar Liquid Mixtures," American Institute of Chemical Engineers Journal 13, No. 6 1099-1107 (1967).

21. Chueh, P. L. and Prausnitz, J. M., "A Generalized Correlation for the Compressibilities of Normal Liquids," American Institute of Chemical Engineering Journal 15, No. 3, 471-472 (1969).

22. Cook, G. A., Argon, Helium, and the Rare Gases, Interscience Publishers, Inc., New York, New York (1961).

23. Correia, Bon P., Schafer, K., and Schneider, M., "Bestimmung der zwischenmolekularen Krafte aus Ultraschalldispersionsmessungen in Gasgemischen," Berichte der Bunsengesellschaft fur Physikalische Chemie 73, No. 6, 507-513 (1969).

24. Dantzler, E. M., Knobler, C. M., and Windsor, M. L., "Second Virial Coefficients of Some Argon-Hydrocarbon Mixtures and Their Comparison With Chromatographic Values," Journal of Chromatography 32, 433-438 (1968).

25. Davidson, N., Statistical Mechanics, McGraw-Hill, Inc., New York, New York (1962).

26. De Boer, J. and Michels, A., "The Influence of the Interaction of More than Two Molecules on the Molecular Distribution-Function in Compressed Gases," Physica 6, 97-114 (1939).

27. DeVaney, W. E., Dalton, B. J., and Meeks, J. C., Jr., "Vapor Liquid Equilibrium of the Helium-Nitrogen System," Journal of Chemical and Engineering Data 8, No. 4, 473-478 (1963).

28. Dokoupil, Z., "Some Solid-Gas Equilibria at Low Temperatures," Progress in Low Temperature Physics, Vol. III, Edited by C. J. Gorter, North-Holland Publishing Company, Amsterdam, Interscience Publishing, Inc., New York, 454-480 (1961).

29. Dokoupil, Z., Van Soest, G., and Swenker, M. D. P., "On the Equilibrium Between the Solid Phase and the Gas Phase of the Systems Hydrogen-Nitrogen Hydrogen-Carbon Monoxide, and Hydrogen-Nitrogen-Carbon Dioxide," Applied Scientific Research A5, 182-240 (1955).

30. Douslin, D. R., Harrison, R. H., Moor, R. T., and McCullough, J. P., "Tetrafluoromethane: P-V-T and Intermolecular Potential Energy Relations," Journal of Chemical Physics 35, 1357-1366 (1961).

31. Drayer, D. E. and Flynn, T. M., "A compilation of the Physical Equilibria and Related Properties of the Hydrogen-Nitrogen System," U. S. National Bureau of Standard Technical Note No. 110 (1961).

32. DuPont de Nemours & Co., E. I., Thermodynamic Properties of Freon 13 Refrigerant, Bulletin T13 (1959).

33. Eckert, C. H., Renon, H., and Prausnitz, J. M., "Molecular Thermodynamics of Simple Liquids," Industrial and Engineering Chemistry. Fundamentals 6, No. 1, 58-67 (1967).

34. Fedoritenko, A. and Ruhemann, M., "Equilibrium Diagrams of Helium-Nitrogen Mixtures," Technical Physics of U S S R 4, 36-43 (1937).

35. Fiske, D. L., "Low Temperature Freon Refrigerants," Refrigerating Engineering 53, 336-339 (1949).

36. Fowler, R. and Graben, H. W., "Nonadditive Third Virial Coefficient for Intermolecular Potentials with Hard-Sphere Cores," Journal of Chemical Physics 50, No. 10, 4347-4351 (1969).

37. Garber, J. D., Gas-Liquid Phase Equilibrium in the Helium-Ethylene and Helium-Propylene Systems Below 260°K and 120 Atmospheres, Ph.D. Thesis, Georgia Institute of Technology, Atlanta, Georgia (1970).

38. Gonikberg, M. and Fastovskii, V., "The Solubility of Gases in Liquids at Low Temperatures and High Pressures, Fourth Article," Foreign Petroleum Technology 9, No. 6, 214-219 (1941).

39. Graben, H. W. and Present, R. D., "Evidence of Three-Body Forces From Third Virial Coefficient," Physical Review Letters 9, 247-248 (1962).

40. Graben, H. W. and Present, R. D., McCulloch, R. D., "Intermolecular Three-Body Forces and Third Virial Coefficients," Physical Review 144, No. 1, 140-142 (1966).

41. Guggenheim, E. A., "The Principle of Corresponding States," Journal of Chemical Physics 13, 253-261 (1945).

42. Hajjar, R. F. and MacWood, G. E., "Second Virial Coefficients and the Force Constants, ϵ_o and r_o, of six Halogen-Substituted Methanes," Journal of Chemical Physics 49, 4567-4570 (1968).

43. Hajjar, R. F. and MacWood, G. E., Determination of the Second Virial Coefficients of Six Fluorochloromethanes by a Gas Balance Method in the Range 40 to 130°C," Journal of Chemical and Engineering Data 15, No. 1, 3-6 (1970).

44. Hamman, S. D., McMananey, W. J., and Pierce, J. F., "Forces Between Polyatomic Molecules," Transaction of Faraday Society 49, 351-357 (1953).

45. Hanley, H. J. M. and Klein, M., "On the Selection of the Intermolecular Potential Function: Application of Statistical Mechanical Theory to Experiment," National Bureau of Standards Technical Note 360, 82 pages (1967).

46. Heck, C. K., Jr., Experimental and Theoretical Liquid-Vapor Equilibrium in Some Binary Systems, Ph.D. Thesis, University of Colorado, Denver, Colorado (1968).

47. Heck, C. K. and Hiza, M. J., "Liquid-Vapor Equilibrium in the System Helium-Methane," American Institute of Chemical Engineers Journal 13, 593-599 (1967).

48. Herring, R. N. and Barrick, P. L., "Gas-Liquid Equilibrium Solubilities for the Helium-Oxygen System," Advances in Cryogenic Engineering 10, 151-159 (1965).

49. Hirschfelder, J. O., Curtiss, C. J., and Bird, R. B., Molecular Theory of Gases and Liquids, John Wiley & Sons, Inc., New York (1964).

50. Hiza, M. J., "Solid-Vapor Equilibria Research on Systems of Interest in Cryogenics," Cryogenics 10, No. 2, 106-115 (1970).

51. Hiza, M. J. and Duncan, A. G., "Equilibrium Gas-Phase Compositions of Ethane and Ethylene in Binary Mixtures with Helium and Neon Below 150°K and a Correlation for Deviations from the Geometric Mean Combining Rule," Advances in Cryogenic Engineering 14, 30-40 (1968).

52. Hiza, M. J., Heck, C. K., and Kidnay, A. J., "Liquid-Vapor and Solid-Vapor Equilibrium in the System Hydrogen-Ethylene," Chemical Engineering Progress Symposium Series No. 88, 57-65 (1968).

53. Hiza, M. J., Heck, C. K., and Kidnay, A. J., "Liquid-Vapor and Solid-Vapor Equilibrium in the System Hydrogen-Ethane," Advances in Cryogenic Engineering 13, 343-356 (1968).

54. Hiza, M. J. and Kidnay, A. J., "Solid-Vapor Equilibrium in the System Helium-Methane," Advances in Cryogenic Engineering 11, 338-348 (1965).

55. Hoover, A. E., Canfield, F. B., Kobayashi, R., and Leland, T. W., Jr., "Determination of Virial Coefficients by the Burnett Method," Journal of Chemical and Engineering Data 9, No. 4, 568-573 (1964).

56. Hudson, G. H. and McCoubrey, J. C., "Intermolecular Forces Between Unlike Molecules," Transactions of the Faraday Society 56, 761-766 (1960).

57. Huff, J. A. and Reed, T. M., "Second Virial Coefficients of Mixtures of Nonpolar Molecules from Correlations on Pure Components," Journal of Chemical and Engineering Data 8, No. 3, 306-311 (1963).

58. Iomtev, M. B., Morozov, V. S., and Chumak, A. V., "Solid-Gas Phase Equilibrium in the System Helium-Carbon Dioxide," Zhurnal Fizicheskoi Khimii 42, No. 8, 2069-2071 (1968).

59. Kalfoglou, N. K. and Miller, J. G., "Compressibility of Gases. V. Mixtures of Spherically Symmetric Molecules at Higher Temperatures. The Helium-Argon and Helium-Tetrafluoromethane Systems," The Journal of Physical Chemistry 71, No. 5, 1256-1264 (1967).

60. Keesom, W. H., Helium, Elsevier, Amsterdam (1942).

61. Kerr, E. C., "Density of Liquid He^4," Journal of Chemical Physics 26, No. 3, 511-514 (1957).

62. Kharakhorin, F. F., "The Phase Relation in Systems of Liquid Gases, First Article, The Binary Mixture Nitrogen-Helium," Foreign Petroleum Technology 9, 397-410 (1941).

63. Kharakhorin, F. F., "Liquid-Vapor Equilibrium in a Helium-Methane System," Inzhenerno-Fizicheskii Zhurnal, Akademiya Nauk Belorusskoi S. S. R. 2, No. 5, 55-59 (1959).

64. Kihara, T., "Determination of Intermolecular Forces from the Equation of State of Gases," Journal Physical Society Japan 3, 265-268 (1948).

65. Kihara, T., "Determination of Intermolecular Forces from the Equation of State of Gases, Journal Physical Society Japan 6, 184-188 (1951).

66. Kihara, T., "Virial Coefficients and Models of Molecules in Gases," Reviews of Modern Physics 25, No. 4 831-843 (1953).

67. Kihara, T., "Virial Coefficients and Models of Molecules in Gases B," Reviews of Modern Physics 27, No. 4, 412-423 (1955).

68. Kirk, B. S., Predicted and Experimental Gas Phase Compositions in Pressurized Binary Systems Containing an Essentially Pure Condensed Phase. Phase Equilibrium Data for the Methane-Hydrogen System from 66.88 to 116.53 ^{o}K and Up to 125 Atmospheres, Ph.D. Thesis, Georgia Institute of Technology, Atlanta, Georgia (1964).

69. Kirk, B. S. and Ziegler, W. T., "A Phase Equilibrium Apparatus for Gas-Liquid Systems and the Gas Phase of Gas-Solid System. Application to Methane-Hydrogen from 66.88 to 116.53 ^{o}K and Up to 125 Atmospheres," Advances in Cryogenic Engineering 10, 160-170 (1965).

70. Kirk, B. S., Ziegler, W. T., and Mullins, J. C., "A Comparison of Methods of Predicting Equilibrium Gas Phase Compositions in Pressurized Binary Systems Containing an Essentially Pure Condensed Phase," Advances in Cryogenic Engineering 6, 413-427 (1961).

71. Kiser, R. W. and Hobrock, D. L., "The Ionization Potential of Carbon Tetrafluoride," Journal of American Chemical Society 87, 922-923 (1965).

72. Knobler, C. M. and Pings, C. J., "Saturated Liquid Density of Carbon Tetrafluoride from 90 to 150 ^{o}K," Journal of Chemical and Engineering Data 10, No. 2, 129-130 (1965).

73. Krichevsky, I. R. and Kasarnovsky, J. S., "Thermodynamical Calculations of Solubilities of Nitrogen and Hydrogen in Water at High Pressures," Journal of the American Chemical Society 57, 2168-2171 (1935).

74. Kunz, R. G. and Kapner, R. S., "Second Virial Coefficients from Tabulated P-V-T Data. Results for $CClF_3$, CCl_2F_2, CCl_3F, and $B(OCH_3)_3$," Journal of Chemical and Engineering Data 14, No. 2, 190-191 (1969).

75. Lange, H. B., Jr. and Stein, F. P., "Volumetric Behavior of Polar-Nonpolar Gas Mixtures: Trifluoromethane-Tetrafluoromethane," Journal of Chemical and Engineering Data 15, 56-61 (1970).

76. Lin, H. -M. and Robinson, R. L., Jr., "Uncertainties in Intermolecular Pair Potential Parameters Determined from Macroscopic Property Data. I. Virial Coefficients," Journal of Chemical Physics 52, No. 7, 3727-

77. Liu, K. F., Phase Equilibria in the Helium-Carbon Dioxide, -Argon, -Methane, -Nitrogen, and -Oxygen Systems, Ph.D. Thesis, Georgia Institute of Technology, Atlanta, Georgia (1969).

78. Longuet-Higgins, H. C. and Wisdom, B., "A Rigid Sphere Model for the Melting of Argon," Molecular Physics 8, 549-556 (1964).

79. MacCormack, K. E. and Schneider, W. G., "Compressibility of Gases at Pressures up to 50 atmospheres. V. Carbon-Tetrafluoride in the Temperature range 0-400 ^{o}C. VI. Sulfur Hexafluoride in the Temperature Range 0-250 ^{o}C," Journal of Chemical Physics 19, 845-848 (1951).

80. MacKendrick, R. F., Heck, C. K., and Barrick, P. L., "Liquid-Vapor Equilibria of the Helium-Carbon Dioxide System," Journal of Chemical and Engineering Data 13, 352-353 (1968).

81. Martin, J. J., "Equations of State," Industrial and Engineering Chemistry 59, No. 12, 34-52 (1967).

82. Martin, J. J. and Hou, Y.C., "Development of an Equation of State for Gases," American Institute of Chemical Engineers Journal 1, No. 2, 142-145 (1955).

83. Mastinu, G., "Apparatus To Determine Excess Molar Volumes. Application to the H_2-N_2 Mixture," Review of Scientific Instruments 38, No. 82, 1114-1116 (1967).

84. Mayer, J. E., "Statistical Mechanics of Condensing Systems. V Two Component Systems," Journal of Physical Chemistry 43, 71-95 (1939).

85. McCain, W. D., Jr., Vapor-Liquid Phase Equilibria of the Binary System Argon-Helium, Ph.D. Thesis, Georgia Institute of Technology, Atlanta, Georgia (1964).

86. Menzel, V. W. and Mohry, F., "Die Dampfducke des CF_4 abd NF_4 und der Tripelpunkt des CF_4," Zeitschrift fur Anorganische und allgememeine Chemie, 210, 257-263 (1933).

87. Michels, A., Wassenaar, T., Wolkers, G. J., Prins, C., and Klunkert, L.v.d., "P-V-T Data and Thermodynamical Properties of Freon 12 (CCl_2F_2) and Freon 13($CClF_3$) Fluorocarbons at Temperatures between 0 and 150°C and at pressures up to 400 atm.," Journal of Chemical and Engineering Data 11, No. 4, 449-452 (1966).

88. Miller, R. C. and Prausnitz, J. M., "Statistical Thermodynamics of Simple Liquid Mixtures," Industrial and Engineering Chemistry Fundamentals 8, No. 3, 449-452 (1969).

89. Montroll, E. W. and Mayer, J. E., "Statistical Mechanics of Imperfect Gases," Journal of Chemical Physics 9, 626-637 (1941).

90. Mullins, J. C., Phase Equilibria in the Argon-Helium and Argon-Hydrogen Systems, Ph.D. Thesis, Georgia Institute of Technology, Atlanta, Georgia (1965).

91. Mullins, J. C. and Ziegler, W. T., "Phase Equilibrium in the Argon-Helium and Argon-Hydrogen Systems from 68 to 108°K and Pressures Up To 120 Atmospheres," Advances in Cryogenic Engineering 10, 171-181 (1965).

92. O'Connell, J. P. and Prausnitz, J. M., "Applications of the Kihara Potential to Thermodynamic and Transport Properties of Gases," Symposium Thermophysical Properties, Papers, 3rd, Lafayette, Indiana, 19-31 (1965).

93. Orentlicher, M. and Prausnitz, J. M., "Thermodynamics of Hydrogen Solubility in Cryogenic Solvents at High Pressures," Chemical Engineering Science 19, 775-782 (1964).

94. Pierotti, R. A., "The Solubility of Gases in Liquids," Journal of Physical Chemistry 67, 1840-1845 (1963).

95. Pierotti, R. A., "Aqueous Solutions of Nonpolar Gases," Journal of Physical Chemistry 69, No. 1, 281-288 (1965).

96. Pierotti, R. A., "On the Sealed-Particle Theory of Dilute Aqueous Solutions," Journal of Physical Chemistry 71, 2366-2367 (1967).

97. Prausnitz, J. M., Molecular Thermodynamics of Fluid-Phase Equilibria, Prentice-Hall, Inc., Englewood Cliffs, New Jersey (1969).

98.. Prausnitz, J. M. and Chueh, P. L., Computer Calculations for High Pressure Vapor-Liquid Equilibrium, Prentice-Hall, Inc., Englewood Cliffs, New Jersey (1968).

99. Prausnitz, J. M., Eckert, C. A., Orye, R. V., and O'Connell, J. P., Computer Calculations for Multi-Component Vapor-Liquid Equilibria, Prentice-Hall, Inc., Englewood Cliffs, New Jersey (1968).

100. Prausnitz, J. M. and Myers, A. L., "Kihara Parameters and Second Virial Coefficients for Cryogenic Fluids and Their Mixtures," American Institute of Chemical Engineers Journal 9, No. 1, 5-11 (1963).

101. Preston, G. T. and Prausnitz, J. M., "A Generalized Correlation for Henry's Law Constants in Nonpolar Systems," Industrial and Engineering Chemistry Fundamentals 10, No. 3, 389-397 (1971).

102. Prigogine, I., The Molecular Theory of Solutions, North-Holland Publishing Company, Amsterdam (1957).

103. Prigogine, I. and Mathot, V., "Application of the Cell Method to the Statistical Thermodynamics of Solutions," Journal of Chemical Physics 20, 49-57 (1952).

104. Reddlich, O. and Kwong, J.N.S., "On the Thermodynamics of Solutions. V An Equation of State. Fugacities of Gaseous Solutions," Chemical Reviews 44, 233-244 (1949).

105. Reed, R. I., Ion Production by Electron Impact, Academic Press, New York, (1962).

106. Reiss, H., "Scaled Particle Methods in the Statistical Thermodynamics of Fluids," Advances in Chemical Physics IX, 1-84 (1965).

107. Reiss, H., Frisch, H. L., and Lebowitz, J. L., "Statistical Mechanics of Rigid Spheres," Journal of Chemical Physics 31, 369-380 (1959).

108. Reuss, J. and Beenakker, J. J. M., "Determination of the Second Virial Coefficient B_{12} of Gas Mixtures," Physica 22, 869-879 (1956).

109. Rodewald, N. D., Davis, J. A., and Kurata, F., "The Heterogeneous Phase Behavior of the Helium-Nitrogen System," American Institute of Chemical Engineers Journal 10, No. 6, 937-943 (1964).

110. Rowlinson, J. S., Summer, F. H., and Sutton, J. R., "The Virial Coefficients of a Gas Mixture," Transactions of the Faraday Society 50, 1-8 (1954).

111. Schindler, D. L., Swift, G. W., and Kurata, F., "Phase-Equilibrium Studies in the Nitrogen-Propane, Helium-Propane, and Helium-Nitrogen-Propane Systems," Proceedings of the Annual Convention Natural Gas Processors Association, Technical Paper 45, 46-51 (1966).

112. Scott, R. L., "Corresponding States Treatment of Non-Electrolyte Solutions," Journal Chemical Physics 25, No. 2, 193-205 (1956).

113. Shah, K. K., "A Comparison of Equations of State," Industrial and Engineering Chemistry 57, 30-37 (1965).

114. Sherwood, A. E., Derocco, A. G., and Mason, E. A., "Nonadditivity of Intermolecular Forces: Effects on the Third Virial Coefficient," Journal of Chemical Physics 44, No. 8, 2984-2994 (1966).

115. Sherwood, A. E. and Prausnitz, J. M., "Third Virial Coefficient for the Kihara, Exp-6, and Square-Well Potentials," Journal of Chemical Physics 41, No. 2, 413-428 (1964).

116. Sherwood, A. E. and Prausnitz, J. M., "Intermolecular Potential Functions and the Second and Third Virial Coefficients," Journal of Chemical Physics 41, No. 2, 429-437 (1964).

117. Shiau, J. F., Ph.D. Thesis in Progress (Chemical Engineering), Georgia Institute of Technology, Atlanta, Georgia (1971).

118. Sikora, P.T., "Combining Rules for Spherically Symmetric Intermolecular Potentials," Journal of Physics B: Atomic and Molecular Physics 3, 1475-1482 (1970).

119. Simon, M., Knobler, C. M., and Duncan, A. G., "The Vapor Pressure of Carbon Tetrafluoromethane from 86 to 146 ^{o}K," Cryogenics 7, No. 6, 138-140 (1967).

120. Sinor, J. E. and Kurata, F., "Solubility of Helium in Liquid Argon, Oxygen, and Carbon, Monoxide," Journal of Chemical and Engineering Data 11, No. 4, 537-539 (1966).

121. Sinor, J. E. and Kurata, F., "The Liquid Phase Volumetric Behavior of the Helium-Methane System," Journal of Chemical and Engineering Data 11, 1-6 (1966).

122. Sinor, J. E., Schindler, D. L., and Kurata, F., "Vapor-Liquid Phase Behavior of the Helium-Methane System," American Institute of Chemical Engineers Journal 12, No. 2, 353-357 (1966).

123. Smith, J. H. and Pace, E. L., "The Thermodynamic Properties of Carbon Tetrafluoride from 12 K to It's Boiling Point. The Significance of Parameter ν," Journal Physical Chemistry 73, 4232-4236 (1969).

124. Smith, G. E., Sonntag, R. E., and Van Wylen, G. J., "Analysis of the Solid-Vapor Equilibrium System Carbon Dioxide-Nitrogen," Advances in Cryogenic Engineering 8, 162-173 (1963).

125. Snider, N. S. and Herrington, T. M., "Hard Sphere Model of Binary Liquid Mixture," Journal of Chemical Physics 47, No. 7, 2248-2255 (1967).

126. Solen, K. A., Chueh, P. L., and Prausnitz, J. M., Thermodynamics of Helium Solubility in Cryogenic Solvents at High Pressures," Industrial and Engineering Chemistry Process Design and Development 9, No. 2, 310-317 (1970).

127. Staveley, L. A. K., "Hard Sphere Model Applied to the Solubility of Gases in Low Boiling-Liquid," Journal of Chemical Physics 53, No. 8, 3136-3138 (1970).

128. Stockbridge, T. R., "Thermodynamic Properties of Nitrogen from 14 to 300 K between 0.1 and 200 Atmospheres," U. S. National Bureau of Standards Technical Note No. 129 (1962).

129. Streett, W. B., "Liquid-Vapor Equilibrium in the System Neon-Argon," Journal of Chemical Physics 42, No. 2, 500-503 (1965).

130. Streett, W. B., "Liquid-Vapor Phase Behavior and Liquid Phase Density in the System Neon-Argon at High Pressures," Journal of Chemical Physics 46, No. 9, 3282-3286 (1967).

131. Streett, W. B., Sonntag, R. E., and Van Wylen, G. J., "Liquid-Vapor Equilibrium in the System Normal Hydrogen-Helium," Journal of Chemical Physics 40, No. 5, 1390-1395 (1964).

132. Terry, M. J., Lynch, J. T., Bunclark, M., Mansell, K. R., and Staveley, A. L. K., "The Densities Liquid Argon, Krypton, Xenon, Osyten, Nitrogen, Carbon Monoxide, Methane, and Carbon Tetrafluoride along the Orthobaric Liquid Curve," Journal of Chemical Thermodynamics 1, 413-424 (1969).

133. Thiele, E., "Equation of State for Hard Sphere," Journal of Chemical Physics 39, No. 2, 474-479 (1963).

134. Tsonopoulos, C. and Prausnitz, J. M., "Equation of State: A Review for Engineering Applications," Cryogenics 9, No. 10, 315-327 (1969).

135. Van Itterbeck, A. and Van Doninck, W., "Measurements on the Velocity of Sound in Mixtures of Hydrogen, Helium, Oxygen, Nitrogen and Carbon Dioxide at Low Temperature," Proceedings of the Physical Society (London) 62B, 62-69 (1949).

136. Watanabe, K., Nakayama, T., and Mottl, J., "Ionization Potentials of Some Molecules," Journal of Quantative Spectroscopy & Radiating Transfer 2, 369-382 (1962).

137. Wertheim, M. S., "Exact Solutions of Percus-Yevick Integral Equation for Hard Spheres," Physical Review Letters 10, No. 8, 321-323 (1963).

138. White, D., Rubin, T., Camky, P., and Johnston, H. L., "The Virial Coefficients of Helium from 20 to 300 K," Journal of Physical Chemistry 64, 1607-1612 (1960).

139. Ziegler, W. T. and Mullins, J. C., Calculation of the Vapor Pressure and Heats of Vaporization and Sublimation of Liquids and Solids, Especially Below One Atmosphere. IV. Nitrogen and Fluorine. Technical Report No. 1, Project A-663, Engineering Experiment Station, Georgia Institute of Technology, Atlanta, Georgia, April 15, 1963 (Contract No. CST - 7404, National Bureau of Standards, Boulder, Colorado).

VITA

Yo Kil Yoon was born January 29, 1940 in Choongchong-Namdo, Korea to the late Soon Chon Park and Sok Koo Yoon. He was reared in Seoul, Korea, where he attended the public schools. After graduating from Seoul Ilsin Elementary School in 1952, he attended Song Dong Middle School for three years and then Kyungi High School for one year. In 1958, he passed the National College Entrace Qualifying Examination. He received the degree Bachelor of Science from Korean Military Academy with the President Award as the first place in his class of 1964.

After serving for two years in the ROK Army, he entered the School of Chemical Engineering, Georgia Institute of Technology in June, 1966 and received the degree Master of Science in Chemical Engineering in June, 1968.

From September, 1968 to March, 1969, he served on the faculty in the Department of Chemistry in Korean Military Academy with the rank of captain. He returned to the Georgia Institute of Technology in March, 1969 and has been employed as a teaching assistant in the School of Chemical Engineering from September 1969 to the present time.

He is a member of the Society of Sigma Xi.

He is married to the former Buhm Jin Key and they have one daughter, Soo Son.